1-2-2013

Impact Of Cryoablation On Tumor Immunity

Jesse Veenstra
Wayne State University,

IMPACT OF CRYOABLATION ON TUMOR IMMUNITY

by

JESSE J. VEENSTRA

DISSERTATION

Submitted to the Graduate School

of Wayne State University,

Detroit, Michigan

in partial fulfillment of the requirements

for the degree of

DOCTOR OF PHILOSOPHY

2013

MAJOR: CANCER BIOLOGY

Approved by:

_____

Advisor Date

_____

_____

_____

_____

_____

ACKNOWLEDGEMENTS

I was fortunate enough to be involved in a project that revolved around one of my great interests, immunology. The work was often challenging and frustrating, but the findings and potential clinical implications have made it a very worthwhile endeavor. This training has provided me with not only a great deal of knowledge, but has helped me develop how I approach any set of problems, which I know will help me become a better clinician in the future. My experience was not only more manageable but remarkably rewarding thanks to the great people around me, and none of the work presented here would have been possible without them.

I would like to thank Dr. Wei for always making time for me and being such a great mentor. She taught me not only how to design and conduct experiments, but more importantly how to think like a true scientist. I was fortunate enough to obtain an F30 fellowship during my time in the lab, which was largely due to Dr. Wei's advice and input. I can list this as one of my greatest accomplishments thanks to her help. She provided a fantastic environment to train in, which I will always be grateful for.

I would also like to thank my committee members: Dr. Stephen Ethier, Dr. David Gorski, Dr. Yi-chi Kong, Dr. Peter Littrup, and Dr. Venuprasad Poojary. It was because of their help and guidance that this project developed into what it is today. I also thank my fellow Wayne State graduate students, in our department as well as others, for providing a fun environment, even in stressful situations. I will fondly look back at my graduate school days thanks to these people.

I would like to give a special thanks to Dr. Heather Gibson and Joyce Reyes, who helped me immensely with conducting experiments. I can't think of how I would have been able to accomplish as much as I was able to without their support. Not only were Heather and Joyce incredibly helpful, but they were great people to be around. I cannot think of better people to work with, and I hope I have the opportunity to work with them again in the future.

Lastly, but certainly not the least, I would like to thank my family for all the support they have provided me over the years. My parents, Jim and Maggie, and my sister, BreeAnn, have helped shape me into the person I am today, and led me into the field of science. I also need to give a special thanks to my wife, Michelle, who has always been there for me even when she has had to work well over 80 hours a week herself. I could not have done all of this without you, and words really can't express how thankful I truly am.

TABLE OF CONTENTS

Acknowledgements……..……....ii

List of Tables……..vi

List of Figures…….……..……....vii

General Introduction……..……1

Materials and Methods……..…...9

Chapter 1: Inflammatory Response to Cryoablation

Abstract…….……...19

Introduction…….…….……21

Results…….....……..…..…25

Discussion…….……..42

Chapter 2: Cryoablation of neu-expressing TUBO Mammary Adenocarcinoma

Abstract…….……...45

Introduction……..…….....47

Results…….…….....……...49

Discussion…….…….……69

Chapter 3: Cryoablation of Her2-expressing D2F2/E2 Mammary Adenocarcinoma

Abstract……..……..……72

Introduction…….……..74

Results……..……..75

Discussion…….....98

General Conclusions…….……..……..…101

Appendix……..104

References…….....106

Abstract……..…126

Autobiographical Statement……..…...128

LIST OF TABLES

Table I PCR Primer Sets ……..…...17

LIST OF FIGURES

Figure 1.1 Tumor cryoablation causes necrosis resulting in polymorphonuclear leukocyte infiltration beginning 1 day post-operatively……..…….....26

Figure 1.2 Fibroblasts and newly synthesized collagen replace necrotic tumor while macrophages clear residual debris……..…..27

Figure 1.3 IL-1β promoter activity is detectable at the healing surgical incision but not the cryoablated tumor *in vivo*..……....29

Figure 1.4 Cryoablation increases IL-1β producing inflammatory infiltrates..……..…….…..30

.

Figure 1.5 CpG ODN stimulation of murine splenocytes..…….…32

Figure 1.6 Flow Cytometry gating strategy..……34

Figure 1.7 Cryoablation and CpG combination therapy elevates DC, NK, and TCR^+ $CD11c^+$ populations in circulation..……...…..36

Figure 1.8 CpG augments endogenous immunity.…….38

Figure 1.9 Cryoablation + CpG elevates DC and TCR^+ $CD11c^+$ populations in circulation……41

Figure 2.1 TUBO mammary adenocarcinoma is sensitive to α-neu Ab..……....50

Figure 2.2 Cryoablation induces transcripts that favor a Th2 environment.……...…52

Figure 2.3 Cryoablation + CpG protects against tumor recurrences..……..54

Figure 2.4 Tumor cryoablation increases protection against TUBO……..……..…….56

Figure 2.5 Tumor cryoablation induces α-neu Ab...…….58

Figure 2.6 Cryoablation primarily induces IgG1 which can be skewed toward IgG2a with the addition of CpG..……..……....60

Figure 2.7 Vaccination with Her2/neu DNA improves α-neu immunity but does not act synergistically with cryoablation..……62

Figure 2.8 Cryoablation does not induce α-neu immunity in NeuT mice.……....64

Figure 2.9 Cryoablation creates a non-conducive environment for vaccine induced immunity in NeuT mice……..……..66

Figure 2.10 CpG does not enhance α-neu immunity in BALB/NeuT mice……..……...68

Figure 3.1 Growth of D2F2/E2 mammary adenocarcinoma induces α-Her2 immunity endogenously……..……76

Figure 3.2 Cryoablation + CpG protects against primary recurrences……..…...78

Figure 3.3 Systemic tumor protection does not occur before resolution of cryoablated tumors ……..……..…81

Figure 3.4 Cryoablation renders systemic protection after resolution of the treated tumor..…….....85

Figure 3.5 Endogenous α-Her2 immunity remains elevated after tumor removal..……88

Figure 3.6 Cryoablation does not diminish systemic α-Her2 immunity induced by D2F2/E2……..…90

Figure 3.7 Addition of CpG to cryoablation reduces transcript levels of key suppressive factors..……....92

Figure 3.8 Cryoablation does not compromise cell-mediated α-Her2 immunity……..…..94

Figure 3.9 Cryoablation does not increase circulating Tregs……..……..97

GENERAL INTRODUCTION

As cancer patients continue to age and accumulate comorbidities they are less able to tolerate aggressive therapies, such as invasive surgery and chemotherapy. Advanced or metastatic cancer also may prohibit surgical resection due to location or extensive invasion. Alternatively, cryoablation, which utilizes freezing temperatures to destroy diseased tissue, has gained increased recognition as an efficient, minimally invasive method of treating solid tumors. The procedure induces necrosis directly by damaging cell membranes and organelles via the formation of ice crystals, and indirectly through osmotic stress and ischemia, resulting from thrombosis of microvasculature (1-4). Cryoablation is an alternative to surgical resection in the treatment of cancers of the breast, prostate, kidney, liver, bone, lung, brain, and skin (5-7). Compared to surgical resection, cryoablation is less damaging to surrounding structures, places less stress on the body, allows for quicker recovery periods, provides improved patient comfort, and is more affordable (8). Importantly, cryoablation allows some patients who are not eligible for traditional surgery, to achieve similar clinical results as surgical resection (8-12). Furthermore, cryoablation promotes the release of tumor-associated antigens from the ablated tumor which have the potential to induce protective tumor-specific immunity (13).

Clinical responses to cryoablation

Systemic anti-tumor effects produced by cryoablation were initially observed in the clinic by Ablin *et al* when they noted spontaneous regression of metastatic lesions following cryoablation of primary prostate tumors in several patients (14, 15). However, this was a rare finding, with only 2 out of 75 treated patients displaying regression of metastatic foci. Based on this finding, Ablin hypothesized that ablation of the tumor resulted in tumor-specific immunity, which was mediated by immune uptake and clearance of the ablated tumor (15). Further support for the concept of 'cryoimmunology' was reported by Blackwood *et al* who performed

palliative cryoablation in patients with advanced cancers and discovered elevated levels of antibodies against DNA, RNA, and tumor cells (16). However, they did not observe any regression of untreated lesions or increased tumor protection. More recently Si *et al* investigated tumor immunity following cryoablation of prostate cancer in 20 patients (17). They observed elevated inflammatory cytokines in sera and increased interferon gamma (IFNγ) secretion in response to stimulation with autologous tumor lysate 4 weeks after cryoablataion, but found the response was transient and unable to prevent disease relapse. Similarly, other cryoablation trials have found a lack of protective immunity (7, 9, 10, 18-26). Although these results have led to increased interest in the immunostimulatory potential of cryoablation, factors leading to clinically beneficial immunity have yet to be elucidated.

Current clinical evidence has supported the use of immune promoting adjuvants with cryoablation to invoke greater tumor-specific immunity. Thakur *et al* evaluated tumor immunity from 6 patients with metastatic renal cell carcinoma (RCC) (27). All patients had lung metastases which were treated with cryoablation in combination with aerosolized granulocyte macrophage colony stimulating factor (GM-CSF), an adjuvant capable of stimulating and expanding leukocytes. T-cell and antibody responses specific to allogeneic RCC lines RC-2 and KCI-18 were elevated in 4 of 6 patients, although the magnitude of increase was not significant. Patients with persistent immune responses were noted to have improved clinical outcomes, however, this referred to the treated metastases only. Growth inhibition or regression of distant tumor foci was not observed, suggesting an ineffective or weak systemic response. Adjuvant modulation of cryoablation induced immunity was also performed by Osada *et al* with the adjuvant krestin (PSK), which is a protein-bound polysaccharide use to promote secretion of tumor necrosis factor alpha (TNFα) (28, 29). Approximately half of patients treated with combination therapy of cryoablation and PSK exhibited an elevated cytokine profile, however no mention of correlating clinical responses were reported. Additionally, pre-clinical studies by Adema and colleagues have used CpG oligodeoxynucleotides (CpG) and saponin based

adjuvants in coordination with cryoablation to dramatically improve magnitude and efficacy of the resulting tumor-specific immune response (30-34).

Although the concept of cryoimmuology is attractive, there has been no clinical benefit consistently observed. Many patients treated with tumor cryoablation suffer from advanced or metastatic cancer, which often leads to compromised host immunity. It may not be feasible for cryoablation treatment alone to induce adequate tumor-specific immunity and overcome immunosuppressive barriers. Additional therapies targeting immunosuppressive effectors, such as T-regulatory cells (Tregs), may be necessary for more consistent immune induction in patients and have shown some activity in pre-clinical studies (31, 35, 36). Although cryoablation may have greater success in treating localized disease, surgical resection will likely remain the initial treatment option until cryoablation produces similar recurrence rates (23, 24, 26, 37, 38). Currently, cryoablation is used primarily in the palliative setting for tumor debulking (i.e. salvage therapy) and pain management, however there is an increasing role for cryoablation in treating single renal masses (39). For palliative care, multiple studies have shown is an effective treatment with a very low complication rate, which improves overall survival and quality of life relative to systemic interventions alone (7, 18, 19, 22, 40).

As technology continues to advance, cryoablation will most likely be utilized for additional treatment applications due to its benefit over other ablation technologies. Unlike other ablation therapies, the ice ball formed during cryoablation is visible on computed tomography, creating a definitive treatment zone that can be manipulated by the operator (41). Other ablation therapies dependent on electrical current (i.e. radiofrequency ablation) are affected by tissue resistance which prevents them from being used in regions with high resistance (i.e. bone and lung), whereas cryoablation has no such limitation (42). Furthermore, patients treated with cryoablation have decreased levels of pain peri- and post-operatively, unlike other ablation therapies that generate intense amounts of heat (18). Additionally, cryoablation is safe to use near major vasculature, preserves the collagenous architecture of the ablated tissues, and

causes less scaring (42). It has also been reported that cryoablation induces significantly greater tumor-specific immunity relative to radiofrequency ablation (RF) in pre-clinical models (31), which may be due denaturation of antigens by RF (43).

Mechanisms of Cryoablation Induced Immunity

Local tissue damage caused by pathogen invasion usually induces the production of pro-inflammatory cytokines from stroma and resident macrophages, which act to upregulate chemotactic and vascular adhesion factors. These factors recruit leukocytes out of circulation to the inflamed region to initiate the innate immune cascade. Granulocytes, monocytes, and natural killer (NK) cells are the first responders and act directly on invading pathogens or perceived threats. Once activated they can produce additional cytokines to further modulate the inflammatory response and recruit additional effectors. Eventually antigen presenting cells (APCs), such as dendritic cells (DCs) and macrophages infiltrate the region to acquire antigen through phagocytosis. APCs initiate adaptive immunity by processing and presenting antigen to T-cells, which account for antigen specific responses. Adaptive immunity can be divided into two major branches, the humoral and cell-mediated responses. Humoral immunity consists of the generation of antigen specific antibody (Ab) or immunoglobulin (Ig) produced by fully differentiated B-cells (plasma cells). Ab acts both directly and indirectly to neutralize and eliminate pathogens and other targets. Cell-mediated responses involve T-cell activation and function. The two main subsets of T-cells include T helper cells (Th / $CD4^+$), which are predominantly responsible for controlling the effector functions of adaptive immunity via cytokine secretion, and cytotoxic T-cells (CTL / $CD8^+$), which directly kill target cells by lysis (i.e. virally infected cells or tumor cells). Another subset of T-cells known as T-regulatory cells (Tregs) can also become activated to serve as a negative regulator. Tregs act to inhibit antigen specific T-cell activity to help maintain a degree of immunologic homeostasis and prevent the development of autoimmunity (44).

Naïve $CD4^+$ T helper cells can be polarized by DCs into two major classes of activated T helper cells, Th1 or Th2, characterized on the basis of their cytokine profiles (45). IFNγ secreting Th1 cells are effective in controlling intracellular bacteria, viruses, and certain tumors by promoting the cytotoxic effector functions of CTLs, NK cells, and macrophages (46-48). Th1 cells also enhance antibody-dependent cell-mediated cytotoxicity (ADCC) through production of IgG2a and IgG1 in mice and humans respectively. Whereas Th2 cells, which secrete interleukin (IL)-4, IL-5 and IL-13, promote humoral immunity via production of IgG1 and IgE in mice and IgG4 and IgE in humans (46). Th2 cells also drive eosinophil mediated elimination of pathogens (i.e. helminthes) and are responsible for the majority of environmental allergies (49). Importantly, Th1 and Th2 cytokines exert reciprocal, inhibitory effects on each other (i.e. IL-12 / IFNγ inhibit IL-4 / IL-13 and vice versa) (50). With regard to cancer immunotherapy, it has been found that Th1 responses are superior in mediating tumoricidal effects relative to Th2 responses, which can even enhance tumor progression (46, 51-54).

DCs activate naïve T helper cells with antigenic and co-stimulatory signals, known as signal 1 (T-cell receptor and MHC II interaction) and 2 (CD28 and B7 interaction) respectively. An additional polarizing signal from the DC is also provided to differentially regulate Th1 and Th2 induction. Induction of Th1 or Th2 biased responses result from two primary mechanisms: pre-commitment of DC toward Th1/Th2 lineages or modulation of DC activation and function to favor one bias over the other (55). DCs and other sentinels of the innate immune system (i.e. macrophages) monitor the surrounding environment using a series of receptors for pathogen-associated molecular patterns (PAMPs) and damaged cell-associated molecular patterns (DAMPs). Signaling through these receptors in combination with other inflammatory mediators, such as cytokines and chemokines, induce variations in DC activation status and functionality, which ultimately determine the DCs propensity to induce type 1 or 2 immune responses (i.e. Th1 or Th2 biased). This model originates from the observation that DCs can change their Th1/Th2 polarizing capabilities in response to different stimuli and environments (56, 57). TNFα,

type 1 interferons (IFNα and IFNβ), and IFNγ are potent inducers of type 1 responses, whereas IL-10, prostaglandin E_2, histamine, and thymic stromal lymphopoietin (TSLP) induce type 2 responses (58). Activated DCs under type 1 conditions produce IL-12 to promote Th1 responses. In contrast, type 2 conditions inhibit IL-12 production and promote IL-10 synthesis, thus favoring a Th2 biased induction (59). If immature DCs acquire antigen but never receive stimuli to mature and express increased co-stimulatory receptors, they take on suppressive characteristics, secreting IL-10 and transforming growth factor beta (TGFβ), which can be directly immunosuppressive and further promote type 2 responses (60). The majority of malignancies induce type 2 promoting conditions in the tumor microenvironment, which can extend to a systemic condition resulting in a Th2 response that supports tumor survival and progression (46). Consequently, one of the paramount challenges in cancer immunotherapy is overcoming tumor-induced immune suppression and creating an environment in which tumor-specific immunotherapy has the greatest probability of success.

Tumor cryoablation produces an inflammatory environment intimately associated with tumor debris, which has the potential to act as an *in situ* tumor-specific vaccine. The resulting immune response induced by tumor cryoablation is determined by several key factors in the microenvironment including the cytokine profile elicited by cryoablation, the amount of antigen released from the tumor, the activation / polarization status of DCs available to acquire antigen, and the recruitment of immune regulatory cells, such as Tregs and myeloid derived suppressor cells (MDSC), which can override immune effector activity (13). The balance of these factors can result in an array of responses, ranging from induction of adaptive anti-tumor immunity to immune suppression. It is also important to consider the degree of necrosis and apoptosis that occurs within the region of cryoablation. Necrotic cells cause an inflammatory response, known as ‘sterile inflammation’, due to the release of ‘danger signals’ which are capable of activating DCs through DAMPs (61, 62). Examples of common endogenous danger signals include heat shock proteins, high mobility group box 1 (HMGB1) DNA, RNA, hyaluronan, IL-1α, and ATP (62,

63). Recent evidence has also implicated actin exposure as the ligand for Clec9A, a DAMP receptor on $CD8\alpha^+$ DCs (mouse Th1 promoting DC) known for potent cross-presentation and antibody responses (64). Although DC activation via Clec9A has not specifically been shown with cryoablation, freeze-thawed cells bind Clec9A (65). While necrotic cells release their contents into the environment, apoptotic cells do not. Several studies have shown that apoptotic cells usually fail to stimulate immune recognition, and may even induce anergic suppression (66, 67), although recent evidence suggests apoptotic cells can be immunostimulatory under certain conditions (68). Therefore, it is important to consider how cell death occurs and what affect it may have on resulting immunity.

Disparity in Cryoimmunology

Although enhanced immune priming after cryoablation has been widely characterized in the pre-clinical setting (31, 32, 34, 69-73), there have been an equivalent number of studies indicating that cryoablation does not elicit any change in tumor-specific immunity (74-76), or worse, induces immune suppression and tumor progression (28, 77-85). Blackwood and Cooper performed cryoablation on immunogenic sarcomas in rats that induced tumor-specific immunity capable of eliminating a second tumor at a distant location. However, they noted regression of the second tumor was very slow or nonexistent if the whole ablated tumor remained *in situ*. Alternatively, if the majority of the ablated tumor was resected and only a small portion remained, regression of the second tumor was faster and absolute (82). Urano et al reported similar findings in BALB/c mice when treating metastatic colon-26 liver nodules generated from a primary tumor in the spleen (28). They found that ablation of a single nodule led to a significant decrease in the number of metastatic nodules present 2 weeks post-operatively. In contrast, ablation of three nodules resulted in an increased number of nodules relative to untreated mice. These results support the notion of an antigenic threshold for inducing

beneficial tumor-specific immunity, with excess antigen inhibiting efficacy of the response, a phenomenon known as high-zone tolerance.

It has also been suggested that cryoablation generates a substantial population of inducible Tregs that inhibit anti-tumor immunity (13, 31, 35, 86-88). In several studies, depletion or inactivation of Tregs in combination with cryoablation led to immune priming and increased tumor protection relative to cryoablation alone, however, a portion of mice remained unprotected, suggesting the presence of additional suppressive factors (31, 35, 36, 86). The inconsistencies in tumor-specific immunity and rejection of distant tumors reflect an inadequate understanding of the mechanisms of immune priming and suppression associated with cryoablation. The discrepancy in findings is, at least in part, due to the wide range of tumor models assessed and their endogenous immunogenicity in respective hosts.

Since cryoablation is an established tool in the clinic, it is important to completely understand the resulting immune response and design strategies to enhance effector mechanisms for controlling tumor recurrences and distant foci. In this project I evaluated cryoablation induced immunity in tumors with known antigens and immunogenicity to test the hypothesis that cryoablation elicits variable levels of tumor protection based on the immunogenicity of the tumor. Both cell-mediated and humoral arms of the immune system were investigated as well as the propensity for Th1 or Th2 biased responses. I also hypothesized that cryoablation induced Th2 biased immunity due to massive levels of tissue inflammation, which can be shifted towards more effective anti-tumor immunity using Th1 promoting adjuvant therapy. The ultimate goal of this project is to elucidate the mechanisms responsible for cryoablation induced immunity, and how they can be therapeutically targeted to produce improved tumor-specific immunity capable of tumor protection.

MATERIALS AND METHODS

Cell culture: All cell lines were maintained *in vitro* in Dulbecco's modified Eagle's medium (DMEM) supplemented with 5% heat-inactivated cosmic calf serum (Hyclone, Logan, UT), 5% heat-inactivated fetal calf serum (Sigma, St. Louis, MO), 10% NCTC 109 medium (Invitrogen, Carlsbad, CA), 2 mM L-glutamine, 0.1 mM MEM non-essential amino acids, 100 units/ml penicillin, and 100 µg/ml streptomycin. All tissue culture reagents were purchased from Invitrogen (Gaithersburg, MD) unless otherwise specified.

Mice: All animal procedures were performed in accordance with the regulation of Wayne State University, Division of Laboratory Animal Resources, following the protocols approved by the Animal Investigation Committee. Six to eight week old BALB/c female mice were purchased from Charles River Laboratory (Frederick, MD). C57BL/6 pIL-1β-DsRed transgenic mice were provided by Akira Takashima (University of Toledo, Toledo, OH). BALB/c pIL-1β-DsRed mice were generated by back-crossing B6 DsRed males with wild-type BALB/c mice. DsRed mice were fed low fluorescent chow to prevent high background levels of fluorescence. Heterozygous BALB/NeuT mice, which express a transforming rat *neu* under the control of the mouse mammary tumor virus promoter, were maintained by breeding with BALB/c mice (89, 90). NeuT females have evidence of atypical ductular hyperplasia in all mammary glands beginning at 3 weeks of age. This hyperplasia progresses to carcinoma *in situ* between 13 and 15 weeks and becomes a palpable tumor between 16 and 18 weeks of age (89-91). Transgene positive mice were identified by PCR.

Cell lines: The neu expressing TUBO mammary adenocarcinoma line was cloned from a spontaneous mammary tumor in a BALB/NeuT female (92). TUBO cells grow progressively in normal BALB/c mice and give rise to tumors which are histologically similar to spontaneous

mammary tumors in NeuT females (91). D2F2 is a mouse mammary tumor cell line derived from a spontaneous mammary tumor that arose in a BALB/c hyperplastic alveolar nodule line D2 (93). D2F2 cells were co-transfected with pRSV2/neo and pCMV/E2, which encodes wild-type human Her2 (94). A stable clone of D2F2/E2 was established and maintained in medium containing 0.6 mg/ml G418 (Geneticin, Invitrogen). To ensure Her2 expression was maintained *in vivo* D2F2/E2 was inoculated subcutaneously into a BALB/c female and allowed to grow for 21 days before the tumor was harvested, dissociated, and the expression of Her2 on the cell surface was verified by flow cytometry.

3T3 Engineered APCs: Antigen presenting cells (APC) 3T3/NKB and 3T3/EKB were generated as previously described (95). Briefly, BALB/c NIH 3T3 cells were transfected with K^d, B7.1, and Her-2 (EKB) or neu (NKB). Stable clones were selected, and maintained in supplemented DMEM (as above) with the addition of 0.6 mg/ml neomycin and 0.6 mg/ml zeocin.

Tumor Inoculation: Mice were inoculated with 2.5 x 10^5 tumor cells in 50 uL of serum free RPMI subcutaneously using a 1 mL syringe and $27^{1/2}$ gauge needle over mammary gland #4 or #9 for primary and rechallenge inoculations respectively. Tumor growth was monitored by palpation and caliper measurement while mice were sedated. Tumor volume was calculated using length and width with the following equation $v = (l \times w^2) / 2$.

DNA Vaccination: DNA vaccination consisted of 50 µg of pGM-CSF and either 50 µg pNeu-$E2_{TM}$ or pVax1 (blank control vector) in a total volume of 50 µL PBS (unless otherwise specified). Vaccination was performed intramuscularly in the left gastrocnemius using a 1mL syringe and $27^{1/2}$ guage needle followed immediately by application of electrode gel and square wave electroporation using a BTX830 (BTX Harvard Apparatus) over the injection site

Surgerical Procedures: Tumors were treated at ~4x7 mm in diameter. Cryoablation was performed using the argon-based CryoCare system with the 1.7mm diameter PERC-15 Percryo CryoProbe – round ice (Endocare). An incision was made along the lateral and medial margins of the tumor and an ellipse of skin was removed directly above the tumor. The tumor was dissected away from the hind limb and retracted from the peritoneal membrane and adjacent skin with a hemostat. The cryoprobe was inserted completely through the center of the tumor and freezing was initiated at 100% power. Each freeze cycle was administered for a full minute followed by the initiation of the thawing cycle, which lasted until the probe could be freed from the tumor (~1 minute). Both freezing and thawing cycles were repeated after the tumor was allowed to return to room temperature. After two freeze-thaw cycles the tumor was placed under the skin and the incision was closed using surgical staples and/or sutures. Sham surgery was identical to cryoablation with the exception of freezing and thawing. Surgical excision was performed using electrocautery, which removed the tumor along with the surrounding mammary tissue.

CpG ODN mu2395: The murine specific class C CpG sequence: 5'-T*C*G*A*C*G*T*T*T*T*C*G*G*C*G*C*G*C*G*C*C*G-3' (Integrated DNA Technologies) was designed by substituting the human hexamer motif (5'-GTCGTT-3') for the optimal mouse motif (5'-GACGTT-3') in the C-Class ODN 2395 (96). 100 µg of CpG was administered peritumorally over 3 injection sites: medial surface of adjacent musculature, caudual and rostral mammary tissue relative to tumor (10 µL/injection).

Splenocyte preparation: Spleens were aseptically harvested from mice in 10% FBS RPMI 1640 medium and dissociated using irradiated frosted glass slides. RBCs were lysed using sterile deionized water and ~ 3 seconds of agitation followed by the addition of an equal volume

of 2x PBS. Splenocytes were cryopreserved in 90% FBS and 5% DMSO and stored at -150°C before ELISPOT or co-culture.

PBMC isolation: Retro-orbital bleeding was performed with heparinized capillary tubes to collect 150 uL of blood into tubes containing heparin (final concentration 0.2 mg/mL). 120 uL of heparinized blood was transferred into 15 mL tubes containing 9 mL DI water. Tubes were inverted several times before 1 mL of 10x PBS was added and mixed. Samples were centrifuged at 400xg for 10 minutes and resuspended in 10% FBS RPMI 1640 medium or flow buffer for further analysis.

TDLN preparation: Tumor draining lymph nodes were aseptically harvested from mice in 10% FBS RPMI 1640 medium and dissociated using two 23 gauge needles to produce a single cell suspension.

Co-culture stimulation: Lymphocyte / splenocyte samples were quantified and assessed for viability using the Cellometer Vision (Nexcelom) cell analysis platform. 3T3 EKB or KB engineered APCs were treated with irradiation or Mitomycin C before being plated in a 24-well plated ($8x10^4$ cells/well). Lymphocyte / splenocyte samples were later added for a final concentration of $1.6x10^6$ cells/mL in a volume of 0.5mL ($8x10^5$ cells/well). Samples were incubated at 37°C 5% CO_2 for 48 hours before supernatents were collected, cleared of debris, and stored at -80°C.

Measurement of tumor specific antibody: Her2 and neu specific IgG levels were quantified via a serum binding assay. Her2 expressing SKOV3 cells or neu-expressing NKB cells were incubated with 50-200x diluted mouse sera for 30 minutes, followed by PE-goat anti-mouse IgG, Fcγ fragment specific (Jackson ImmunoResearch) for 30 minutes. A standard curve for α-Her2

IgG levels was generated using serial dilutions (1000 – 2 ng/mL) of anti-c-ErbB2/c-neu (Ab5, TA-1; Calbiochem) which recognizes an epitope in the extracellular domain of Her2. A similar standard curve for α-neu IgG levels was generated using anti-c-ErbB2/c-neu (Ab4, 7.16.4; Calbiochem) which recognizes an epitope in the extracellular domain of neu. Normal mouse serum was used as a negative control. Flow cytometric analysis was performed with a BD FACSCanto II (Becton Dickinson). Median fluorescent intensity (MFI) for each sample was used to calculate an Ab5 or Ab4 equivalent for Her2 and neu respectively.

Area under the curve analysis for antibody: Area under the curve (AUC) for antibody levels was measured for each mouse using the equation ((Day Y) – (Day X)) x (Ab X + Ab Y) / 2 between two time points where Day Y follows Day X. The sum of the values for all time points makes up the AUC.

IFN γ ELISPOT: Anti-mouse IFNγ (AN-18; eBioscience) 2.5 μg/mL was used to coat a 96-well HTS IP plate (Millipore) overnight at 4°C. Splenocyte samples were suspended in RPMI 1640 medium with a total of $2x10^5$ cells added to each well (final concentration 10^6 splenocytes/mL). To measure Her2 or neu specific responses, $2x10^4$ engineered APCs, EKB, NKB, or KB were also added to the wells. Following incubation, cells were removed and biotinylated anti-mouse IFNγ (R4-6A2; eBioscience) 2 μg/mL was added. Biotinylated Ab was detected using UltraAvidin-HRPO (Leinco) 1 μg/mL. Spots were developed using the AEC substrate kit (BD Pharmingen) and enumerated with the ImmunoSpot analyzer (CTL). Results were expressed as number of cytokine producing cells per 10^6 cells.

Flow cytometry analysis: Approximately $2x10^6$ PBMC or lymphocytes were incubated for 15 min on ice in flow buffer (0.25% FBS in 1x PBS) with anti-mouse CD16/CD32 (2.4G2) (BD Pharmingen) to block Fc receptors. Cells were subsequently stained with the eFluor 780 viability

dye (eBioscience) and the following: α-CD4 (GK1.5), α-CD8α (53-6.7), α-CD19 (1D3), α-CD25 (PC61;Biolegend), α-TCRβ (H57-597), α-CD11c (N418), α-CD11b (M1/70), α-CD49b (DX5), and α-Ly6G (RB6-8C5). All antibodies from eBioscience unless otherwise indicated. For intracellular staining of Foxp3, cells were surface labeled with α-CD4 and α-CD-25, fixed, permeabilized with Fixation/Permeabilization buffer (eBioscience), and washed with a 1X Permeabilzation buffer (eBioscience) before 30 minute incubation with α-Foxp3 (FJK-16s). All samples were washed 2x in flow buffer before analyzed using a BD FACSCanto II cytometer (Becton Dickinson) and FlowJo software (Tree Star). All populations enumerated as percentage of viable singlets.

Protein Multiplexing: Cell culture supernatant or serum/plasma samples were diluted 2 fold for quantification. The Cytokine Mouse Magnetic 10-Plex or 20-Plex kits (Life Technologies) were used with the Magpix platform (Luminex) to quantify the following proteins: FGF basic, GM-CSF, IFNγ, IL-1α, IL-1β, IL-2, IL-4, IL-5, IL-6, IL-10, IL-13, IL-12 (p40/p70), IL-17, IP-10, KC, MCP-1, MIG, MIP-1α, TNF-α, and VEGF. The assay was performed according to the manufacturer's instructions.

TGFβ ELISA: NUNC Maxisorp 96-well plates were coated with rat anti-mouse TGFβ (BD Pharmingen) (4 μg/mL) diluted in bicarbonate buffer and incubated at 4˚C overnight. The following day the plate was washed 5x with wash buffer (0.05% Tween-20 in 1x PBS) before blocking the plate using blocking buffer (0.5% BSA in wash) for 2 hours at room temperature. In a separate 96-well plate, 100 μL of sample was added to each well. To activate latent TGFβ to the immunoreactive form, samples must be acidified, and then neutralized. Briefly, 20 μL of 1N HCl was added to each well, followed 10 minutes later by 20 uL of 1N NaOH. 100 μL of each sample was transferred to the TGFβ coated plate and incubated at 4˚C overnight. The following day the plate was washed 5x before adding biotinylated rat anti-mouse TGFβ (BD Pharmingen)

(2 μg/mL) diluted in blocking buffer. The plate was incubated for 1 hour at room temperature and washed 5x. UltraAvidin-HRPO (Leinco) (1 μg/mL) diluted in blocking buffer was added to the plate and incubated for 30 minutes at room temperature. The plate was washed 6x before TMB substrate (BD OptEIA) was added for colorimetric development. Substrate development was stopped by adding an equal volume of 1M sulfuric acid. Absorbance was read on the Synergy 2 plate reader (BioTek) at 450 and 570 nm, with wavelength subtraction (450-570).

Histology: Tumor samples were collected and placed in 10% buffered formalin. Slide preparation and staining were performed by the histology core. Images were collected using the SCN400 slide scanner (Leica Microsystems).

***In vivo* Imaging**: DsRed IL-1β mice were anesthetized and imaged in the In-Vivo MS FX PRO (Carestream). Fluorescent spectra were collected for 30 seconds, which were merged with white light images.

RNA isolation: Total RNA was isolated from cells using TRIzol (Invitrogen) as recommended by the manufacturer. Briefly, up to 10^7 cells were lysed in 1 mL TRIzol and incubated at room temperature for 5 minutes. 200 μL chloroform was added followed by vigorous shaking for 15 seconds. Samples were centrifuged for 15 minutes at 12 kRPM at 4^{o}C and the aqueous layer was transferred to a new tube. The RNA was precipitated by addition of 600 μL isopropanol, thorough mixing and incubation at room temperature for 10 minutes. The RNA was pelleted by centrifugation at 12 kRPM at 4^{o}C for 10 minutes followed by washing with 70% DEPC ethanol. Samples were resuspended in 15 μL DEPC water and heated to 55^{o}C for 5 minutes prior to quantification by absorption at 260 and 280 nm.

First strand cDNA synthesis: Reverse transcription was performed with up to 4 µg total RNA using ProtoScript first stand cDNA synthesis kit (New England Biolabs). Briefly, 1 µg of RNA was diluted to 3 µL with nuclease-free water and combined with 1 µL of oligo dT and incubated at 70^{o}C for 5 min after which the samples were placed on ice. 5 µL of M-MuLV reaction mix was distributed to each sample, followed by 1 µL of M-MuLV enzyme mix. Samples were incubated at 42^{o}C for 1 hour followed by 5 minutes at 70^{o}C to deactivate the enzyme. The volume was then increased to 50 µL per µg RNA initially added and samples were stored at -20^{o}C until use.

Quantitative real-time PCR (qPCR): Quantitative PCR was performed with the equivalent of 10 ng RNA per cDNA sample using iTaq Universal SYBR Green Supermix (BioRad) per manufacturer recommendations. Samples were run on a StepOnePlus real-time PCR system (Applied Biosystems). Primers were used at a final concentration of 500 nM and sequences are listed in Table I. Analysis for relative gene expression was performed using the $2^{-\Delta\Delta CT}$ method (97). The expression of each gene in each sample was performed in duplicates and the level was normalized relative to B2-microglobulin (B2M).

Statistical analysis: Statistical analyses were conducted using GraphPad Prism 6. Error bars shown represent SEM unless otherwise noted. Survival percentages were calculated using the Kaplan-Meier method (98). *P* values less than 0.05, 0.01, and 0.001 were noted as *, **, and ***, respectively.

Name	Geme	RefSeq# (Fwd / Rev)	Primer (5'->3')
β2 microglobulin	B2M	F	CCTGGTCTTTCTGGTGCTTG
		R	TTCAGTATGTTCGGCTTCCC
Monocyte chemotactic protein-1	CCL2	NM_011333.3_F	AGTAGGCTGGAGAGCTACAAGAGG
		NM_011333.3_R	AAACTACAGCTTCTTTGGGACACC
CCL5 (RANTES)	CCL5	NM_013653.3_F	GCTCCAATCTTGCAGTCGTGTTTG
		NM_013653.3_R	TCTCTGGGTTGGCACACACTTG
Trans-acting T-cell-specific transcription factor GATA-3	GATA3	F	AGGATGTCCCTGCTCTCCTT
		R	GCCTGCGGACTCTACCATAA
Granulocyte colony-stimulating factor	Csf3	NM_009971.1_F	TGCAGCAGACACAGTGCCTAAG
		NM_009971.1_R	GGTGGCAAAGTTGGCAACATCC
Forkhead box P3	Foxp3	F	TCCAAGTCTCGTCTGAAGGC
		R	GCGAAAGTGGCAGAGAGGTA
histidine decarboxylase	Hdc	NM_008230.5_F	AGCCACGGACTTCATGCATTGG
		NM_008230.5_R	AGGACCGAATCACAAACCACAGC
Interleukin 4	IL-4	F	CGAGCTCACTCTCTGTGGTG
		R	TGAACGAGGTCACAGGAGAA
Interleukin 5	IL5	NM_010558.1_F	GGTGAAAGAGACCTTGACACAGC
		NM_010558.1_R	AGCCTCATCGTCTCATTGCTTG
Interleukin 6	IL6	NM_031168.1_F	TCCTCTCTGCAAGAGACTTCCATC
		NM_031168.1_R	TGGTTGTCACCAGCATCAGTCC
Interleukin 10	IL10	F	CCCTGGGTGAGAAGCTGAAG
		R	CACTGCCTTGCTCTTATTTTCACA
Interleukin 13	IL13	NM_008355.3_F	AACGGCAGCATGGTATGGAGTG
		NM_008355.3_R	AATCCAGGGCTACACAGAACCC
Interleukin 17A	IL17A	NM_010552.3_F	TCCAGGGAGAGCTTCATCTGTGTC
		NM_010552.3_R	TTGGACACGCTGAGCTTTGAGG
Interferon gamma	INFγ	F	GCGTCATTGAATCACACCT
		R	GAGCTCATTGAATGCTTGGC
Interferon-induced 17 kDa protein	Isg15	F	AGCAATGGCCTGGGACCTAAAG
		R	AGTCACGGACACCAGGAAATCG
2'-5'-oligoadenylate synthetase 1	OAS1	NM_011852.2_F	AGCCTTTGATGTCCTGGGTCATGG
		NM_011852.2_R	AAGCAGGTAGAGAACTCGCCATCC
2'-5'-oligoadenylate synthetase 2	Oas2	NM_145227.3_F	TGAAAGTGTCGAGTTCGATGTCC
		NM_145227.3_R	TCAGACCGCAGTTGACCTAGTG
Prostaglandin E synthase	Ptges	NM_022415.3_F	TCTCCTGGCTGCAAATCTGGAC
		NM_022415.3_R	ACAGTGCTTTGCTCTGTGCTGTG
RAR-related orphan receptor gamma T	RORγT	F	CCGCTGAGAGGGCTTCAC
		R	TGCAGGAGTAGGCCACATTACA
T-box transcription factor 21	Tbet	F	GTGAAGGACAGGAATGGGAA
		R	GGTGTCTGGGAAGCTGAGAG
Transforming Growth Factor beta	Tgfb1	NM_011577.1_F	TGACGTCACTGGAGTTGTACGG
		NM_011577.1_R	TCGAAAGCCCTGTATTCCGTCTC

Tumor necrosis factor alpha	TNFα	F	ATGAGAGGGAGGCCATTTG
		R	CAGCCTCTTCTCATTCCTGC
OX40L	Tnfsf4	NM_009452.2_F	GGCAAAGGACCCTCCAATCCAAAG
		NM_009452.2_R	AGTTGCCCATCCTCACATCTGG
Thymic stromal lymphopoietin	TSLP	NM_021367.2_F	ATCGAGGACTGTGAGAGCAAGC
		NM_021367.2_R	TCTCTTGTTCTCCGGGCAAATG

Table I. PCR Primer Sets

CHAPTER 1

Inflammatory Response to Cryoablation

ABSTRACT

Cryoablation causes mechanical destruction and ischemia of the treated tumor which triggers mobilization of the innate immune system to clear the necrotic tissue. Polymorphonucleocytes (PMNs) are one of the first cells to arrive and infiltrate the necrotic tumor, followed by macrophages and lymphocytes replacing them several days thereafter. Because cryoablation causes necrosis primarily by membrane disruption, dying cells spill a portion of their intracellular contents into the surrounding environment. Some of these components are danger signals which elicit additional immune activation and have the potential to induce adaptive immunity. Here we analyze the progression of the innate immune cascade in response to tumor cryoablation.

Histological examination of ablated tumors found PMNs infiltrating the tissue by 1 day post-operatively, which dissipated by day 3. New leukocytic infiltration at the peripheral margins of the tumor was also observed at this time. Macrophages and fibroblasts were seen throughout the entirety of tumor by day 9, with increasing numbers seen as the tissue continued to heal. To observe inflammatory infiltrates *in vivo*, fluorescent imaging monitoring the activity of the IL-1β promoter was analyzed in pIL-1β-DsRed transgenic mice. DsRed fluorescence was observed at the surgical incision, indicative of IL-1β activation during wound healing, but could not be detected within sham or cryoablated treated tumors *in vivo*. However, when tumors were harvested from mice and imaged *ex vivo*, DsRed fluorescence was found to be significantly increased in mice treated with cryoablation relative to sham surgery, indicating infiltration of IL-1β producing inflammatory leukocytes.

In preparation for adding adjuvant stimulation during cryoablation, the activity of human and mouse specific class B and C CpG oligodeoxynucleotides (CpG) were evaluated *in vitro* with murine splenocytes. Surface expression of MHCII, CD80, and CD54 were elevated with all CpG treatments. Additionally, quantitative transcript analysis found elevated levels of interferon induced transcripts (i.e. *Isg15*, *Oas1*, and *Oas2*) with human and mouse specific CpGs, suggesting both CpGs have similar stimulatory capacity in mice. *In vivo*, treatment with CpG elevated levels of IL-1β, IL-2, IL-6, IL-12, IFNγ, and TNFα in tumor draining lymph nodes (TDLN) and plasma 2 days post-operatively, indicative of Th1 biased responses. Dendritic cell (DC) and natural killer (NK) cell populations were also significantly increased by CpG treatment, further demonstrating the immune stimulatory activity of CpG.

INTRODUCTION

Following cryoablation, the tissue can be divided into two approximate zones, a central and peripheral zone. The central zone comprises the core of the frozen tissue and results in complete coagulative necrosis, while the peripheral zone contains both necrotic and apoptotic cells (99). The formation of intracellular ice crystals results in mechanical trauma to cellular structures, whereas extracellular ice formation draws water away from pericellular spaces, effectively creating an osmotic gradient that further stresses membranes and organelles (100, 101). The formation of extracellular crystals also causes additional mechanical trauma which becomes pronounced with increased freezing. After freezing has been completed, thawing of frozen tissues leads to reduced extracellular osmolarity via melting ice, promoting lysis of already fragile cells (102). Additionally, repeated freeze-thaw cycles dramatically increase cellular death leading to more complete ablation. The subsequent damage to the endothelium in the vasculature feeding the ablated area results in thrombus formation resulting in increased ischemia, leading to further cell death (101). After thawing is complete, reactive hypereamia and increased vascular permeability lead to tissue congestion and edema. The process of wound repair begins at the margins of the treated area where neutrophils initially invade (102-104). Over the following months the necrotic tissue is eventually cleared by macrophages and replaced with fibroblasts and newly formed collagen (101).

Cytokines in the interleukin (IL)-1 family function as powerful mediators and regulators of inflammatory responses to pathogens and tissue injury. Of the eleven members in this family, IL-1β is the most well characterized. On exposure to pathological stimuli, IL-1β is produced by activated leukocytes such as neutrophils, monocytes, macrophages, and dendritic cells (DCs), leading to induction and promotion of additional inflammatory responses (105). Thus IL-1β promoter activity can be used as an indicator of inflammatory infiltrates and their migration into tissues (106).

Sentinels of the innate immune system, such as DCs and macrophages, can be activated by pathogen-associated molecular patterns (PAMPs) which are expressed and produced by a variety of infectious agents. The activated innate effectors function to limit proliferation and spread of infectious organisms until the host can mount an adaptive immune response against the pathogen. Recognition of PAMPs is accomplished by members of the Toll-like family of receptors (TLRs), which form homo- or hetero-dimers (107). Signaling through most members of the TLR family results in activation of multiple transcription factors (i.e. NF-κB, AP1, CEBP, and CREB), which directly upregulate inflammatory cytokine and chemokine gene expression (108). A major PAMP recognized by the immune system is bacterial DNA. Differences in the methylation status of cytosine – guanine dinucleotides (CpG) results in a much greater frequency of unmethylated CpG motifs in prokaryote DNA relative to eukaryote DNA (108). The innate immune system can discriminate against these differences and detect unmethylated CpG motifs using TLR9, which is expressed intracellularly, within the endosomal compartment (109). TLR9 molecules between species have diverged from one another as each species has dealt with its own complement of pathogens. Thus, the optimal sequence motifs for stimulating immune activation in one species (e.g. mice) may differ from those that are optimal for another species (e.g. humans) (110). The optimal human hexamer motif (5'-GTCGTT-3') differs from the optimal mouse motif (5'-GACGTT-3') by changing a thymine to an adenine near the 5' end (96). Plasmacytoid dendritic cells and B-cells are the primary cell types that express TLR9, although mice have additional expression on monocytes, macrophages, and myeloid dendritic cells (108). Activation of these cells by CpG initiates stimulatory pathways that results in the indirect maturation, differentiation, and expansion of additional DCs, T-cells, NK cells, and macrophages (111-114). These cells subsequently secrete cytokines that generate a pro-inflammatory (i.e. IL-1β, IL-6, IL-18, and TNFα) and strongly Th1 biased (IFNγ and IL-12) environment (114, 115). These type 1 immune promoting conditions enhance cytotoxic T-cell

responses and inhibit Th2 mediated suppression, which is associated with the most efficacious anti-tumor immunity (46).

Synthetic oligodeoxynucleotides (ODNs) containing similar CpG motifs to those found in bacterial DNA bind to TLR9 and produce comparable immune activation (96, 116-118). However, synthetic ODN differ from bacterial DNA in that they have a partially or completely phosphorothioated backbone instead of a phosphodiester backbone, as well as a poly G tail at the 3' end, 5' end, or both. The phophorothioated modification protects the ODN from being degraded by nucleases in the body, while the poly G tail enhances cellular uptake (119). Sequences with variations in the number and location of CpG dimers, as well the base sequences flanking the CpG motif, have been shown to activate TLR9 to elicit variable immune stimulation (96). Three major classes of synthetic CpG ODNs have currently been described (A,B, and C) (108, 120). Class A CpG ODN utilize a mixed phosphodiester-phosphorothioate backbone and contain a single hexameric purine– pyrimidine–CG–purine–pyrimidine motif flanked by self-complementary bases, resulting in a palindromic sequence. Class A ODN primarily induce secretion of IFNα from plasmacytoid DCs, which supports maturation of other DCs (121). Class B CpG ODN use a fully phosphorothioated backbone and largely activate B-cells but also stimulate DC maturation, although to a lesser extent than class A CpG ODN (122). Class C CpG ODN, like class B, also use a fully phosphorothioated backbone. A portion of the class C sequence also contains a palindrome, similar to the structure observed in class A ODNs. Appropriately, Class C ODN are capable of stimulating both plasmacytoid DCs and B-cells equally well, making them the most versatile of the three classes (120).

CpG ODNs have been used in more than 50 clinical trials, many of which are phase I studies designed to investigate safety and immunomulatory properties of CpG in combination with vaccines, monoclonal antibodies, or allergens (108). Multiple phase II studies are currently underway to evaluate CpG activity in the treatment of cancer, allergy and asthma, or as a vaccine adjuvant. Interestingly, a phase II trial using local irradiation in combination with

intratumoral CpG injection to treat B-cell lymphoma resulted in one complete response and three partial responses out of twenty patients, which was mediated by cytotoxic T-cell (123). These results suggest that *in situ* tumor vaccination achieved with local tumor ablation modalities can provide improved clinical outcomes when combined with CpG.

RESULTS

Tumor cryoablation causes necrosis resulting in inflammatory infiltration and subsequent fibroblast expansion. To evaluate the innate immune response to cryoablation we examined hematoxylin and eosin (H&E) stained tumor sections post-operatively. The vast majority of ablated tumors underwent complete coagulative necrosis evident by the lack of nuclear staining (Figure1.1). Cryoablation also caused marked disruption in cellular architecture unlike other common causes of coagultive necrosis (e.g. ischemia), which provides evidence of the resulting mechanical damage due to ice formation. One day after cryoablation, polymorphonucleocytes (PMNs) were observed largely in the peripheral regions of the tumor and perivascular areas (Figure1.1). Consistent with the classical wound healing cascade, the majority of PMNs were no longer present by the third day after cryoablation (124). By 6 days post-operatively a definitive band of infiltrates could be seen around the entire periphery of the tumor (Figure1.2). Deeper infiltrates were seen in the tumor at 9 days, which appeared to be predominantly macrophages and fibroblasts. Over the next 6 weeks fibroblasts continued to proliferate and produce collagen, eventually forming the majority of the remaining tissue. Accumulation of hemosiderin, an iron storage complex, was also observed in macrophages, suggestive of previous tissue hemorrhage and subsequent red blood cell phagocytosis (Figure1.2 arrow).

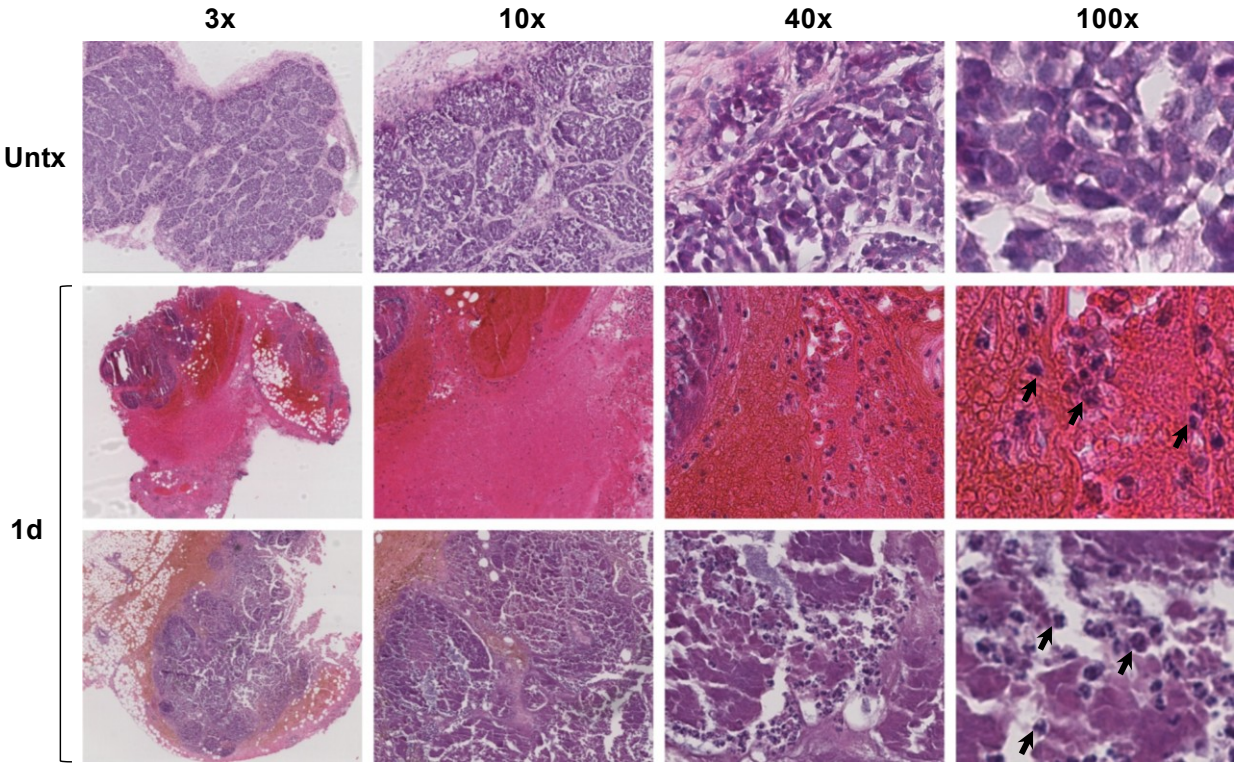

Figure 1.1. Tumor cryoablation causes necrosis resulting in polymorphonuclear leukocyte infiltration beginning 1 day post-operatively. BALB/c mice were inoculated with $2.5x10^5$ cells of TUBO mammary adenocarcinoma, which grew to ~4x7mm before undergoing treatment with cryoablation. Mice were euthanized 1 day post-operatively to harvest ablated tumors (n=2). Tissues were fixed, sectioned, and stained with H&E. Images collected at 3, 10, 40 and 100x magnification. Untreated (Untx) tumor was collected for reference (top). Cryoablation produced coagulative necrosis, with no evidence of viable tumor cells remaining. Numerous polymorphonucleocytes were observed infiltrating along regions of necrotic tumor (arrows).

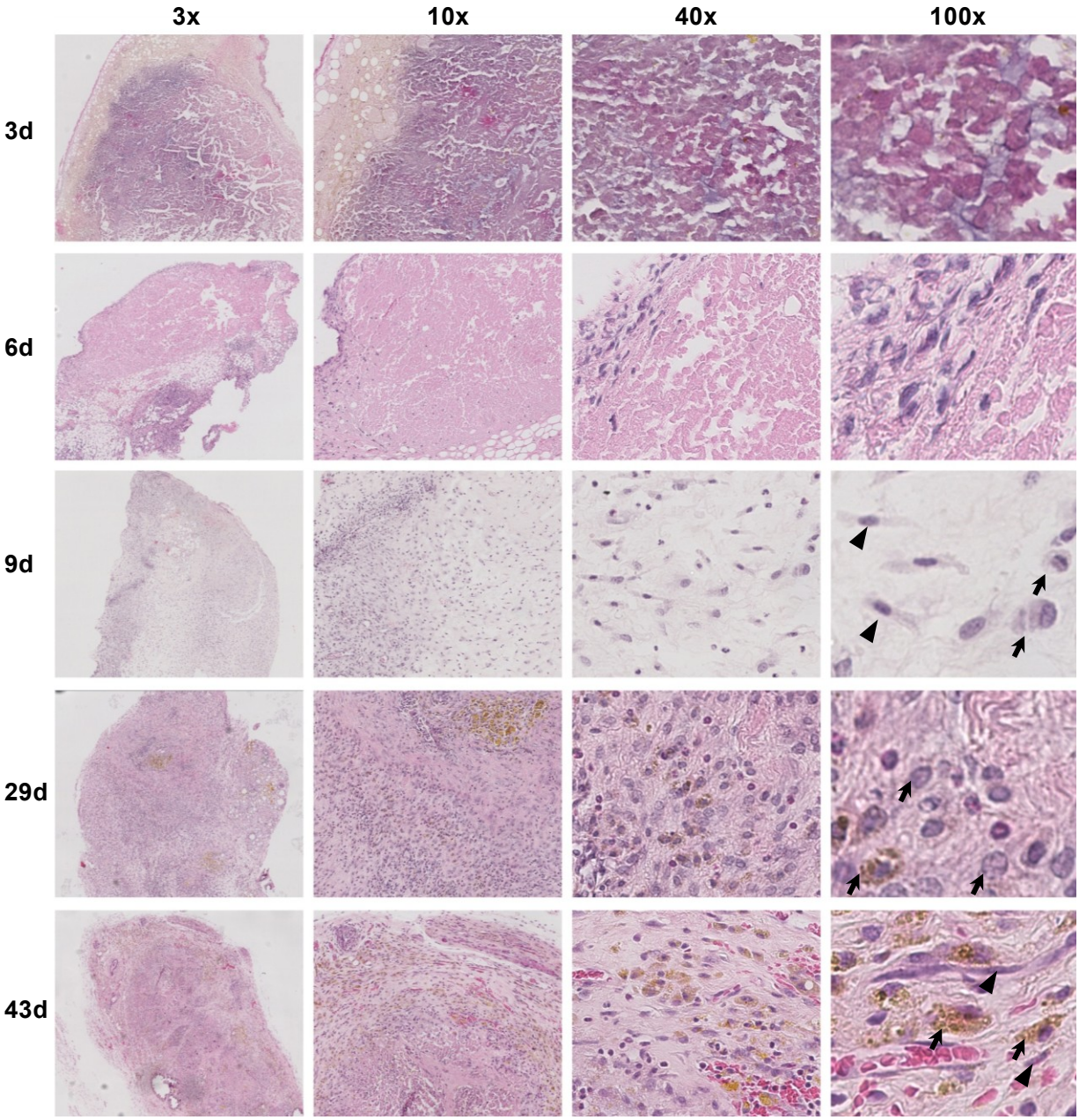

Figure 1.2. Fibroblasts and newly synthesized collagen replace necrotic tumor while macrophages clear residual debris. Mice were euthanized 3, 6, 9, 29, and 43 days post-operatively to harvest ablated tumors. Tissues were fixed, sectioned, and stained with H&E. Images collected at 3, 10, 40 and 100x magnification. By day 3 the majority of Polymorphonuclear leukocytes were no longer present. By day 6 a definitive border of infiltrates was observed around the peripheral edge of the tumor with small numbers of cells penetrating further into the tissue. Large numbers of macrophages (arrows), fibroblasts (arrow heads), and other infiltrates could be seen throughout the entire tumor by day 9. Increased numbers of fibroblasts and new collagen deposition were observed between 29 and 43 days. Hemosiderin accumulation in macrophages was also evident. Representative images for each time point are shown.

Cryoablation increases IL-1β promoter activity within the tumor. To evaluate infiltration of IL-1β producing inflammatory cells *in vivo*, fluorescent imaging monitoring the activity of the IL-1β promoter was analyzed in BALB/c pIL-1β-DsRed transgenic mice, which utilize the IL-1β promoter to drive expression of the fluorescent marker gene, DsRed. pIL-1β-DsRed mice were inoculated with $2.5x10^5$ cells of D2F2/E2 mammary adenocarcinoma, which grew to ~4x7mm before undergoing treatment with cryoablation or sham surgery. Mice were imaged pre-operatively and 4 hours post-operatively, with no detectable fluorescence observed. DsRed fluorescence was detected at the surgical incision site 20 hours post-operatively and remained elevated for 8 days (Figure1.3). By the twelfth day fluorescence was no longer detectable at any location. Surprisingly, no fluorescence specific to cryoablated or sham treated tumors was observed at any time point, suggesting DsRed fluorescence may not be detectable through intact skin.

To confirm these suspicions, mice were imaged 15 days post-operatively and euthanized (Figure1.4A). Tumors from sham and cryoablation treated mice were harvested and cut into representative slices for imaging (Figure1.4B-C). A whole spleen from a cryoablation treated mouse was also collected to serve as a control. *Ex vivo* imaging revealed that cryoablation treated tumors had significantly greater DsRed fluorescence relative to sham treated tumors (Figure1.4D-E). This finding provides direct evidence of significant inflammatory infiltration into ablated tumors, consistent with the infiltration observed in histological analysis.

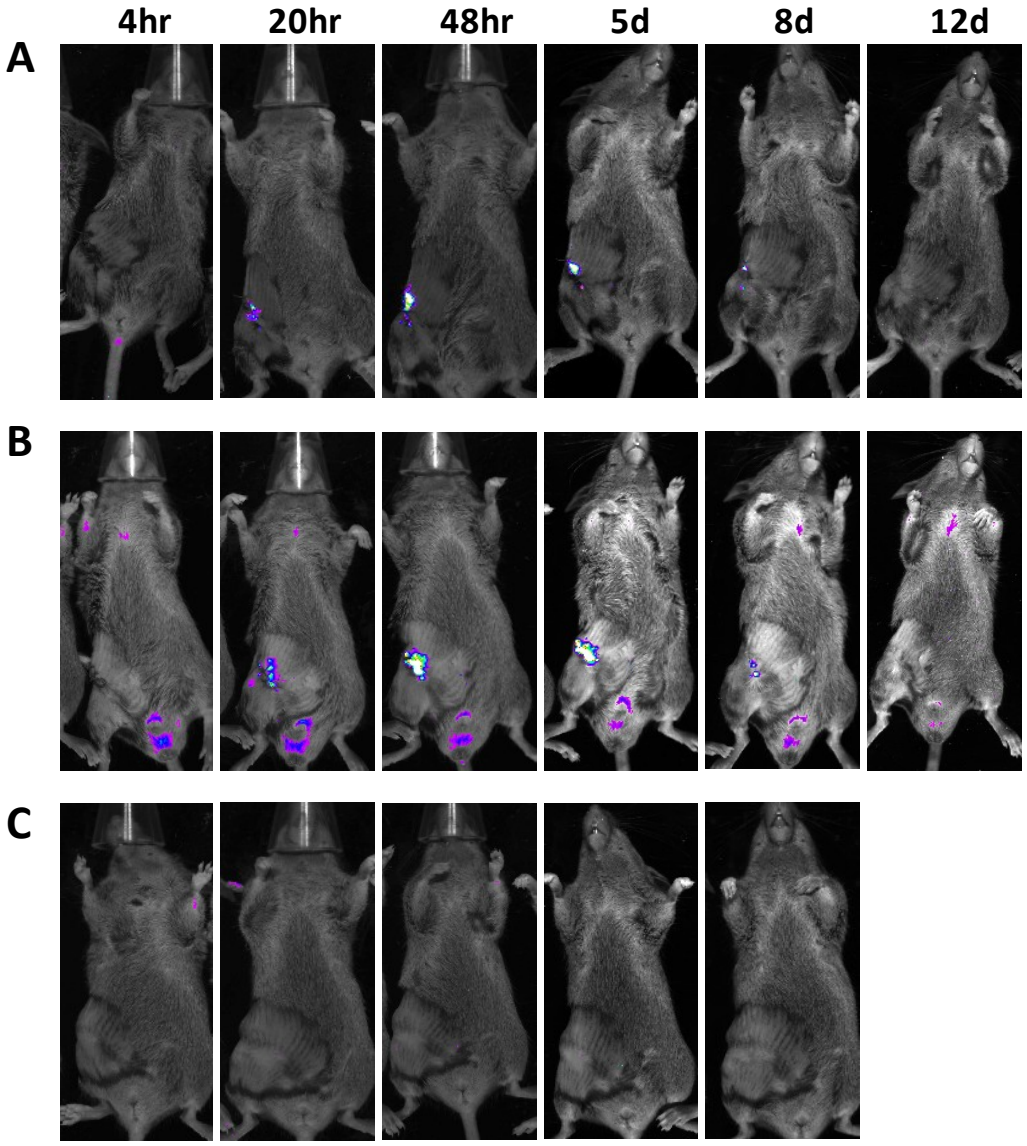

Figure 1.3. IL-1β promoter activity is detectable at the healing surgical incision but not the cryoablated tumor *in vivo*. BALB/c pIL-1β-DsRed transgenic mice were inoculated with $2.5x10^5$ cells of D2F2/E2 mammary adenocarcinoma, which grew to ~4x7mm before undergoing treatment with cryoablation or sham surgery (n=2). Mice were treated with (A) cryoablation, (B) sham surgery, or (C) left untreated. Mice were imaged post-operatively at indicated time points. Representative images shown.

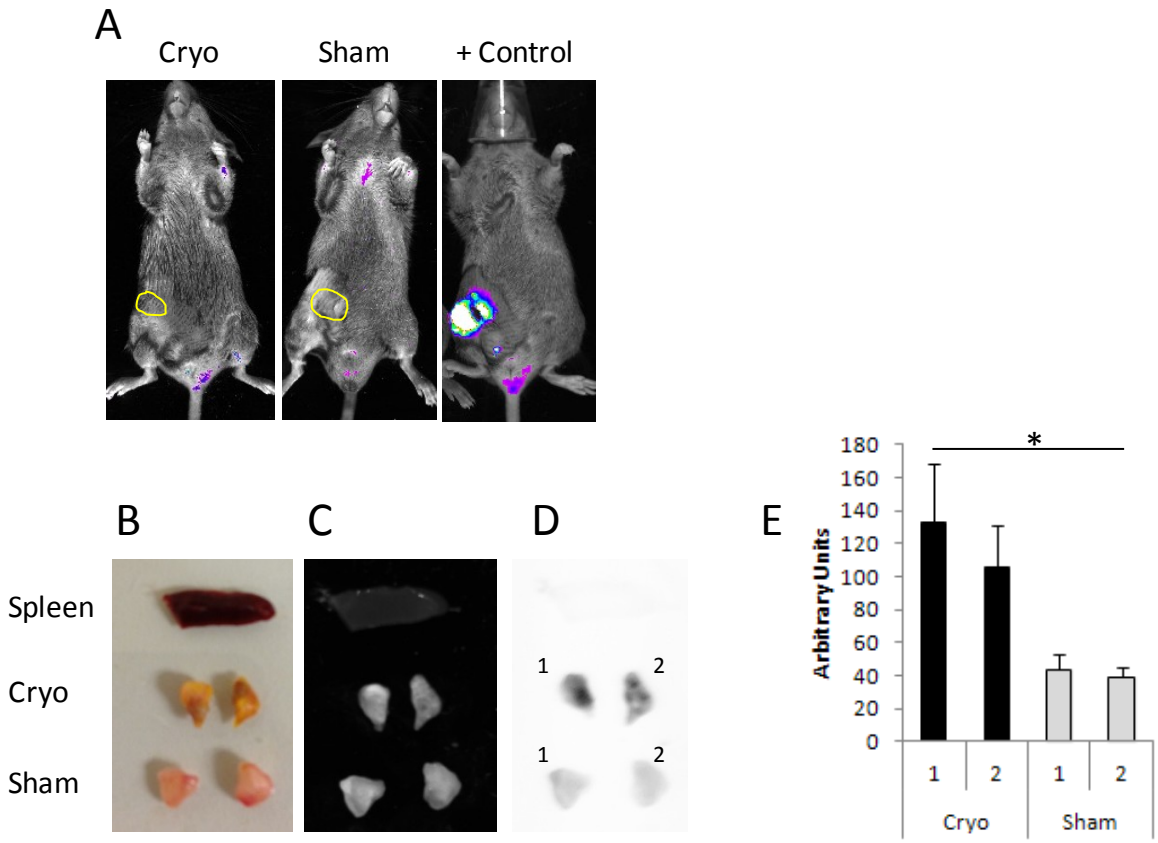

Figure 1.4. Cryoablation increases IL-1β producing inflammatory infiltrates. (A) Fifteen days post-operatively mice were imaged for DsRed fluorescence and euthanized (approximate border of the tumor outlined in yellow). A mouse with an open incision at 20 hours post-operatively was used as a positive control. Tumors were harvested, representative portions cut to equivalent sizes (1 and 2), and imaged with the following channels (B) Color (C) Grey scale (D) inverted DsRed fluorescence. The spleen from the cryoablation treated mouse was used as a control tissue. (E) Average DsRed fluorescent intensity and standard deviation of each tumor slice quantified using ImageJ densitometry software. *P<0.05 Unpaired t-test using means of slices.

CpG ODN stimulation of murine splenocytes. Human and mouse specific class B and C CpG ODN were assessed for immunostimulatory activity with mouse splenocytes. A mouse specific CpG ODN (mu2395) was constructed by substituting the human hexamer motif (5'-GTCGTT-3') for the optimal mouse motif (5'-GACGTT-3') in the class C ODN 2395 (96). We also evaluated human specific ODN 2006, which is a class B CpG, similar to the CpG ODNs currently used in clinical trials (125). Freshly isolated mouse splenocytes ($2x10^6$ cells/mL) were treated with 1μM of CpG ODN 2006, 2395 or mu2395 for 24 hours in 10% FBS RPMI. Surface expression of MHCII, CD80 (B7.1), and CD54 (ICAM-1) were quantified on viable cells using flow cytometry (Figure1.5A-B). The expression of these markers were similarly elevated with all CpG treatments, indicating equivalent efficacy with each CpG ODN. RNA was also isolated from CpG 2395 and mu2395 treated splenocytes for subsequent transcript analysis. Transcript levels of interferon inducible targets (*Isg15*, *Oas1*, and *Oas2*), TNFα and IL-6 were elevated to comparable levels relative to untreated splenocytes, suggesting both CpG ODNs have similar capability to stimulate DCs and B-cells in the mouse (Figure1.5C). These results indicate CpG ODN 2395 and mu2395 elicit similar immunostimulatory effects in murine splenocytes.

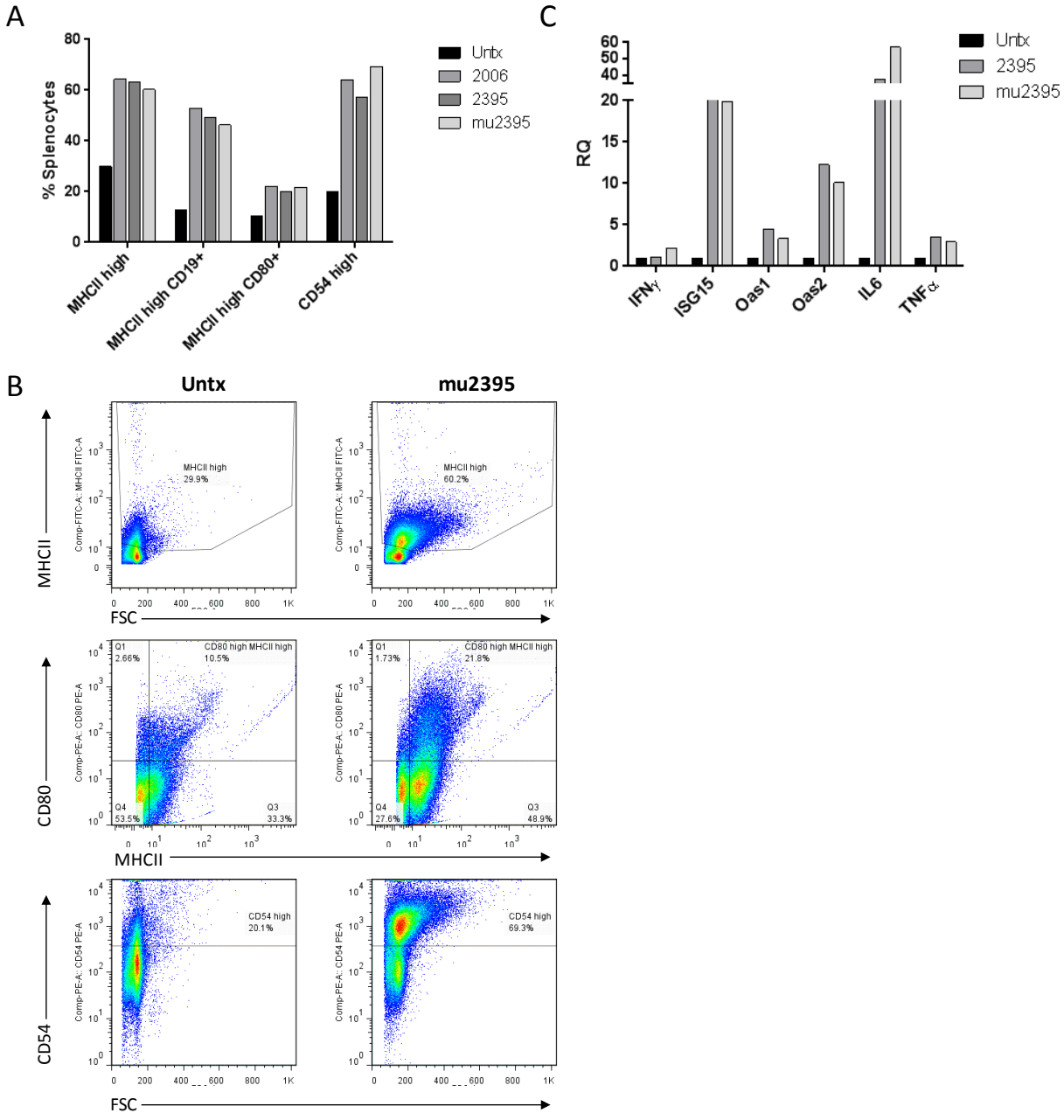

Figure 1.5. CpG ODN stimulation of murine splenocytes. Splenocytes (2x10^6 cells/mL) were treated with 1μM of CpG ODN 2006, 2395 or mu2395 for 24 hours in 10% FBS RPMI. Cells were collected for (A) flow cytometry and (C) RNA isolation and subsequent transcript analysis via qPCR. Transcript levels expressed as quantity relative to untreated splenocytes (RQ). (B) Representative dot plots and gating strategy of untreated and CpG ODN mu2395 treated splenocytes for surface expression of MHC II, CD80, CD19, and CD54.

Analysis of immune populations by flow cytometry. Total PBMC or lymphocytes were acquired and gated on viable singlets. T-cells were initially gated on $TCR\beta^{+}$ $CD11c^{-}$ cells and subsequently gated on CD4 and CD8α (Figure1.6). Dendritic cells (DC) were identified as $TCR\beta^{-}$ $CD11c^{+}$ cells, and natural killer (NK) cells were identified $CD49b^{+}$ $TCR\beta^{-}$ cells. An additional population of $TCR\beta^{+}$ $CD11c^{+}$ cells was also noted.

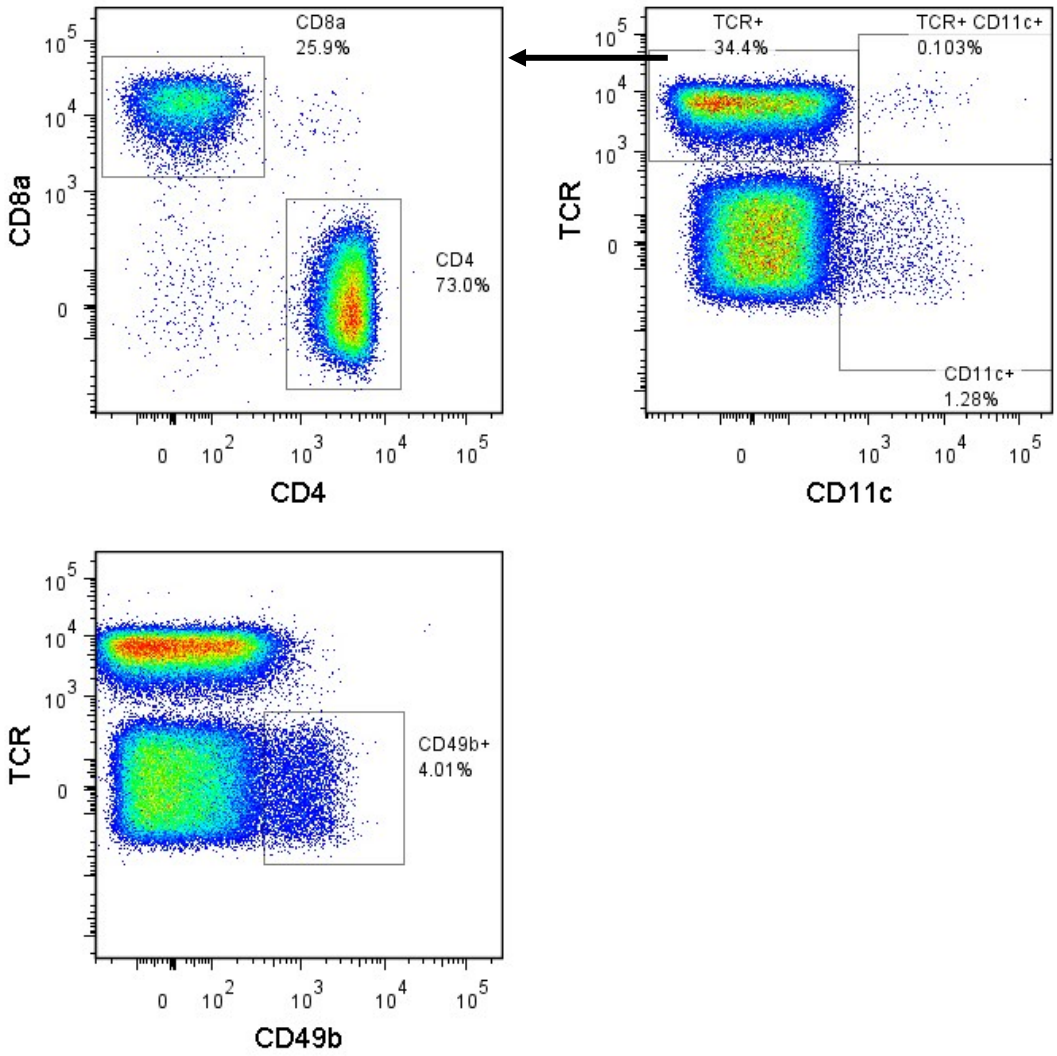

Figure 1.6. Flow Cytometry gating strategy. Total PBMCs or lymphocytes were acquired and gated on viable singlets. $CD4^+$ and $CD8^+$ T-cells were initially gated on $TCR\beta^+$ $CD11c^-$ cells. Dendritic cells were identified as $TCR\beta^-$ $CD11c^+$ cells. Natural Killer (NK) cells were identified as $CD49b^+$ $TCR\beta^-$ cells.

Cryoablation and CpG combination therapy rapidly elevate DC and NK populations in circulation. Fifteen days after inoculation, D2F2/E2 mammary adenocarcinomas (~4x7mm) were treated with cryoablation with or without peritumoral CpG, tumor excision, peritumoral CpG injection or sham surgery (n=6). Mice were euthanized 2 days post-operatively and PBMCs and TDLNs harvested, which were subsequently stained for TCRβ, CD4, CD8α, and CD11c for flow cytometry analysis (Figure1.7A). Tissues from naïve mice were also collected as a control (n=5). No significant differences between groups were observed in total $TCR\beta^+$, CD4 and CD8 T-cell populations (data not shown). Treatments using CpG more than tripled populations of DCs and an unexpected population of TCR^+ $CD11c^+$ cells (Figure1.7B). Several reports suggest that $CD11c^+$ T-cells represents a group of antigen experienced T-cells and may correlate with cytotoxic T-cell activity (126-131), however the functional relevance of these cells in this situation is unknown. Therefore, CpG treatment elevates the percentage of DCs in circulation and also increases the percentage of TCR^+ $CD11c^+$ cells, however the functional impact of the later population is unknown.

NK cells were approximately two-fold higher in mice treated with cryoablation (11±1.4%), excision (8±0.5%), CpG (10±0.5%), and sham surgery (8±0.4%) relative to naïve mice (4.7±0.5%). NK cells still further increased in mice treated with cryoablation and CpG combination therapy (17±0.6%). In TDLN no significant differences were observed in any populations with the exception of an increase in the TCR^+ $CD11c^+$ population with CpG treatment (Figure1.7C). No concurrent increase was observed with cryoablation and CpG combination therapy, suggesting trafficking to the TDLN may be delayed or impaired after cryoablation. These data further confirm CpG elevates the percentage of DCs and TCR^+ $CD11c^+$ cells in circulation.

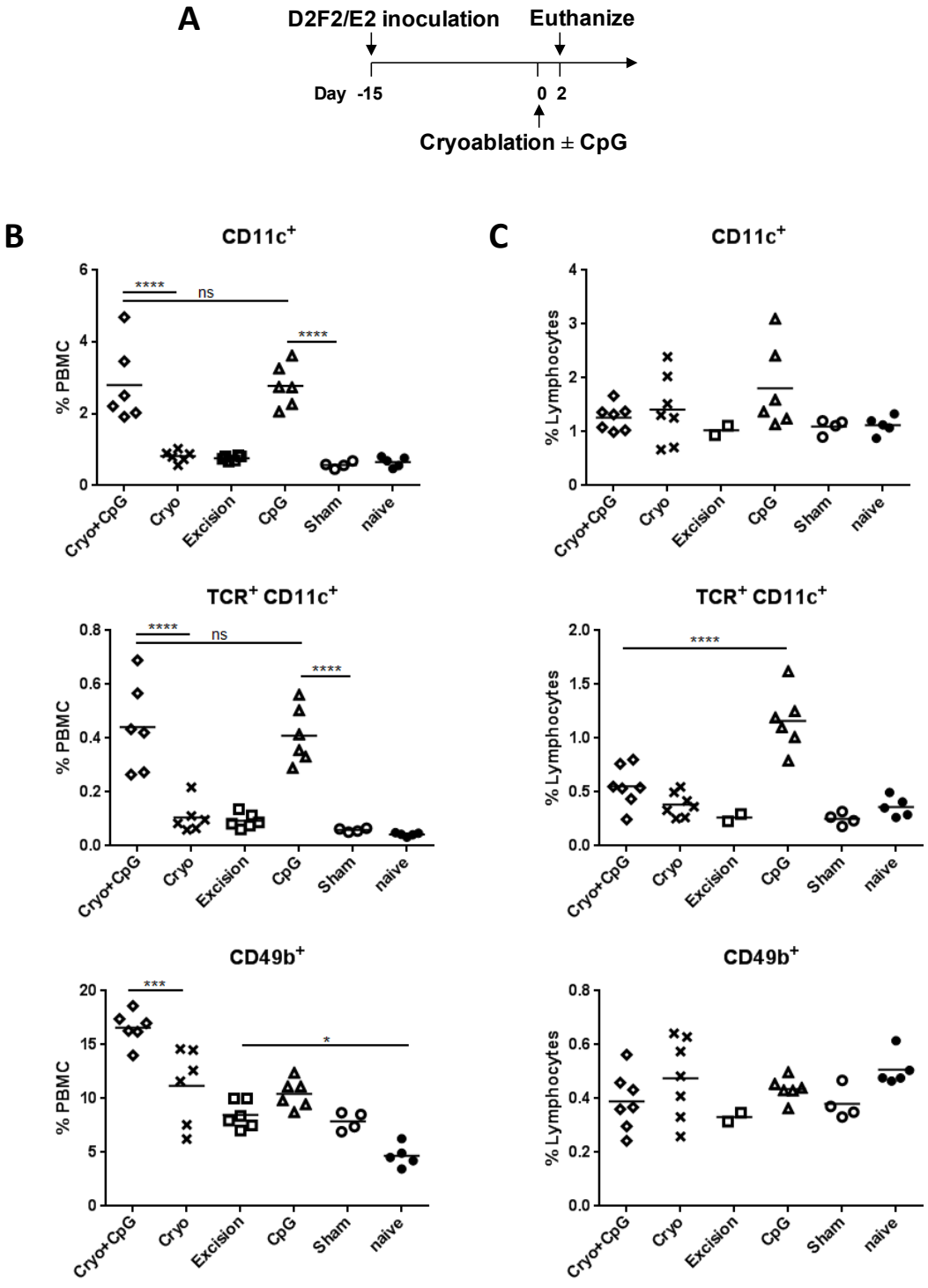

Figure 1.7. Cryoablation and CpG combination therapy elevates DC, NK, and TCR$^+$ CD11c$^+$ populations in circulation. (A) Experimental scheme outlining timing of tumor inoculation and treatments. Fifteen days after inoculation, D2F2/E2 mammary adenocarcinomas (~4x7mm) were treated with cryoablation ± CpG, tumor excision, peritumoral CpG injection or sham surgery (n= 6). Mice were euthanized 2 days post-operatively with (B) PBMCs and (C) TDLN harvested. Cells were stained for TCRβ, CD4, CD8α, CD11c, and CD49b for flow cytometry analysis. One-way ANOVA with Tukey's test. ***P<0.001 ****P<0.0001

CpG treatment increases Th1 cytokines. TDLNs and plasma were collected from mice in the previous experiment 2 days post-operatively. Single cell suspensions were prepared from TDLN and stimulated for 48 hours with 3T3/EKB, which stably express K^d, B7.1, and Her2. Supernatents were collected and analyzed with magnetic-bead protein multiplexing to detect GM-CSF, IFNγ, IL-1β, IL-2, IL-4, IL-5, IL-6, IL-10, IL-12 (p40/p70), and TNF-α, or TGFβ by ELISA. Mice treated with cryoablation, tumor excision, and sham surgery produced comparable results for all cytokines measured, however, these groups had significantly higher levels of IL-1β, IL-2, IL-4, and IL-6 relative to naïve mice, indicative of endogenous tumor induced immunity (Figure1.8A). CpG treatment, either alone or in combination with cryoablation, produced significantly higher levels of IL-1β, IL-2, IL-4, IL-6, IL-12, and TNFα, indicating activation of a Th1 biased response and subsequent macrophage activation (IL-1β and IL-6) (48). Interestingly, combination therapy of cryoablation and CpG produced much lower levels of IFNγ and IL-12 relative to CpG treatment alone, suggesting cryoablation may partially suppress CpG induced responses.

A similar pattern of cytokine levels was observed in the plasma between groups, however, IFNγ and IL-12 levels were now elevated to comparable levels in mice treated with CpG, with or without cryoablation (Figure1.8B). The discrepancy in IFNγ and IL-12 patterns between the TDLN and plasma suggest cryoablation may promote immunosuppressive mechanisms that dampen CpG induced responses. Alternatively, cryoablation may partially impede trafficking to the TDLN due to increased vascular permeability and edema, without having an effect on CpG's ability to activate PBMCs, as was suggested in Figure 1.7.

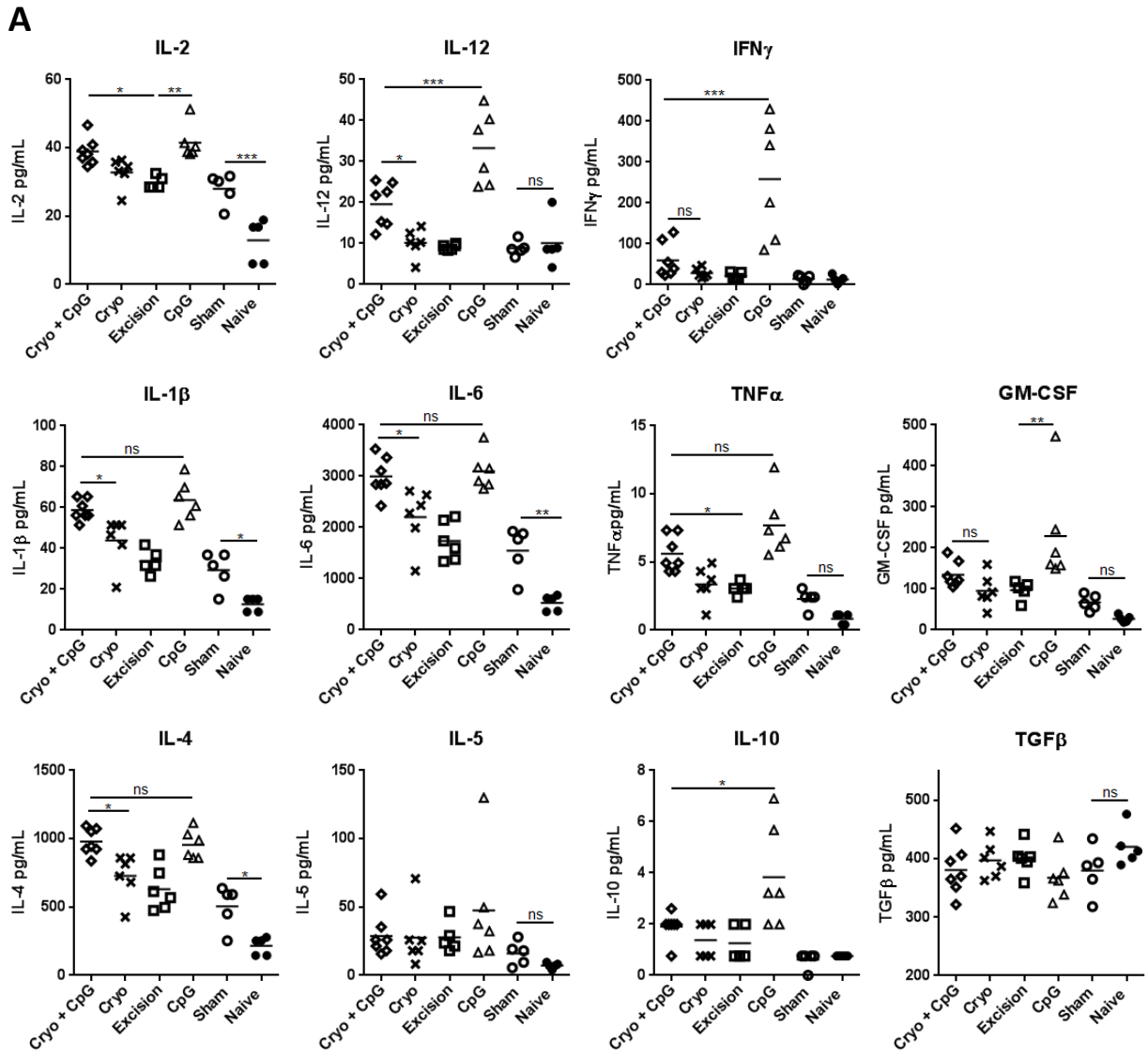

Figure 1.8. CpG augments endogenous immunity. Mice were euthanized 2 days post-operatively for TDLN and plasma collection. (A) $8x10^5$ LN cells were co-cultured with $8x10^4$ 3T3/EKB cells in a total volume of 0.5mL of 10% FBS RPMI at 10% CO_2 37˚C for 48 hours. Supernatents were collected and analyzed with Magpix based multiplexing. (B) Magpix of plasma. **P*<0.05 ***P*<0.01 ****P*<0.001 *****P*<0.0001 One-way ANOVA with Tukey's post-test. Continued

B

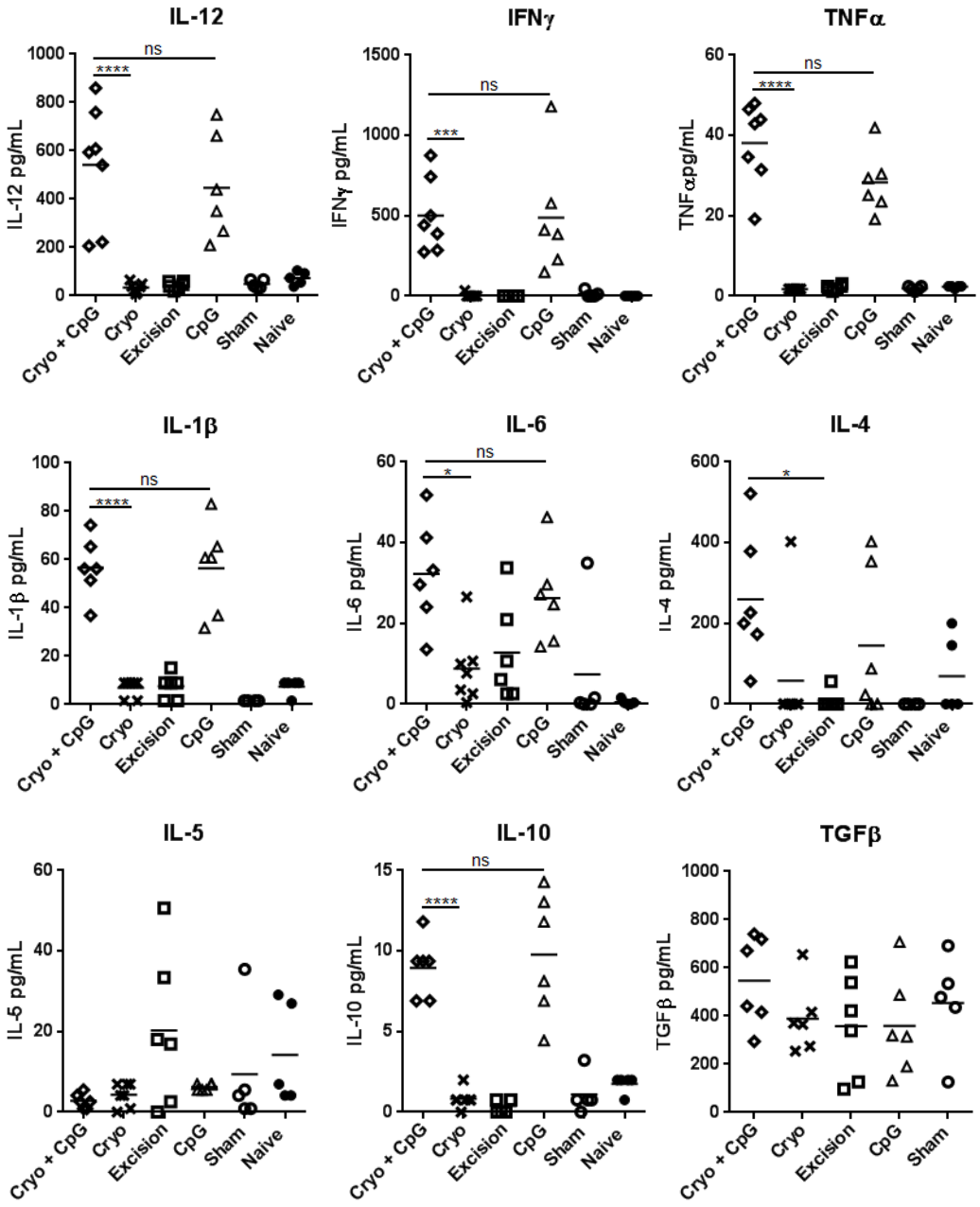
IL-12
IL-12 pg/mL
1000
800
600
400
200
0
ns
****
IFNγ
IFNγ pg/mL
1500
1000
500
0
ns
***
TNFα
TNFαpg/mL
60
40
20
0
ns
****
IL-1β
IL-1β pg/mL
100
80
60
40
20
0
ns
****
IL-6
IL-6 pg/mL
60
40
20
0
ns
*
IL-4
IL-4 pg/mL
600
400
200
0
*
IL-5
IL-5 pg/mL
60
40
20
0
IL-10
IL-10 pg/mL
15
10
5
0
ns
****
TGFβ
TGFβ pg/mL
1000
800
600
400
200
0
Cryo + CpG
Cryo
Excision
CpG
Sham
Naive

Cryoablation and CpG combination therapy elevates DC and TCR^+ $CD11c^+$ populations in circulation. To investigate changes in T-cell and DC populations in CpG treated mice, BALB/c mice with TUBO adenocarcinomas (~4x7 mm) were treated with cryoablation and CpG, CpG alone, or left untreated. Heparinized blood was collected on day 7 and 12 post-operatively for collection of peripheral blood mononuclear cells (PBMC), which were subsequently stained for TCRβ, CD4, CD8α, and CD11c for flow cytometry analysis. No significant differences between groups were observed in total $TCR\beta^+$, CD4 and CD8 T-cell populations (data not shown). Cryoablation resulted in a significant elevation in DC populations relative to untreated mice at day 7, which could be further elevated with the addition of CpG (Figure1.9A). However, DCs returned to comparable levels of untreated mice by day 12. Similarly, CpG treatment, with or without cryoablation significantly increased TCR^+ $CD11c^+$ cells at day 7 which returned to comparable levels of untreated mice by day 12.

To test if this was a tumor-specific phenomenon, we also performed the same analysis in mice inoculated with D2F2/E2. Once tumors grew to ~4x7 mm, mice were treated with cryoablation ± peritumoral CpG, tumor excision, peritumoral CpG injection, or sham surgery (n=6-7). PBMCs were collected at day 7, 14, and 22 post-operatively for flow cytometry analysis. Similar to TUBO, treatments using CpG more than doubled percentages of DCs and quadrupled TCR^+ $CD11c^+$ percentages at day 7, which fell to comparable levels of all tumor experienced groups by day 14 (Figure1.9C-D), indicating DC expansion and activation via treatment with CpG. Furthermore, untreated tumor-bearing mice significantly elevated percentages of DCs relative to naïve mice at all time points, indicating tumor induced DC expansion. Immunity induced by D2F2/E2 will be further elaborated on in chapter 3. These data further confirm CpG elevates the percentage of DCs and TCR^+ $CD11c^+$ cells in circulation.

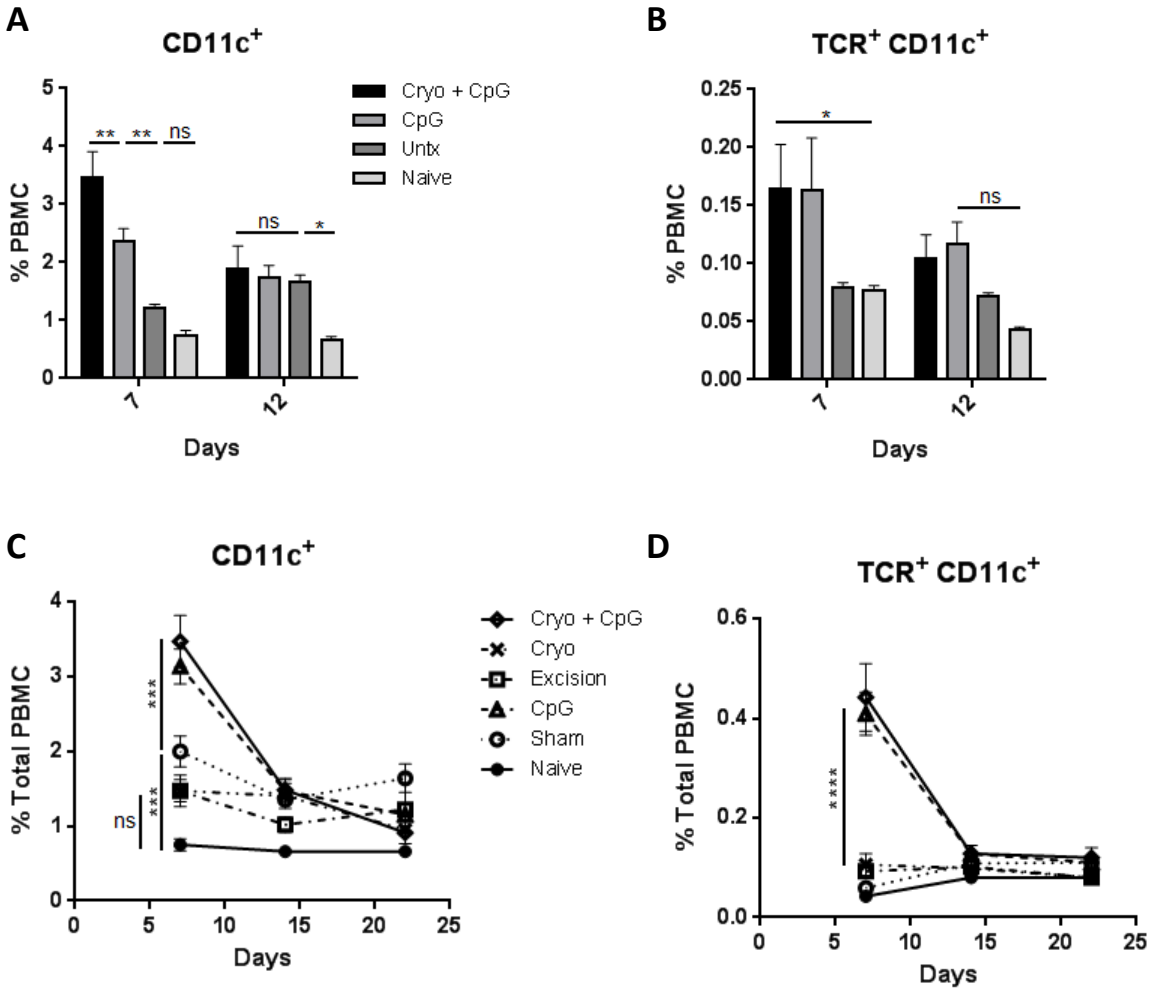

Figure 1.9. Cryoablation + CpG elevates DC and TCR$^+$ CD11c$^+$ populations in circulation. Seven and twelve days after treatment of the TUBO mammary adenocarcinomas (~4x7mm) mice were bled and PBMC harvested (n=3-4). Cells were stained for TCRβ, CD4, CD8α, and CD11c for flow cytometry analysis. Viable singlets were gated on and selected for (A) TCRβ$^-$ CD11c$^+$ cells or (B) TCRβ$^+$ CD11c$^+$ cells. (C-D) The same analysis was performed 7, 14, and 22 days after treatment of D2F2/E2 mammary adenocarcinomas (~4x7mm) (n=6-7). *P<0.05 ** P<0.01 ***P<0.001 **** P<0.0001 One-way ANOVA with Tukey's post-test.

DISCUSSION

Following cryoablation tumor infiltration by polymorphonucleocytes was evident on day 1, which subsided by day 3. Thereafter, macrophages, fibroblasts and other infiltrates invaded the peripheral edges of the tumor. As the necrotic tumor was cleared by macrophages, activated fibroblasts filled the void and began the synthesis of new collagen. These findings are consistent with current knowledge about the progression of immune infiltration in cryoablation treated tumors. Additionally, we confirmed our tumors behave in a similar manner to other tissues undergoing cryoablation (102-104). Using pIL-1β-DsRed mice (106), we found elevated IL-1β promoter activity in freshly resected tumor, which was treated 15 days earlier with cryoablation relative to sham treated mice, further supporting our histological findings. Unfortunately, *in vivo* imaging was not able to detect these differences, prohibiting the possibility of characterizing movements and accumulation of inflammatory infiltrates within the tumor in individual mice. Modifications to the system to further improve fluorescent intensity or examination by intra-vital imaging improve may lead to effective *in vivo* imaging applications.

In advanced disease, it may not be feasible for cryoablation treatment alone to induce tumor-specific immunity and overcome immunosuppressive barriers developed in the tumor microenvironment (13). The wound healing process following cryoablation may also induce multiple factors, such as prostaglandin E2 and thymic stromal lymphopoietin, that create a suppressive Th2 biased microenvironment (132, 133). Furthermore, the chronic inflammatory nature of the healing tissue promotes greater immunosuppression, in part mediated through increased TGFβ production by macrophages and fibroblasts (134). In anticipation of these suppressive effect, we choose to investigate adjuvant therapy using CpG ODN based on its ability to produce strongly polarized type 1 immunity and subsequent Th1 responses (111-114). A mouse specific class C ODN (mu2395) was designed because of the ability of class C ODNs to stimulate both plasmacytoid DCs and B-cells equally well. Despite the presence of the mouse

specific motif in mu2395, it performed equally well as the human specific ODN 2395 in stimulating murine splenocytes. Expression of MHC and co-stimulatory receptor CD80 (B7.1) more than doubled with either CpG treatment. Indirect stimulation of lymphocytes was also evident by upregulation of the intercellular adhesion molecule CD54 (ICAM-1) compared to unstimulated splenocytes. It is unknown if other variations in immunostimulatory properties between mouse and human specific CpGs exist in murine immune cells, therefore we decided to use mu2395 throughout our studies.

In vivo, peritumoral treatment with CpG significantly elevated levels of IL-1β, IL-2, IL-6, IL-12, IFNγ, and TNFα in tumor draining lymph nodes (TDLN) and plasma 2 days post-operatively, indicative of a Th1 biased response (48). In contrast, only low to undetectable responses resulted from treatment with cryoablation, tumor excision, or sham surgery. Although combination therapy of cryoablation and CpG produced significantly elevated levels of IFNγ and IL-12 in TDLN relative to cryoablation alone, levels were significantly lower relative to CpG treatment alone, suggesting cryoablation may dampen CpG induced responses. However, plasma levels of IFNγ and IL-12 were elevated to comparable levels in mice treated with CpG alone or in combination with cryoablation, indicating equivalent stimulation of PBMCs. This is further evident by the elevated levels of DC and NK populations seen in mice treated with cryoablation and CpG. Therefore, cryoablation does not affect CpG mediated stimulation of PBMCs, but may inhibit local responses, as observed in TDLN. Decreased IFNγ and IL-12 responses in TDLN could be due to local immune suppression, in part mediated by TGFβ and IL-10, as a result of massive tissue inflammation produced by cryoablation (134-136). Alternatively, cryoablation may partially impede or slow DC trafficking to the TDLN due to increased vascular permeability, tissue congestion, and increased chemotactic factors present in the ablated region (137).

These findings suggest extensive tissue damage resulting from cryoablation may induce local immune suppression. Although the immune stimulatory effect of CpG treatment is

dampened by cryoablation in TDLN, Th1 biased responses are still significantly increased relative to mice treated with cryoablation alone. Thus, adjuvant therapy, such as CpG, may be a necessary addition to cryoablation to elicit immune activation.

CHAPTER 2

Cryoablation of neu-expressing TUBO Mammary Adenocarcinoma

ABSTRACT

Tumor cryoablation has previously been shown to elicit a variety of anti-tumor responses, ranging from stimulation to suppression, and may promote tumor growth in some situations (13, 31, 35, 86, 87). We hypothesize that anti-tumor immunity and overall outcome induced by cryoablation is determined, at least in part by the immunogenic nature of the tumor. Here we test cryoablation's capacity to induce anti-tumor immunity against an antigenic BALB/c mouse mammary adenocarcinoma, TUBO, which expresses rat Her2/neu (neu). We show that TUBO is sensitive to α-neu antibody (Ab), which can mediate regression of established tumors *in vivo*. Thus, we sought to determine if cryoablation induces α-neu Ab to protect mice against subsequent tumor rechallenge, and if addition of the TLR9 agonist CpG to cryoablation further augments immunity.

In BALB/c mice, cryoablation successfully treated TUBO with a recurrence rate of ~26% and protected ~65% of mice from subsequent tumor rechallenge on the contralateral side. Surgical excision of TUBO produced no recurrences, but did not provide increased protection upon rechallenge. Cryoablation also induced significantly elevated levels of α-neu Ab relative to tumor excision. Peri-tumoral injection of CpG immediately following cryoablation decreased the recurrence rate to 0% and protected nearly 100% of mice from subsequent tumor rechallenge. Combination therapy also significantly increased α-neu Ab above all other groups. When α-neu IgG1 and IgG2a subclasses were quantified cryoablation was found to primarily induce IgG1, suggestive of a Th2 biased response, which was skewed toward IgG2a with the addition of CpG. Additionally, analysis of transcripts in tumor draining lymph nodes (TDLN) found upregulated levels of factors favoring a Th2 biased environment. Therefore, cryoablation may

serve as an effective treatment modality to induce tumor immunity, although it may be a Th2 biased response. Combination treatment with CpG further augmented anti-tumor immunity induced by cryoablation to promote Th1 responses and amplify protection.

In neu tolerant BALB/NeuT (NeuT) mice, cryoablation of TUBO was insufficient to overcome self-tolerance to produce α-neu immunity. To initiate α-neu immunity, NeuT mice were vaccinated with Her2/neu DNA before cryoablation, tumor excision, or sham surgery. No exogenous tumor rechallenge was performed due to the development of spontaneous mammary tumors at approximately 16 to 18 weeks of age in NeuT females. Interestingly, cryoablation treated mice produced similar levels of α-neu Ab to sham treated mice, whereas mice treated with tumor excision had significantly higher levels of Ab. Additionally, tumor excision significantly delayed the onset of spontaneous mammary tumors relative to cryoablation and sham treated groups. When CpG was used in combination with cryoablation, no additional benefit was observed over cryoablation alone. These results suggest cryoablation of a very weakly or non-antigenic tumor, as in this case, is not capable of inducing tumor-specific immunity. Furthermore, cryoablation in this scenario may actually result in an immunosuppressive environment, evident by decreased vaccine induced α-neu Ab and tumor protection relative to tumor excision.

INTRODUCTION

Her-2 is a tyrosine kinase growth factor receptor and a member of the epidermal growth factor receptor (EGFR/ErbB) family. When Her2 is overexpressed or mutated it increases signal transduction to mitogenic (i.e. MAPK) and survival (i.e. phosphatidylinositol 3-kinase/Akt) pathways. These changes ultimately contribute toward the initiation and progression of neoplastic transformation (138). Approximately 25% of human breast carcinomas overexpress Her2, making it one of the most plausible targets for therapeutic intervention (138-140).

The rat homologue of human Her-2 is referred to as neu. A single point mutation at amino acid position 664 in the transmembrane domain transforms neu into a constitutively active transforming oncogene (89, 90, 92, 141). BALB/NeuT mice express the activated rat neu transgene (NeuT) driven by the mouse mammary tumor virus promoter. NeuT females develop atypical ductular hyperplasia in all mammary glands beginning at 21 days of age, which progresses to carcinoma *in situ* between 91 and 105 days, and ultimately into palpable tumors between 112 to 130 days (89-91). Endogenous expression of rat neu in NeuT mice eliminates neu-reactive lymphocytes via central tolerance. Thus, NeuT mice have a much higher degree of tolerance against rat neu than wild type BALB/c mice, which have no previous exposure to neu. This allows us to analyze a tumor expressing a true self-antigen.

TUBO is a neu^{+} BALB/c mammary adenocarcinoma line established *in vitro* from a lobular carcinoma that arose spontaneously in a BALB/NeuT female. TUBO is considered an antigenic tumor due to cellular expression of transformed rat neu. Antigenic tumors have proteins the immune system can potentially recognize due to modifications from the tumor or surrounding microenvironment (i.e. mutation or glycosylation), although many tumors evade antigenic recognition by inhibiting effector responses (142, 143). While α-neu immunity is readily induced in BALB/c mice by active vaccination, inoculation with TUBO and subsequent tumor growth is not capable of producing such a response. Therefore, TUBO is representative of

tumors that express antigen(s) the immune system can potentially recognize but does not respond against without specific intervention. For example, aberrant tumor expression of Her2, MUC-1, melanoma-associated antigen 3 (MAGE-A3), or carcinoembryonic antigen (CEA) does not elicit host immunity, but targeted therapy against these molecules can induce tumor-specific immunity (144-152).

We have previously shown that Her2/neu DNA vaccination can inhibit and protect mice against Her2/neu$^+$ tumor growth (145, 153-157). The most effective constructs for inducing anti-tumor immunity and overcoming tolerance in Her2 and NeuT transgenic mice were found to be hybrid DNA vaccines, which utilize heterologous (xenogenic) Her2/neu to improve immunogenicity through cross-reactive epitopes. These constructs encode fusion proteins of human Her2 and rat neu. The hybrid vaccine used in the following studies utilizes DNA encoding a chimeric $NeuE2_{TM}$ protein. This is a transmembrane neu-Her2 fusion protein with neu at the NH_2 terminus and Her2 at the COOH terminus, and a truncated Her2 intracellular domain (155, 158). All vaccinations include pGM-CSF, which encodes for the adjuvant murine granulocyte macrophage colony-stimulating factor.

We hypothesize that cryoablation can elicit anti-tumor immunity from an antigenic tumor through the liberation of tumor associated antigens and endogenous danger signals released by ablated cells. Additionally, we believe using the TLR9 ligand CpG to promote Th1 biased responses will improve cryoablation induced immunity and anti-tumor protection. Lastly, it seems reasonable tumor cryoablation may promote vaccine induced immunity through the release of additional tumor antigen which may subsequently bind to vaccine induced antibody. Uptake of the resulting immune complexes by dendritic cells would lead to cross-presentation and possibly a greater anti-tumor response.

RESULTS

TUBO mammary adenocarcinoma is sensitive to α-neu Ab. Previous studies have shown that induction of α-neu Ab through DNA vaccination in BALB/c mice provided complete protection from challenge with TUBO mammary adenocarcinoma in a prophylactic setting (92, 159). To test the therapeutic effect of vaccination, BALB/c mice with established TUBO tumors (~3x5 mm) were vaccined with an admix of pNeuE2 and pGM-CSF, which resulted in α-neu Ab levels up to 134±7 μg/mL, sufficient to cause complete tumor regression (Figure2.1A). Mice vaccinated with a control plasmid, empty pVax, and pGM-CSF produced very low levels of α-neu Ab (0.5±0.5 μg/mL) 34 days after vaccination, until mice had to be euthanized due to excessive tumor burden (Figure2.1B). The lack of α-neu Ab induction demonstrates that a growing TUBO tumor does not induce endogenous α-neu immunity. Interestingly, α-neu Ab levels in vaccinated tumor-bearing mice began to decline after day 34, shortly after tumors had completely regressed, suggesting that immune-mediated death of TUBO contributes to α-neu responses. These observations were further validated in non-tumor bearing BALB/c mice similarly vaccinated with pNeuE2. Vaccinated BALB/c mice produced 19.5±4 μg/mL of α-neu Ab 27 days after vaccination relative to 92.4±5 μg/mL in vaccinated tumor-bearing mice (Figure2.1C). This finding supports the notion that immune mediated death of neu^+ TUBO amplifies vaccine induced α-neu immunity until the tumor has completely regressed, at which point α-neu Ab levels begin to decline.

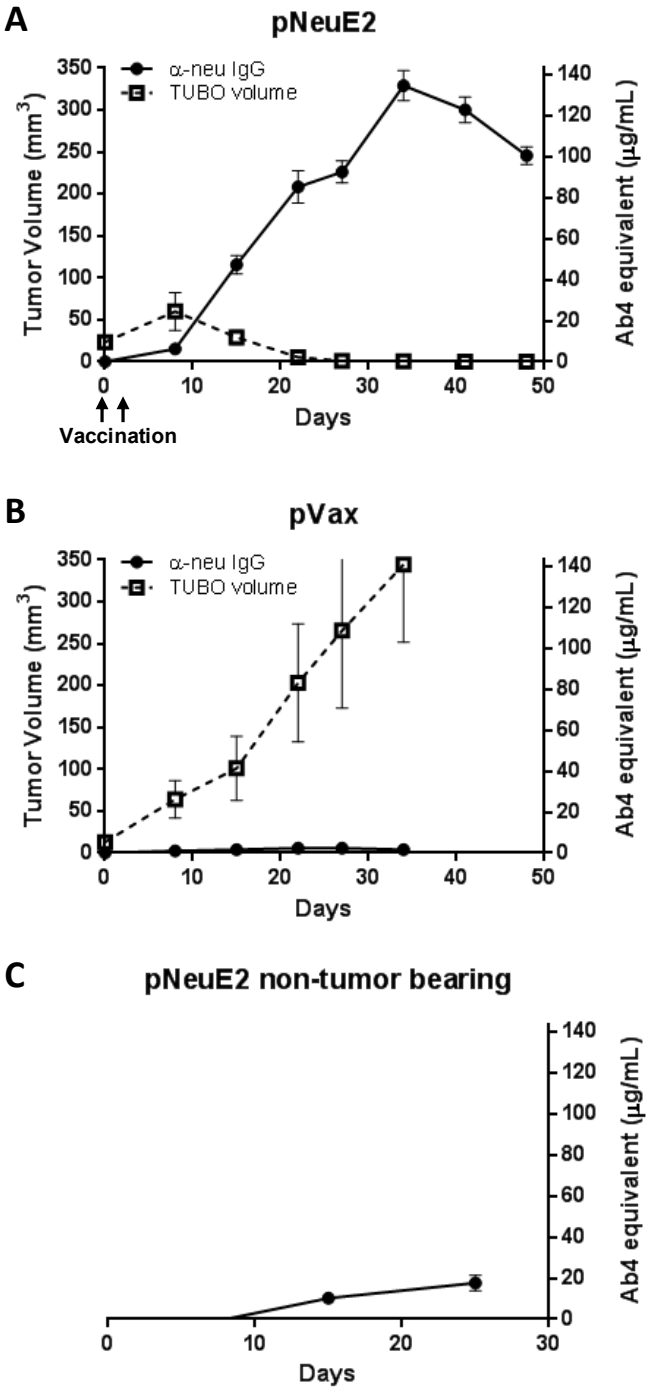

Figure 2.1. TUBO mammary adenocarcinoma is sensitive to α-neu Ab. Thirteen days after inoculation with $2.5x10^5$ cells of TUBO mammary adenocarcinoma (~3x5 mm) BALB/c mice were vaccinated with an admix of 30 µg of pGM-CSF and (A) 30 µg pNeuE2 or (B) 30 µg of pVax on day 0 and 2 (n=4). Sera and tumors measurements were collected at weekly intervals. TUBO volume (mm^3) and α-neu IgG (Ab4 equivalent µg/mL) are plotted on the left and right y-axis respectively. (C) Non-tumor bearing BALB/c mice were vaccinated with pGM-CSF and pNeuE2 as previously described (n=7). Data representative of three independent experiments.

Cryoablation induces transcripts that favor a Th2 environment. To develop a better understanding of how cryoablation modulates immunity we evaluated a panel of immune-related transcripts in TDLNs 6 days after cryoablation using quantitative real-time PCR (qPCR). TDLNs were harvested 6 days post-operatively (Figure2.2A) to allow adequate time for trans-migration between the tumor and TDLN, as well as induction of immune populations (160). The panel of targets that was selected included cytokines, chemokines, transcription factors, and other factors known to contribute toward Th1 or Th2 biases.

Multiple transcripts were significantly elevated throughout the panel of targets, including both Th1 and Th2 contributing factors (Figure2.2B). Cytokines representative of a Th1 response, such as IFNγ and TNFα, were upregulated after cryoablation, although the Th2 cytokine IL-4 was also significantly increased. Other factors known to promote Th2 bias such as IL-10, prostaglandin E synthase (Ptges), thymic stromal lymphopoietin (TSLP), and OX40 Ligand (Tnfsf4) were also significantly elevated (59, 161). TGFβ, which directly inhibits T-cell activity, was also significantly increased (162). Of the master transcription factors analyzed, only GATA3 (Th2) was significantly elevated, but not Tbet (Th1), Foxp3 (T regulatory cells) or RORγT (Th17). These findings support the notion of a dynamic post-cryoablation environment in the TDLN which could potentially promote or suppress an effective anti-tumor immune response, although the majority of the significantly elevated transcripts favor a Th2 biased response.

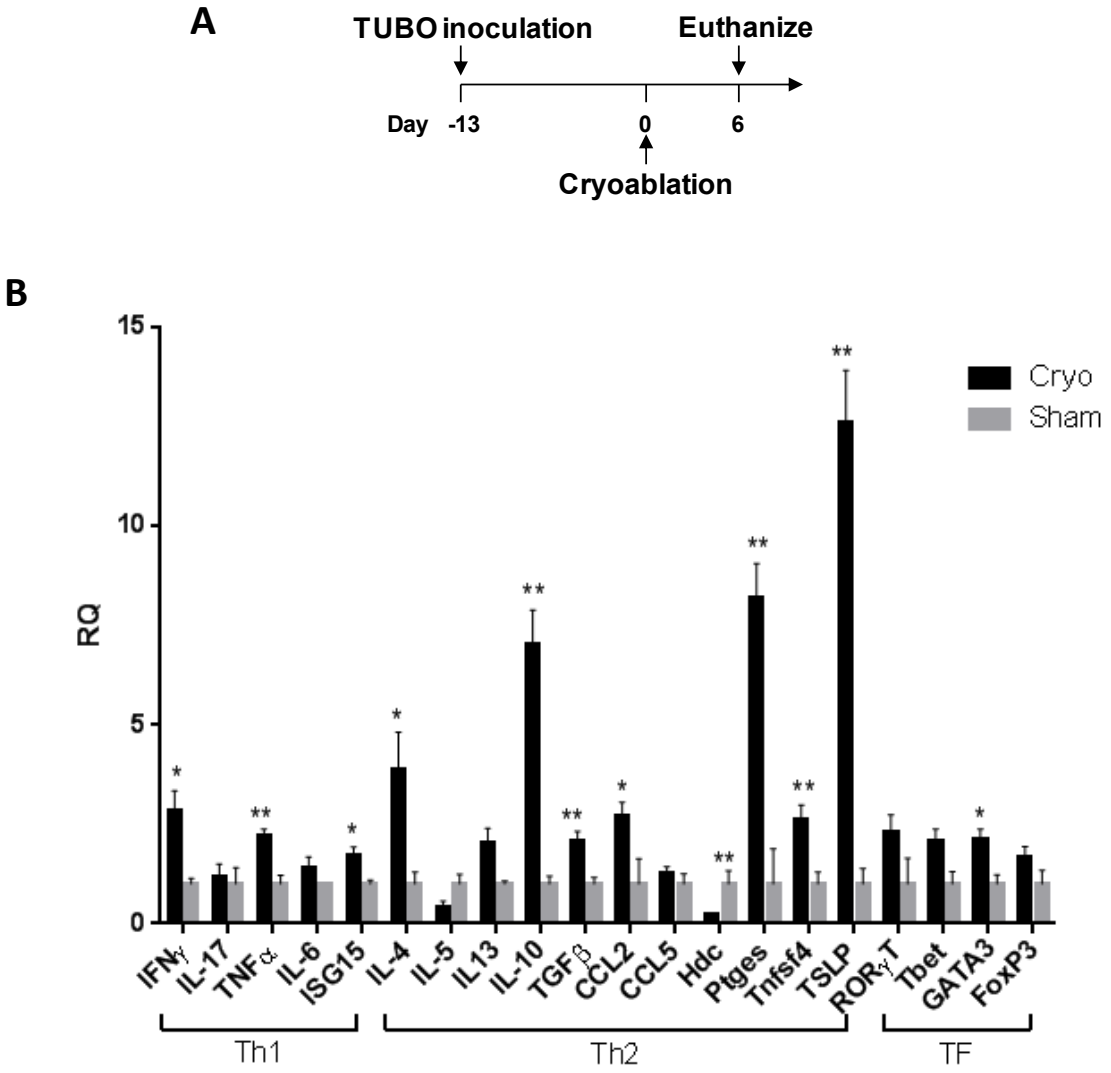

Figure 2.2. Cryoablation induces transcripts that favor a Th2 environment. (A) Thirteen days after inoculation with $2.5x10^5$ cells of TUBO mammary adenocarcinoma (~3x5 mm) BALB/c mice were treated with either cryoablation (n=7) or sham surgery (n=4). (B) Tumor draining lymph nodes (TDLN) were harvested 6d post-operatively and lymphocytes stimulated for 3 hr using 50 nM PMA / 1μM ionomycin. RNA was isolated for cDNA synthesis and subsequent qPCR analysis. Transcript levels measured are relative to the sham group (RQ). Brackets show Th1 and Th2 biased transcripts and master transcriptions factors (TF). **P*<0.05 ***P*<0.01 Unpaired t-test.

Peritumoral injection of CpG oligodeoxynucleotide (CpG) with cryoablation reduces recurrences. Cryoablation is an established procedure to eliminate and/or debulk solid tumors in the clinical setting, however, this seldom results in beneficial anti-tumor immunity. We tested the feasibility of promoting cryoablation induced immunity by adding CpG, a potent Th1 activator. CpG acts as a ligand for Toll-like receptor 9 (TLR9) which is present on dendritic cells (DCs), B-cells, monocytes/monocytes, and natural killer (NK) cells (163, 164). CpG mediated activation of plasmacytoid DCs stimulates synthesis and secretion of type I interferons, which subsequently induces production of IL-12 by conventional DCs, thus promoting Th1 activity (164).

Tumor recurrence data from mice treated with either cryoablation alone (n=28) or combination therapy of cryoablation and CpG (n=15) were compiled from 4 independent experiments. Mice from each experiment were treated when tumor dimensions reached approximately 4x7 mm in size, after which they were monitored for recurrence at the primary tumor location at least 30 days post-operatively and as long as 90 days (Figure2.3). Cryoablation had a recurrence rate of ~26%, with tumor recurrences detected between 34-60 days post-operatively. Surgical excision of similar size tumors, along with adjacent mammary tissue, produced no observed recurrences (n=24) (data not shown). This discrepancy is likely because cryoablation in mice does not achieve the same degree of margins as excision does. The margins, or lethal isotherm, achievable in mice may not reach micro tumor foci not intimately associated with the primary tumor. However, when CpG was combined with cryoablation the recurrence rate fell to 0%. This finding argues the addition of CpG to cryoablation may elevate local anti-tumor immunity to prevent recurrences.

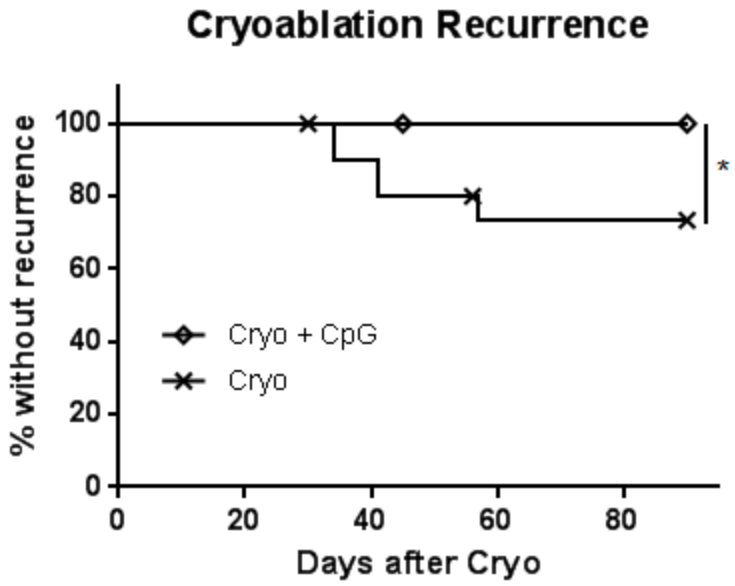

Figure 2.3. Cryoablation + CpG protects against tumor recurrences. Results pooled from 4 independent experiments with all mice monitored at least 30 days post-operatively for recurrence – Cryo + CpG (n=15) Cryo (n=28). Symbols indicate censored subjects within an experiment due to experimental endpoint. *P<0.05 Log-rank test.

Cryoablation induces systemic anti-tumor immunity which is enhanced with peritumoral CpG injection. BALB/c mice were inoculated with $2.5x10^5$ TUBO cells which grew for twenty days to ~4x7 mm in diameter. Tumors were treated with cryoablation ± peritumoral CpG, surgical excision, peritumoral CpG injection, or left untreated (n=6-8) and monitored for 57 days (Figure2.4A). All tumors treated with cryoablation ± peritumoral CpG or surgical excision completely regressed with the exception of two mice in the cryoablation group that developed recurrences at day 41 and 57. CpG treatment alone did not cause tumor regression but did slow tumor growth relative to untreated mice (Figure2.4B). Mice treated with CpG or left untreated were eventually euthanized due to progressive tumor burden or skin ulcerations.

On day 57, all mice that cleared the primary tumor were rechallenged with $2.5x10^5$ TUBO cells on the contralateral side. An additional group of naïve mice also received TUBO inoculation at the same time as a control (n=7). Mice were monitored for an additional 45 days after tumor rechallenge. All naïve mice and 5/6 of mice treated with surgical excision developed tumors from the second rechallenge, indicating tumor excision does not induce systemic anti-tumor immunity capable of consistently protecting mice. Cryoablation protected 7/11 mice from rechallenge, whereas combination therapy of cryoablation and CpG further augmented anti-tumor immunity, protecting 15/16 mice (Figure2.4C). Thus, cryoablation of an antigenic but non-immunogenic tumor induced systemic anti-tumor immunity capable of protecting mice from tumor growth at a distant site, which was further enhanced with the use of CpG.

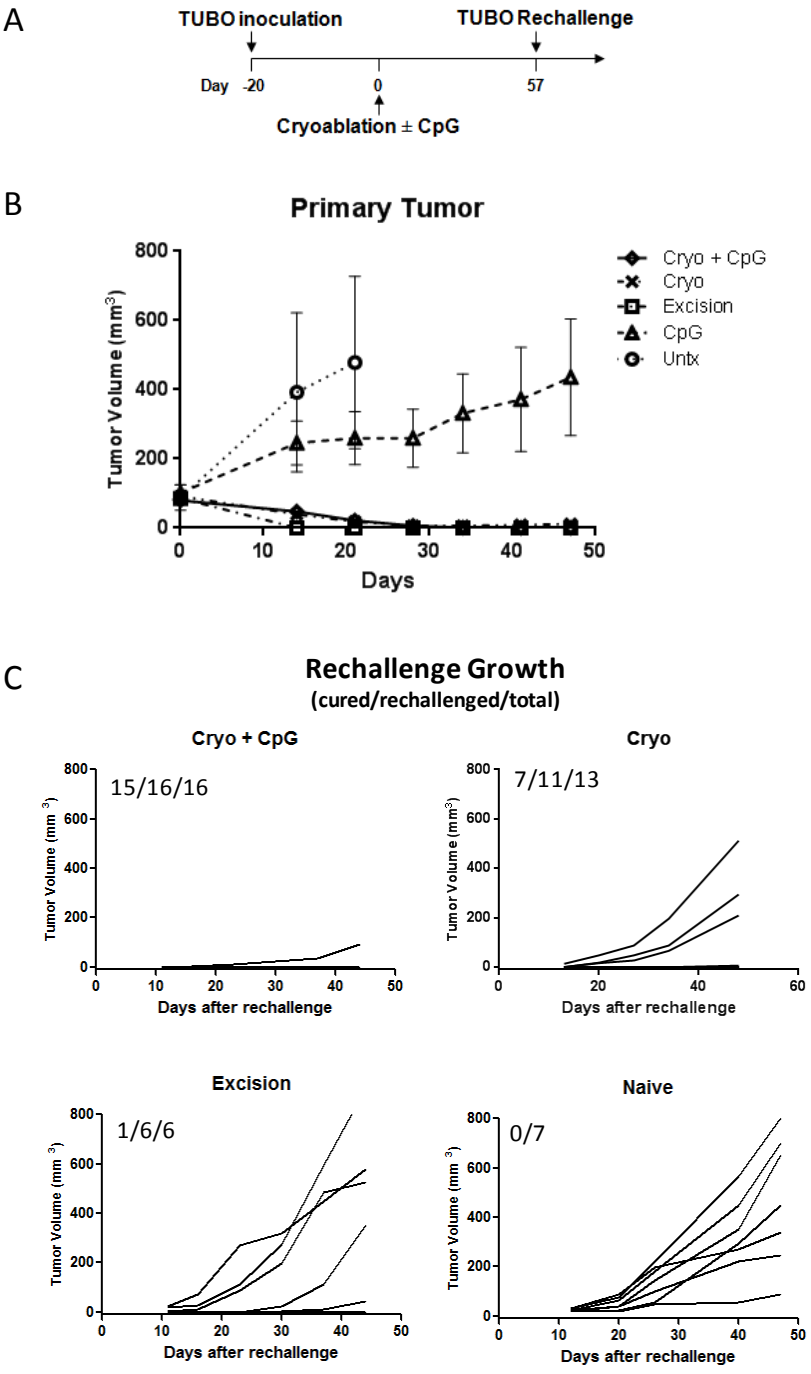

Figure 2.4. Tumor cryoablation increases protection against TUBO. (A) Experimental scheme outlining timing of tumor inoculation and treatment. Twenty days after inoculation TUBO mammary adenocarcinomas (~4x7mm) were treated with cryoablation ± peritumoral CpG, tumor excision, peritumoral CpG injection, or left untreated (n= 6-8). (B) Primary tumor growth of TUBO was monitored over time showing mice treated with CpG or left untreated continued to have progressive tumor growth. Untreated mice were euthanized at day 20 due to tumor burden. (C) Fifty-seven days later, tumor free mice were rechallenged with $2.5x10^5$ TUBO cells on the contralateral side. Tumor growth was monitored over the course of 45 days, with any palpable tumor growing considered a failure in tumor protection. Number of mice (cured/rechallenged/total) shown. Data pooled from two independent experiments.

Cryoablation induces α-neu Ab which is further amplified by CpG. Since TUBO was shown to be sensitive to α-neu Ab (Figure2.1) we sought to determine if cryoablation or other treatments induced α-neu Ab to render tumor protection. Sera from the previous experiment were collected for α-neu Ab quantification (Figure2.5). Both untreated mice and mice treated with surgical excision produced very low α-neu IgG (1.5±0.7 and 1.5±0.03 μg/mL respectively). Mice treated with cryoablation produced increased levels of α-neu IgG beginning 14 days post-operatively (16±7 μg/mL) which began to plateau at day 21 (10±3 μg/mL). Mice treated with peritumoral injection of CpG alone produced 22±7 μg/mL of α-neu IgG, which slowed tumor growth relative to untreated mice but was not able to cause regression (Figure2.4B).

When CpG was used in combination with cryoablation, α-neu IgG levels continually increased to 58±16 μg/mL at day 41, which plateaued thereafter and remained elevated to day 70. As expected, this plateau correlated with clearance of the treated tumor. Area under the curve (AUC) analysis found significant differences occurring between cryoablation + CpG and cryoablation groups, as well as the cryoablation and excision groups. Additionally, α-neu IgG induced from cryoablation + CpG appeared to be greater than a simple additive response from cryoablation alone and CpG alone. These observations taken together with our previous findings in Figure2.1 are indicative of α-neu IgG playing a critical role in immune mediated tumor death of TUBO. Contrarily, α-neu IgG in mice treated with CpG alone was capable of slowing tumor growth but unable to mediate tumor regression, which implicates the presence of an immunosuppressive tumor microenvironment.

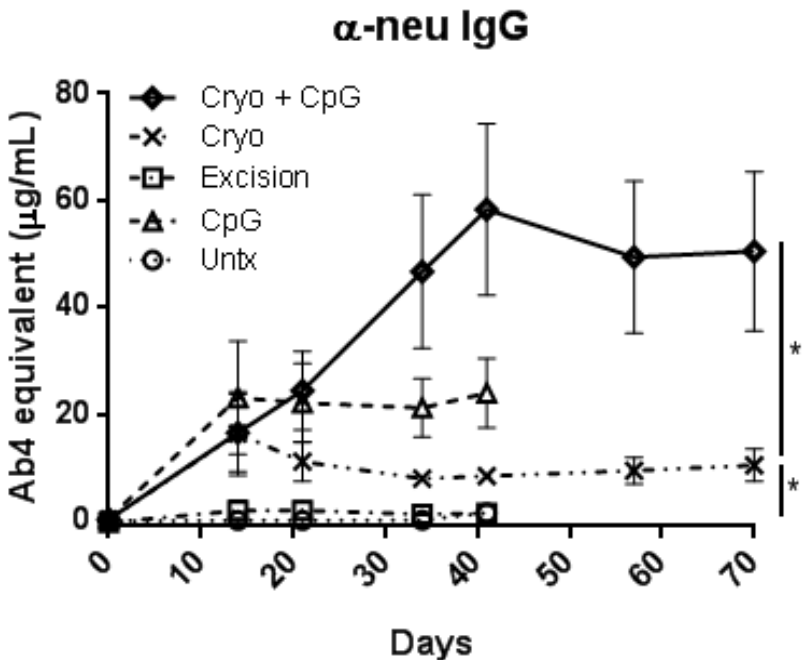

Figure 2.5. Tumor cryoablation induces α-neu Ab. Sera was collected throughout the experiment for α-neu IgG quantification. Area under the curve (AUC) analysis was performed for cryoablation groups at day 70. AUC analysis was also performed between cryoablation and excision groups at day 41. *P<0.05 unpaired t-test with Welch's correction. Data representative of two independent experiments.

Cryoablation primarily induces α-neu IgG1 which can be skewed toward IgG2a with the addition of CpG. To further characterize α-neu Ab we assessed levels of IgG2a and IgG1, which are representative of Th1 and Th2 responses respectively (165). IFNγ (Th1) and IL-4 (Th2) are the main factors regulating subclass switching to IgG2a and IgG1 respectively, with each response also antagonizing the other (166). Using AUC analysis, cryoablation + CpG treated mice produced significantly higher levels of IgG2a relative to cryoablation treated mice, with no such difference detected for IgG1 (Figure2.6A-B). Ab measurements at a representative time point (day 41) display variable IgG2a and IgG1 levels in either group treated with CpG, but a consistently increased IgG1 level relative to IgG2a within the cryoablation alone group (Figure2.6C). To help illustrate this point IgG1 and IgG2a percentages of total α-neu IgG were calculated. The percentage of IgG1 in cryoablation treated mice (76±5%) was consistently elevated relative to cryoablation + CpG (46±11%) or CpG (38±10%) treated groups (Figure2.6D). Whereas the percentage of IgG2a in cryoablation treated mice (12±4%) was significantly lower relative to cryoablation + CpG (38±8%) or CpG (38±6%) treated groups. These data suggest addition of CpG is capable of converting the IgG1 dominant response produced in cryoablation toward an IgG2 response.

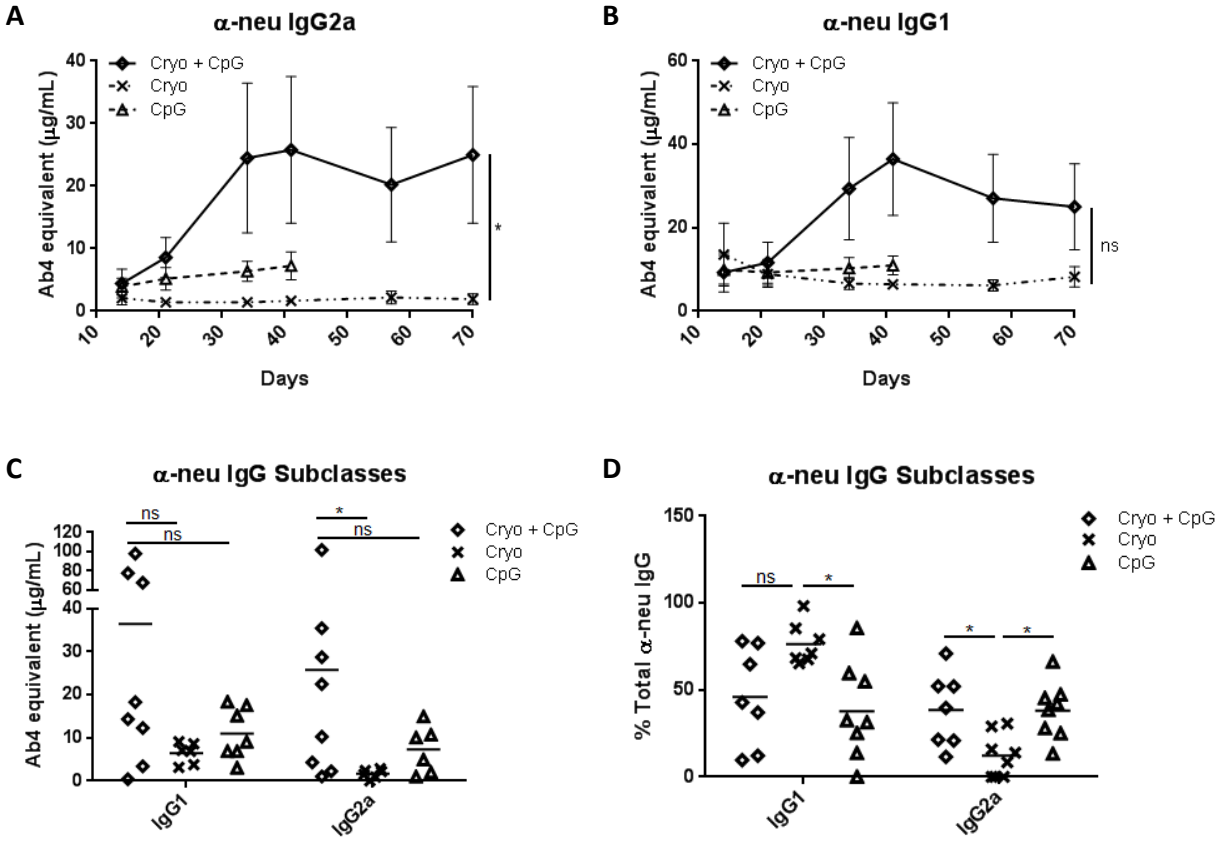

Figure 2.6. Cryoablation primarily induces IgG1 which can be skewed toward IgG2a with the addition of CpG. Sera was collected throughout the experiment for α-neu IgG subclass quantification. Area under the curve analysis was performed for (A) IgG2a and (B) IgG1 levels at day 70. **P*<0.02 Mann Whitney test. (C) α-neu IgG quantification at day 41. **P*<0.05 One-way ANOVA with Dunn's post-test. (D) Percent total α-neu IgG was calculated for IgG2a and IgG1 subclasses. Data shown (day 21) is representative of Ab subclass profile through day 70. **P*<0.05 One-way ANOVA with Tukey's post-test.

Vaccination with Her2/neu DNA induces α-neu immunity but does not act synergistically with cryoablation. We next investigated if α-neu immunity induced from Her2/neu DNA vaccination can be augmented by tumor cryoablation. Thirteen days after inoculation with $2.5x10^5$ cells of TUBO mammary adenocarcinoma (~3x5 mm) BALB/c mice were randomly divided into 6 groups and vaccinated with an admix of 30 μg of pGM-CSF and 30 μg pNeuE2 or 30 μg of pVax on day 0 and 2 (n=5-7). Eight days after the first vaccination mice were treated with cryoablation, tumor excision, or sham surgery (Figure2.7A). Tumors regressed in all groups with the exception of pVax and sham treated. Three mice treated with pVax and cryoablation also had tumors recur at day 34 and 41(Figure2.7B).

Mice vaccinated with pVax and treated with excision or sham surgery produced very low levels of α-neu IgG (1.5±0.7 and 0.7±0.03 μg/mL respectively) (Figure2.7C). Mice treated with pVax and cryoablation produced detectable levels of α-neu IgG beginning 8 days post-operatively (7±3 μg/mL), which increased to 13±6 μg/mL at day 15 and eventually plateaued at day 22 (11±5 μg/mL). Vaccination with pNeuE2 induced significantly higher levels of α-neu Ab in all groups relative to vaccination with pVax. Interestingly, mice treated with pNeuE2 and sham surgery produced higher levels of α-neu Ab (123±6 μg/mL) than mice treated with pNeuE2 and cryoablation (80±15 μg/mL) or pNeuE2 and excision (56±14 μg/mL). Increased Ab levels in pNeuE2 and sham treated mice can be attributed to vaccine mediated immunogenic death of TUBO, which is no longer possible once tumors have been treated with cryoablation or surgical excision. Area under the curve analysis found no significant differences between pNeuE2 vaccinated mice treated with cryoablation or surgical excision, suggesting cryoablation does not further enhance vaccine induced immunity, as originally hypothesized.

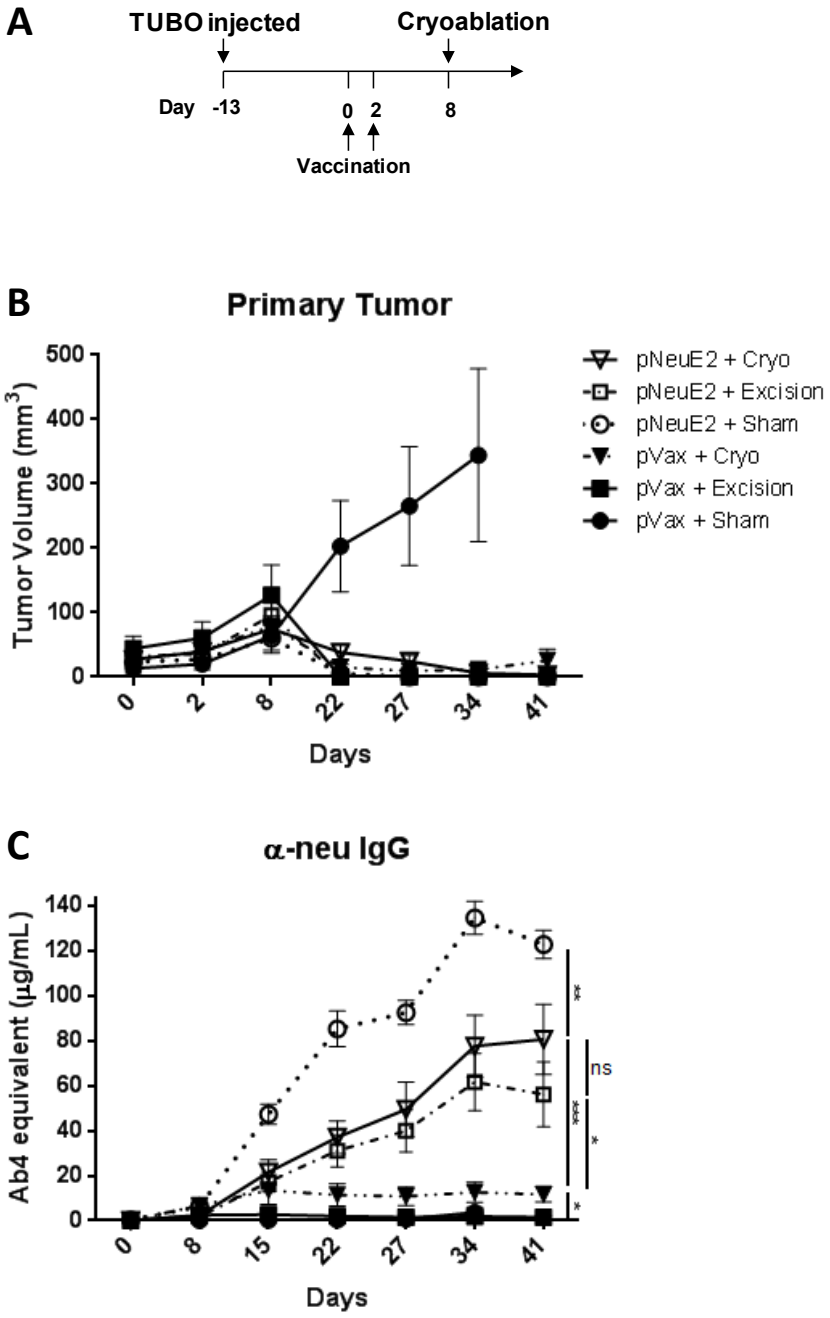

Figure 2.7. Vaccination with Her2/neu DNA improves α-neu immunity but does not act synergistically with cryoablation. (A) Thirteen days after inoculation with $2.5x10^5$ cells of TUBO mammary adenocarcinoma (~3x5 mm) BALB/c mice were randomly divided into 6 groups and vaccinated with an admix of 30 µg of pGM-CSF and either 30 µg pNeuE2 or 30 µg of pVax on day 0 and 2 (n=5-7). Eight days after the first vaccination mice were treated with cryoablation, tumor excision, or sham surgery. (B) Tumor growth of TUBO was monitored over time showing all groups caused tumor regression with the exception of mice treated with pVax and sham surgery, which were euthanized at day 34 due to tumor burden. (C) Sera was collected throughout the experiment for α-neu IgG quantification. Area under the curve analysis was performed at day 41. **P*<0.05 ***P*<0.01 ****P*<0.001 One-way ANOVA with Tukey's post-test. Data representative of two independent experiments.

Cryoablation does not induce α-neu immunity in NeuT mice. To study cryoablation induced immunity against a tumor associated self-antigen we used tolerant BALB/NeuT female mice. Female NeuT mice were separated into four groups (n=6-10) and vaccinated with an admix of 50 μg of pGM-CSF and 50 μg of pNeuE2 or 50 μg of pVax at 77, 87, and 105 days of age. Mammary pads 4 and 5, which endogenously develop recognizable carcinoma *in situ*, were treated with cryoablation or sham surgery at 91 days of age (Figure2.8A). Growth of spontaneous tumors were monitored for an additional 100 days or until mice had to be euthanized due to tumor burden (Figure2.8B). As expected, mice vaccinated with pNeuE2 exhibited delayed outgrowth of spontaneous mammary tumors compared to mice vaccinated with pVax, which was independent of cryoablation.

Mice vaccinated with pVax and treated with cryoablation or sham surgery produced no measurable α-neu Ab, verifying cryoablation alone is not capable of producing α-neu immunity against a fully tolerant antigen (Figure2.8C). Both groups vaccinated with pNeuE2 produced similar levels of α-neu Ab (5-10 μg/mL), which began to decline after peaking at 120 days. No significant differences between cryoablation and sham surgery treated groups were found, suggesting cryoablation does not contribute toward vaccine induced immunity in NeuT mice.

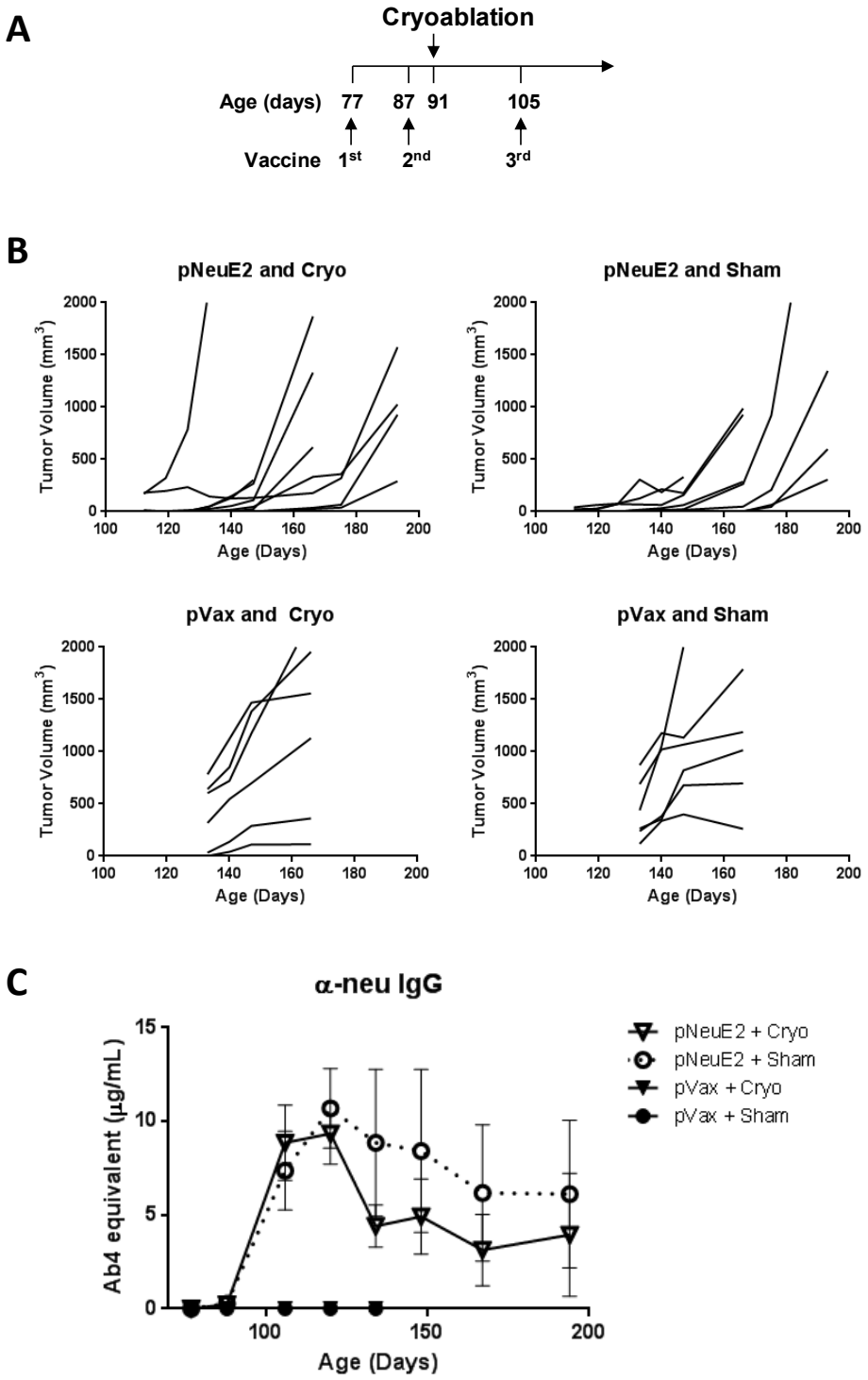

Figure 2.8. Cryoablation does not induce α-neu immunity in NeuT mice. (A) 77 day old female BALB/NeuT mice were placed into four groups (n=6-10) and vaccinated with an admix of 50 μg of pGM-CSF and 50 μg of pNeuE2 or 50 μg of pVax at 77, 87, and 105 days of age. Mammary pads 4 and 5 were treated with cryoablation or sham surgery at 91 days of age. (B) Spontaneous tumor growth was monitored over time. (C) Sera was collected for α-neu IgG quantification. Only mice vaccinated with pNeuE2 produced α-neu IgG. Levels between cryoablation and sham treated mice were not significantly different.

Cryoablation creates a non-conducive environment for vaccine induced immunity in NeuT mice. To further test the effects of cryoablation on α-neu immunity in NeuT mice we inoculated fifty-eight day old female NeuT mice with $2.5x10^5$ TUBO. Mice were randomly divided into three groups (n=8-9) and vaccinated with an admix of 50 μg of pGM-CSF and 50 μg of pNeuE2 at 70 and 80 days of age. Primary tumors (~4x6mm) were treated with cryoablation, excision, or sham surgery 4 days after the second vaccination (Figure2.9A). Tumor growth was monitored until mice reached 200 days of age or until mice were euthanized due to excessive tumor burden (Figure2.9B). Unlike BALB/c mice, no regression of primary tumors was evident in sham treated mice, indicating vaccination alone is not sufficient to treat NeuT mice in a therapeutic setting.

Cryoablation and sham treated mice produced similar levels of α-neu Ab (5±1.5 μg/mL) peaking at 97 days and declining thereafter (Figure2.9C). Unexpectedly, excision treated mice produced significantly higher levels of α-neu Ab (13±3μg/mL) peaking at 112 days, which remained elevated longer than other groups. Furthermore, excision significantly delayed the development of spontaneous tumors relative to cryoablation treated mice, even protecting several mice out to 200 days (Figure2.9D). These results, taken together with our previous NeuT findings, argue that cryoablation exerts a negative impact on vaccine induced immunity, similar to an untreated tumor.

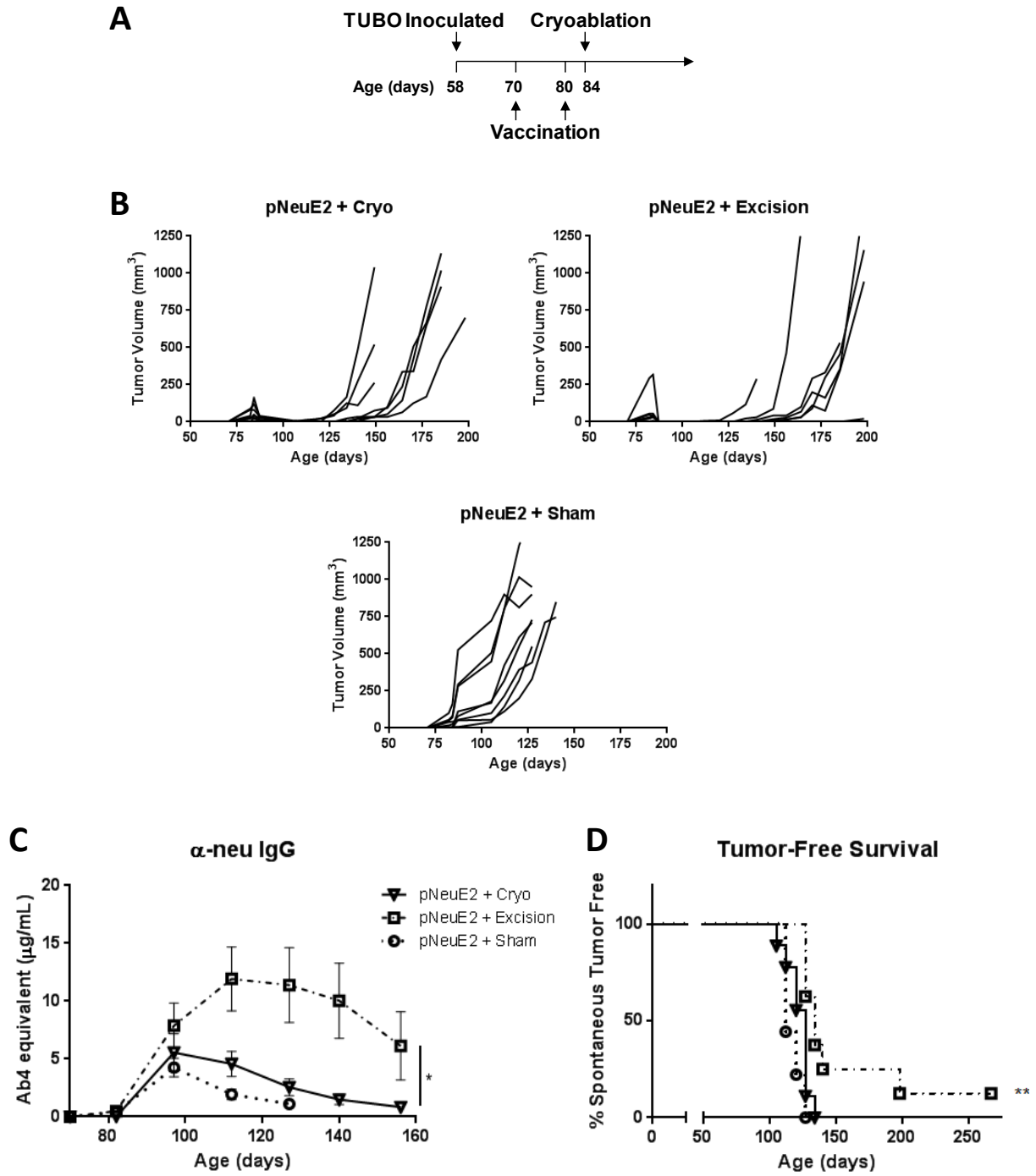

Figure 2.9. Cryoablation creates a non-conducive environment for vaccine induced immunity in NeuT mice. (A) Fifty-eight day old female BALB/NeuT mice were randomly divided into three groups (n=8-9) and inoculated with $2.5x10^5$ TUBO. All mice were vaccinated with an admix of 50 µg of pGM-CSF and 50 µg of pNeuE2 at 70 and 80 days of age. Primary tumors (~4x6mm) were treated with cryoablation, excision, or sham surgery 4 days after the second vaccination. (B) Tumor growth was monitored over time. (C) Sera was collected for α-neu IgG quantification and area under the curve analysis. **P*<0.05 One-way ANOVA with Tukey's post-test. (D) Mice were monitored for development of spontaneous tumor formation in all ten mammary glands, with any palpable tumor growing considered a failure in spontaneous tumor free survival. ***P*<0.01 Log-rank test.

Cryoablation and CpG combination therapy does not enhance α-neu immunity in NeuT mice. In NeuT mice, cryoablation appears to support an immunosuppressive environment that blunts efficacy of vaccine induced immunity. In attempt to reverse this effect, we used CpG in combination therapy with cryoablation. Additionally, NeuT mice were vaccinated on an accelerated schedule over two days in attempt to bolster vaccine induced immunity. Seventy-five day old female NeuT mice were randomly divided into two groups (n=7/group) and inoculated with $2.5x10^5$ TUBO. All mice were vaccinated with an admix of 60 μg of pGM-CSF and 60 μg of pNeuE2 at 76 and 78 days of age. Primary tumors (~4x7mm) were treated with cryoablation ± CpG at 96 days of age. (Figure2.10A). Tumor growth was monitored until mice reached 180 days of age or until mice were euthanized due to excessive tumor burden (Figure2.10B).

Cryoablation with or without CpG produced similar levels of α-neu Ab (13±4 μg/mL), which peaked at 127 days and declined thereafter (Figure2.10C). Similar protection from spontaneous tumor development was also observed in both groups (Figure2.10D). Two mice in the cryoablation treated group had substantially elevated α-neu Ab levels beginning at 127 days relative to all other mice, which correlated to prolonged protection from spontaneous tumor development. No reason for an increased response in these two mice was found. The addition of CpG to cryoablation in NeuT mice was not able to enhance α-neu Ab or tumor protection relative to cryoablation alone.

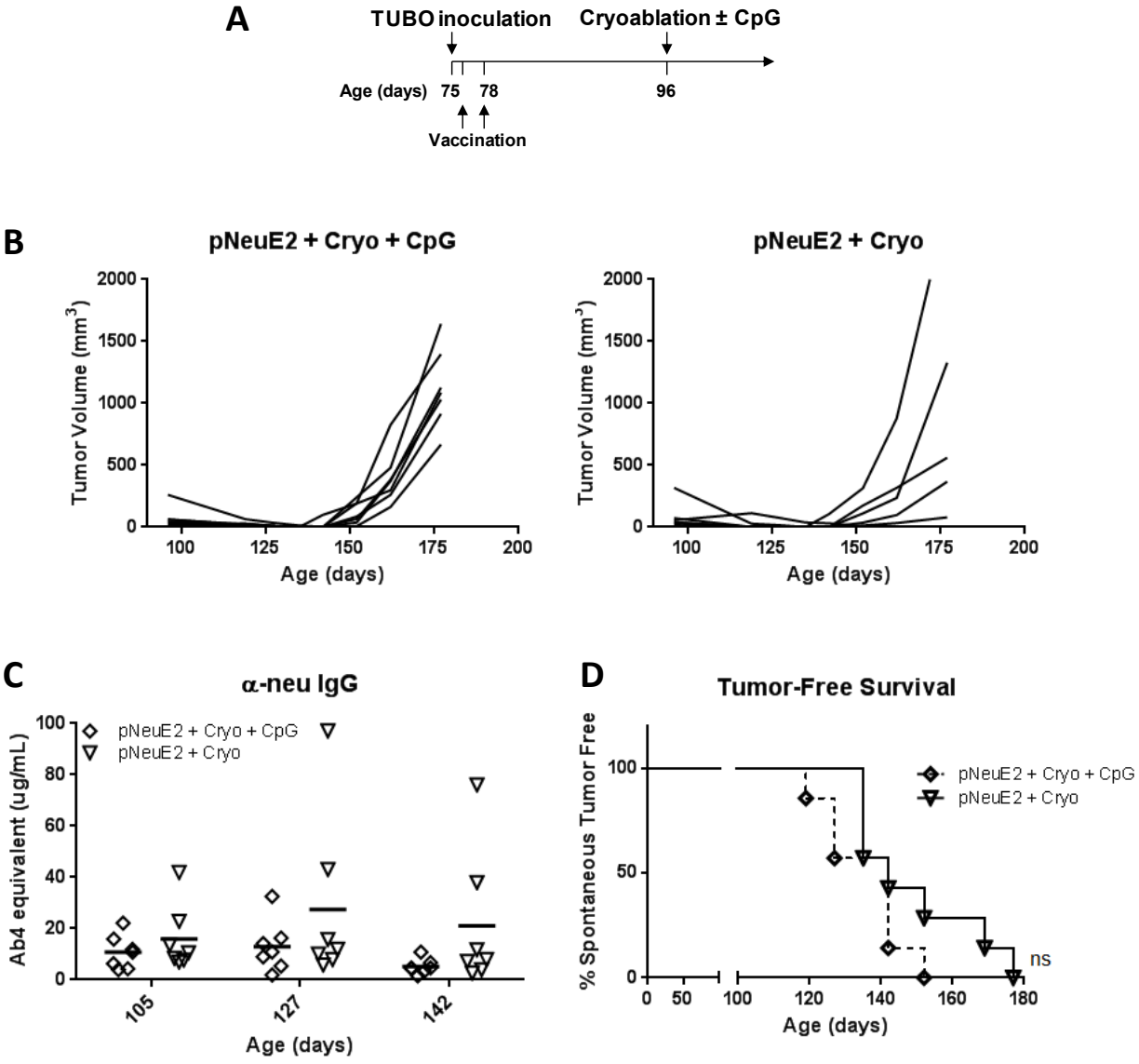

Figure 2.10. CpG does not enhance α-neu immunity in BALB/NeuT mice. (A) Seventy-five day old female BALB/NeuT mice were randomly divided into two groups (n=7/group) and inoculated with $2.5x10^5$ TUBO. All mice were vaccinated with an admix of 60 µg of pGM-CSF and 60 µg of pNeuE2 at 76 and 78 days of age. Primary tumors (~4x7mm) were treated with cryoablation ± CpG at 96 days of age. (B) Tumor growth was monitored over time. (C) Sera was collected for α-neu IgG quantification. Levels between groups were not significantly different. Unpaired t-test. (D) Mice were monitored for development of spontaneous tumor formation in all ten mammary glands, with any palpable tumor growing considered a failure in spontaneous tumor free survival. No significant differences detected - Log-rank test.

DISCUSSION

We found that TUBO, an antigenic tumor, was sensitive to α-neu Ab, which caused regression of established tumors *in vivo*. In BALB/c mice, cryoablation of TUBO induced α-neu Ab, which was capable of protecting over half of mice from subsequent tumor rechallenge, whereas tumor excision did not provide increased tumor protection. The addition of the TLR9 agonist CpG to cryoablation augmented induction of α-neu Ab and protected nearly 100% of mice from tumor rechallenge. Cryoablation upregulated transcripts indicative of a Th2 biased response, which consequently resulted in an IgG1 dominant Ab response. Addition of CpG to cryoablation skewed Ab responses toward IgG2a, suggestive of a Th2 to Th1 shift. Importantly, retrospective analysis of 4 independent experiments found cryoablation of TUBO had resulted in a 26% recurrence rate, which fell to 0% when CpG was used in combination therapy, providing further support for concurrent CpG treatment with cryoablation.

Growth of TUBO in BALB/c mice did not induce α-neu immunity despite high levels of rat neu. Thus, TUBO may resemble human cancers with viral etiology or gene mutations that result in expression of neo-antigens the immune system can recognize but does not without exogenous manipulation (47). The mechanisms of immune escape TUBO utilizes are not fully understood, but our previous studies have found depletion of Tregs was sufficient to mediate tumor regression, suggesting Tregs contribute toward tumor induced immune suppression (95). It is possible immune escape of TUBO is, in part, mediated by tumor STAT3 activity, which is known to be critically involved in tumor mediated expansion and activation of immunosuppressive Tregs, tumors associated macrophages, and myeloid derived suppressor cells (MDSC) (167, 168). In support of this, we have found high transcript levels of granulocyte-colony stimulating factor (G-CSF) in TUBO, which is highly dependent on STAT3 signaling (169), and concomitant increases of MDSC in the spleen (Supplemental Figure1-2). Additionally, an attempt to knock-down STAT3 expression by shRNA silencing in TUBO was

unsuccessful in mediating any decrease in STAT3, indicating its importance to TUBO survival (170). Although TUBO is able to evade immune recognition when left untreated, the physical damage caused by cryoablation results in the release and presentation of neu to induce tumor-specific immunity.

Although cryoablation induced immunity was able to protect ~65% of mice from subsequent tumor rechallenge, it resulted in a Th2 biased response as evident by a dominant IgG1 Ab response. This bias may result from the induction of immunosuppressive factors, such as prostaglandin E2, thymic stromal lymphopoietin, OX40 ligand, TGFβ and IL-10, as present in Figure 2.2. Upregulation of these factors is not unexpected considering the degree of tissue inflammation and subsequent wound healing that is associated with cryoablation (51, 58, 134-136). Cryoablation induced tumor protection was significantly improved with the addition of CpG, which not only elevated α-neu Ab but also skewed the response toward IgG2a, indicative of Th1 biased immunity. These findings are further corroborated by Nierkens and den Brok, who reported similar Th1 induction with CpG treatment (30-34).

Additionally, CpG used in combination with cryoablation decreased recurrences from 26% to 0%, which does not appear to be entirely mediated by systemic α-neu immunity based on cases of mice without tumor recurrence developing new tumor growth at the rechallenge site (Figure2.4C). Therefore, CpG may act to eliminate recurrences by elevating local immune activation in coordination with cryoablation. This process is likely mediated by increased Th1 responses, as seen in chapter 1, which promote cytotoxic activities of effectors, such as cytotoxic lymphocytes, NK cells, and macrophages (46, 47). For example, Kawarada et al reported that repeated peritumoral injection of CpG resulted in inhibition of tumor growth in IE7 fibrosarcoma, B16 melanoma, and 3LL lung carcinoma lines, which was mediated by both NK and tumor-specific $CD8^+$ T cells (171). Furthermore, Haabeth et al found Th1 derived IFNγ rendered macrophages directly cytotoxic to cancer cells and induced them to secrete the

angiostatic chemokines CXCL9 and CXCL10 (48). Taken together, these findings strongly support the incorporation of CpG treatment in cryoablation.

To further evaluate cryoablation's immunostimulatory capacity we treated tumor-bearing tolerant BALB/NeuT females. Cryoablation, with or without CpG, was incapable of inducing α-neu immunity, which was expected considering NeuT mice develop central tolerance against neu. This finding illustrates the necessity of a tumor associated neo-antigen for cryoablation to induce tumor-specific immunity.

Although cryoablation did not induce α-neu immunity in NeuT mice, we hypothesized it may be able to modulate Her2/neu vaccine induced responses due to the release of neu from the treated tumor. Cryoablation did not boost vaccine induced immunity relative to sham treated mice, however, treatment with surgical excision increased Ab levels, which delayed the onset of spontaneous mammary tumors. The disparity between cryoablation and surgical excision treated mice suggest cryoablation exerts a negative impact on vaccine induced responses. If cryoablation did not impact vaccine induced immunity we would expect similar results between cryoablation and excision groups based on the lack of immune induction previously observed with excision (Figure2.4-5). However, it appears tumor excision eliminates a suppressive environment created by the tumor, whereas cryoablation leaves necrotic tumor *in situ* that may promote immunosuppression via upregulation of factors favoring a Th2 biased environment (51, 58, 135, 136). Addition of CpG to cryoablation was unable to improve responses over cryoablation alone, which warrants further efforts to counteract immune suppression induced by cryoablation. Additional therapies targeting Tregs (i.e. α-CTLA-4, α-CD25, and cyclophosphamide) in combination with cryoablation have also shown increased responses in pre-clinical models (31, 35, 36). Thus, treatments targeting both stimulatory and suppressive components of cryoablation may lead to greater tumor protection still.

CHAPTER 3

Cryoablation of Her2-expressing D2F2/E2 Mammary Adenocarcinoma

ABSTRACT

The impact of cryoablation was further tested in the mouse mammary adenocarcinoma D2F2/E2, which was transfected to express wild type human Her2. In contrast to TUBO, D2F2/E2 does not rely on Her2/neu signaling for survival. We show that tumor growth of D2F2/E2 in BALB/c mice, without any manipulation, induces α-Her2 humoral and cell-mediated responses, which fail to slow tumor growth. Thus, we sought to determine if cryoablation affects this endogenous α-Her2 immunity and tumor protection.

In BALB/c mice, cryoablation eliminated D2/F2/E2 tumors with a recurrence rate of ~29%, which could be decreased to 0% if CpG was used in combination therapy. Cryoablation protected approximately 10% and 65% of mice from tumor rechallenge on the contralateral side at 13 and 41 days post-operatively respectively. Combination treatment with cryoablation and CpG protected 33% and 86% of mice respectively. Discrepancy in tumor protection between short and long rechallenge time points is suggestive of transient immunosuppression that dissipates once ablated tumors have been cleared from the host. Systemic α-Her2 cell-mediated responses were not augmented by any treatment. However, Her2 specific Th1 responses (IL-2, IL-12, and IFNγ) were amplified in tumor draining lymph nodes (TDLNs) in mice treated with cryoablation and CpG. Additionally, treatment with cryoablation and CpG skewed α-Her2 antibody (Ab) towards IgG2a when compared with cryoablation alone. Analysis of transcripts in tumor draining lymph nodes after cryoablation showed upregulation of immune regulatory molecules that favor an immunosuppressive environment, which could be reversed with the addition of CpG.

Therefore, an immunogenic D2F2/E2 tumor that is not controlled by the endogenous Her2 specific immunity can be completely ablated with the addition of CpG to cryoablation. Although levels of systemic α-Her2 immunity were not significantly altered, elevated α-Her2 Th1 responses emerged in TDLNs along with IgG2a skewed α-Her2 Ab. Furthermore, an immune suppressive profile in contralateral TDLNs following cryoablation could be reversed with the addition of CpG. These findings warrant the inclusion of CpG or other Th1 promoting adjuvants in combination with cryoablation.

INTRODUCTION

D2F2 is a tumor line derived from a spontaneous mammary tumor that arose in a prolactin induced BALB/c hyperplastic alveolar nodule line D2 (93). D2F2 cells were subsequently transfected with pCMV/E2 encoding wild type human Her2, to produce the D2F2/E2 line (94). Because there is no selective pressure to maintain expression of Her2 *in vivo*, it may potentially be lost. Therefore, a D2F2/E2 subline with stable Her2 expression was selected by passaging D2F2/E2 in BALB/c. We have previously reported that a parallel tumor line, D2F2/neu, which was transfected to express mutant neu, was relatively insensitive to α-neu antibody (Ab) (157). Similarly, we show D2F2/E2 is uninhibited by α-Her Ab, and inoculation of BALB/c mice with D2F2/E2 results in induction of α-Her2 antibody (Ab). Furthermore, splenocytes from D2F2/E2 bearing mice have low basal levels of α-Her2 IFNγ activity relative to naïve mice. Although D2F2/E2 induces endogenous α-Her2 immunity in BALB/c mice, it is not sufficient to inhibit tumor growth. We hypothesized that cryoablation augments endogenous α-Her2 immunity to provide increased tumor protection.

RESULTS

D2F2/E2 mammary adenocarcinoma induces α-Her2 immunity endogenously without exogenous manipulation. To test if D2F2/E2 induced Her-2 specific immune responses, BALB/c mice were inoculated with $2.5x10^5$ cells of D2F2/E2 cells which were allowed to grow for thirteen days before initial sera and tumor measurements were collected (day 0). Additional sera and tumor measurements were collected at day 8, 17, 24, and 30 (Figure3.1A). Tumor growth correlated with a parallel increase in α-Her2 Ab, which reached 102±9 μg/mL on day 30, but did not inhibit tumor progression (Figure3.1B). Since D2F2/E2 cells are likely resistant to Ab, similar to D2F2/neu, we tested for the presence of α-Her2 cell-mediated immunity. Spleens from 3 mice were collected at day 17 for α-Her2 IFNγ ELISPOT analysis. Spleens from naïve BALB/c mice were also collected as a negative control. Splenocytes were isolated and stimulated for 48 hours with either 3T3/EKB, which stably express K^d, B7.1, and Her2 (EKB only), or control 3T3/KB cells. Tumor-bearing mice had a significantly elevated IFNγ response relative to naïve mice when stimulated with 3T3/EKB cells (Figure3.1C). Together these data indicate that D2F2/E2 induces endogenous α-Her2 humoral and cell-mediated immunity in BALB/c mice, but failed to control tumor growth.

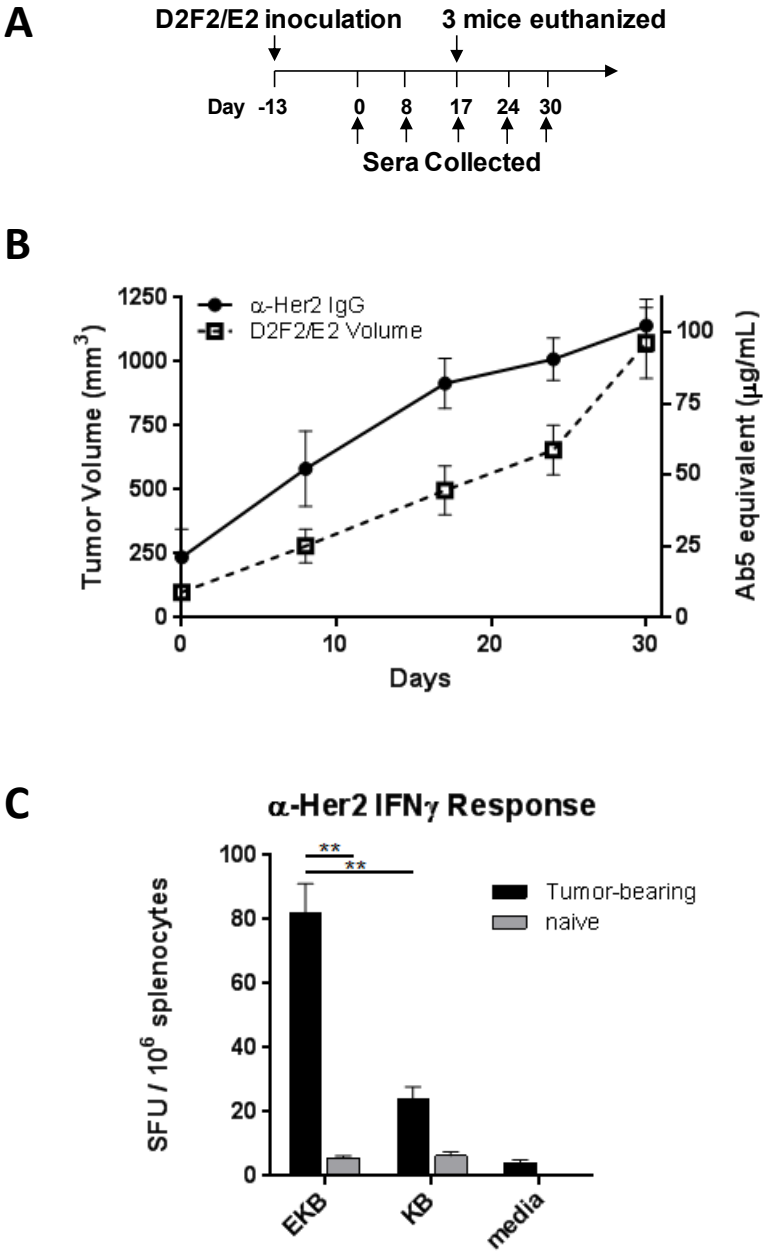

Figure 3.1. Growth of D2F2/E2 mammary adenocarcinoma induces α-Her2 immunity endogenously. (A) BALB/c mice were inoculated with $2.5x10^5$ cells of D2F2/E2 mammary adenocarcinoma which were allowed to grow for thirteen days (~4x7 mm) before initial sera and tumor measurements were collected (day 0). Additional sera and tumor measurements were collected on days 0, 8, 17, 24, and 30 (n=9). (B) α-Her2 IgG levels were quantified and correlated with tumor volume. D2F2/E2 volume (mm^3) and α-Her2 IgG (Ab5 equivalent µg/mL) are plotted on the left and right y-axis respectively. (C) Both naïve mice and tumor-bearing mice were euthanized at day 17 to collect spleens for IFNγ ELISPOT (n=3/group). Splenocytes were isolated and stimulated with either 3T3/EKB or 3T3/KB for 48hr. Results expressed as spot forming units (SFU). ***P*<0.01 Unpaired t-test.

Peritumoral injection of CpG oligodeoxynucleotide (CpG) with cryoablation reduces recurrences. Similar to cryoablation of TUBO, a portion of cryoablated D2F2/E2 tumors recurred. Since CpG in combination with cryoablation resulted in no recurrences, the same was tested in D2F2/E2. Tumor recurrence data from mice treated with either cryoablation alone (n=24) or combination therapy of cryoablation and CpG (n=25) were compiled from 4 independent experiments. Mice from each experiment were treated when tumor dimensions reached approximately 4x7 mm in size, after which they were monitored for recurrence at the treated location at least 30 days post-operatively and as long as 60 days (Figure3.2). Comparable to TUBO, cryoablation resulted in an overall recurrence rate of ~29%, with tumor recurrences detected between 24-58 days post-operatively. Surgical excision of similar size tumors, along with adjacent mammary tissue, produced no observed recurrences (n=23) (data not shown). Cryoablation and CpG combination therapy reduced the recurrence rate to 0%, indicating that CpG elevates localized anti-tumor immunity or modifies the tumor microenvironment to prevent recurrences, further supporting the role of CpG in combination therapy with cryoablation.

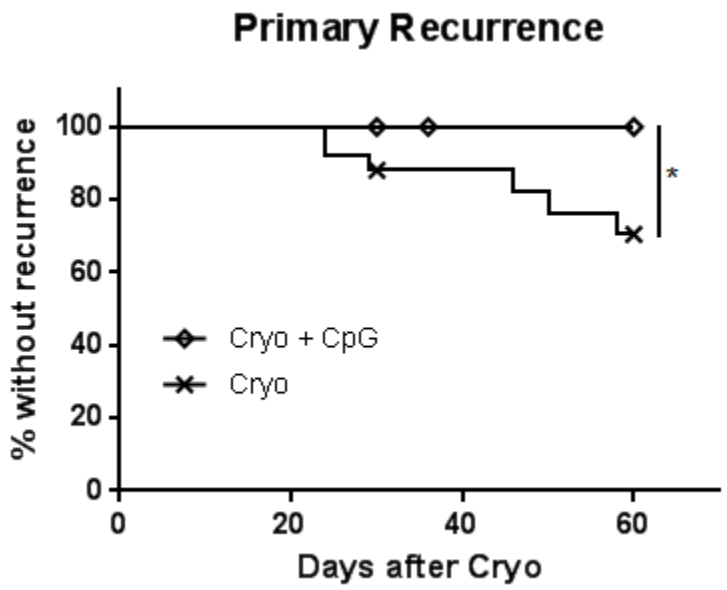

Figure 3.2. Cryoablation + CpG protects against primary recurrences. Results pooled from 4 independent experiments with all mice monitored at least 30 days after cryoablation for primary recurrence – Cryo + CpG (n=24) Cryo (n=25). Symbols indicate censored subjects due to experimental endpoint. *P<0.05 Log-rank test.

Systemic tumor protection does not occur before resolution of cryoablated tumors. BALB/c mice were inoculated with $2.5x10^5$ D2F2/E2 cells which were allowed to grow until the tumor measured ~4x7 mm in diameter. Tumors were treated with cryoablation ± peritumoral CpG, surgical excision, peritumoral CpG injection, or left untreated (n=6-9) and monitored for 30 days (Figure3.3A). All tumors treated with cryoablation ± peritumoral CpG or surgical excision completely regressed by day 30 with the exception of two mice in the cryoablation group that developed recurrent growth at day 24. CpG treatment alone did not significantly change tumor growth relative to untreated mice (Figure3.3B). To test if cryoablation resulted in protective immunity, mice were rechallenged with $2.5x10^5$ D2F2/E2 cells on the contralateral side 13 days post-operatively, while the ablated tumor was undergoing clearance. An additional group of naïve mice also received D2F2/E2 inoculation as a control (n=10). Mice were monitored for an additional 17 days after the rechallenge for tumor growth.

Naïve mice, as well as tumor-bearing mice in CpG and untreated groups, developed tumors at the rechallenge site, indicating that endogenous α-Her2 immunity induced in D2F2/E2-bearing mice is insufficient to reject tumor challenge at a distant site (Figure3.3C). However, rechallenge tumor growth was significantly delayed in untreated tumor bearing mice relative to naïve mice, suggesting that tumor induced α-Her2 immunity has a partial inhibitory effect (Figure3.3D-E). When primary tumors were treated with cryoablation or excision, 1/9 and 3/7 mice were protected respectively. However, when CpG was used in combination with cryoablation 8/17 mice were protected, although the increase was not significant (p=0.09). Rechallenge tumors that did grow in cryoablation ± CpG treated mice grew at comparable rates to untreated mice, while tumors in the excision group grew significantly slower than other groups (Figure3.3C). These results suggest tumor induced α-Her2 immunity may be too weak to elicit tumor regression due to concurrent tumor related immunosuppression. Procedures that debulk the primary tumor appear to be beneficial in relieving tumor induced immunosuppression, thus supporting endogenous anti-tumor immunity and promoting greater tumor protection. However,

tissue inflammation resulting from cryoablation may also contribute to increased immune suppression as evident by increased growth in rechallenge tumors relative to excision treated mice. The addition of CpG to cryoablation may partially abrogate immune suppression as discussed in chapter 1 and 2.

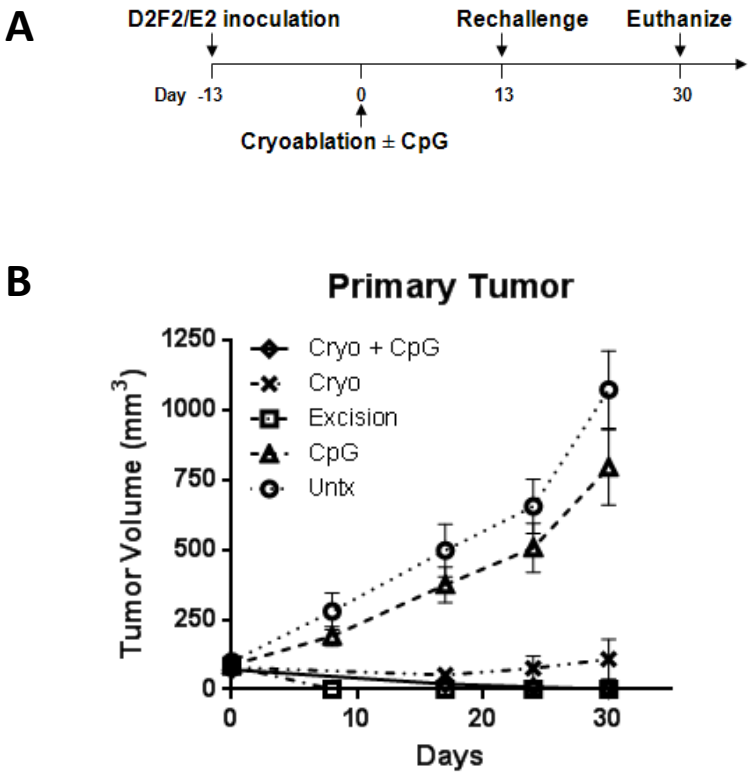

Figure 3.3. Systemic tumor protection does not occur before resolution of cryoablated tumors. (A) Experimental scheme outlining timing of tumor inoculation and treatment. Thirteen days after inoculation D2F2/E2 mammary adenocarcinomas (~4x7mm) were treated with cryoablation ± peritumoral CpG, tumor excision, peritumoral CpG injection, or left untreated (n= 6-9). (B) Primary tumor growth of D2F2/E2 was monitored over time showing untreated mice and CpG treated mice with progressive tumor growth. Continued

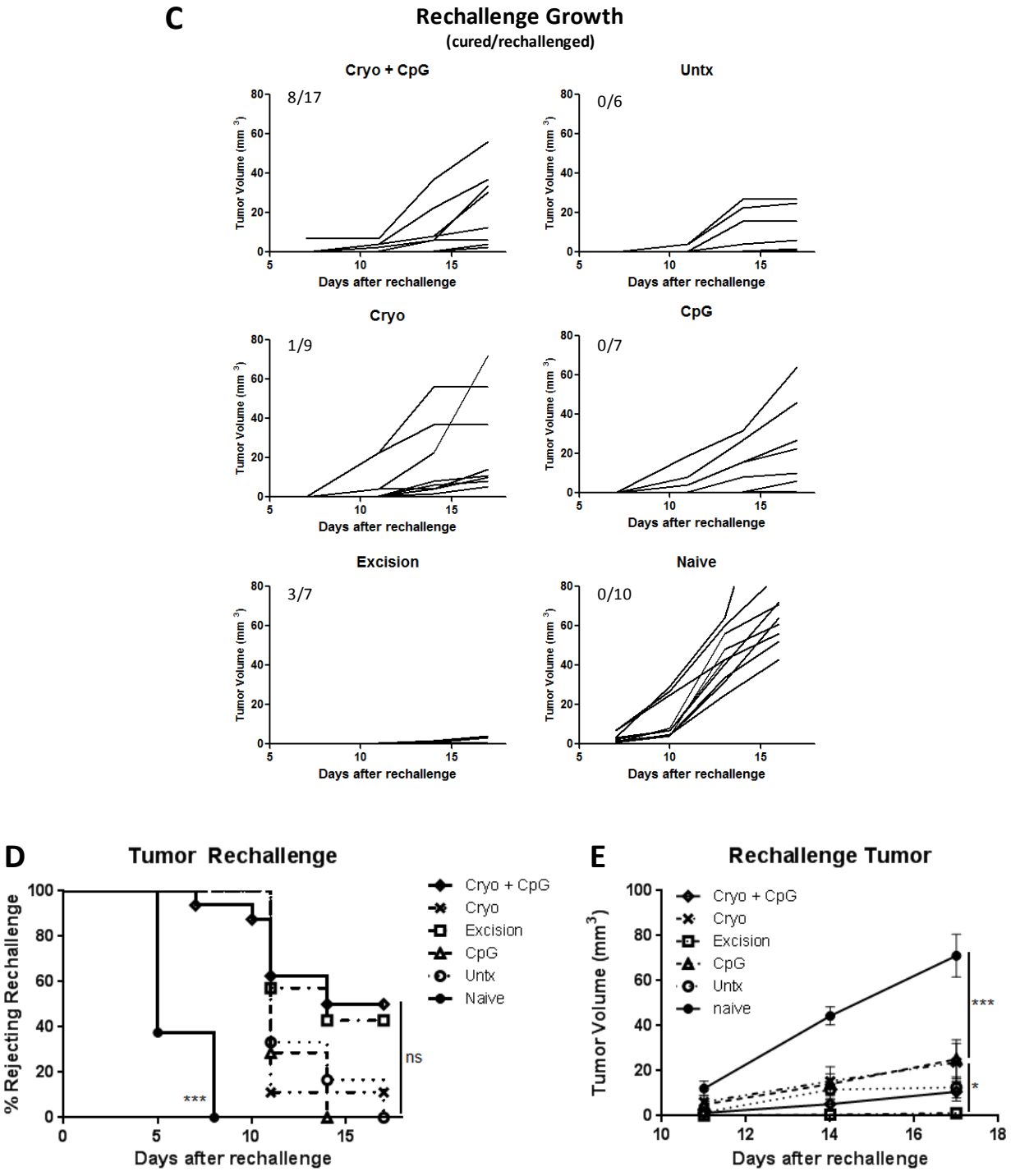

Figure 3.3. Systemic tumor protection does not occur before resolution of cryoablated tumors. (C) Thirteen days later, mice were rechallenged with $2.5x10^5$ D2F2/E2 on the contralateral side. Mice were monitored for tumor growth over the course of 17 days, with any palpable tumor growing considered a failure in tumor protection. Number of mice (cured/rechallenged) shown. (D) Percent of mice rejecting tumor rechallenge. ***P<0.001 Log-rank test. (E) Mean rechallenge tumor volume. *P<0.05 ***P<0.001 One-way ANOVA with Sidak's multiple comparisons test. Data pooled from two independent experiments.

Protective tumor immunity is present after complete resolution of the primary tumor. Because cryoablation did not enhance protective α-Her2 immunity before ablated tumors had been cleared from mice (Figure3.3), we sought to determine if protection changed once treated tumors had fully resolved. BALB/c mice were inoculated with $2.5x10^5$ cells of D2F2/E2 cells which were allowed to grow until they measured ~4x7 mm in diameter. Tumors were treated with cryoablation ± peritumoral CpG, tumor excision, peritumoral CpG injection, or sham surgery (n=6-7) and monitored for 41 days (Figure3.4A). All tumors treated with cryoablation ± peritumoral CpG or surgical excision completely regressed by day 41 with the exception of one mouse in the cryoablation group that developed a recurrence appearing at day 29. CpG treatment alone did not significantly change tumor growth relative to untreated mice (Figure3.4B). Forty-one days post-operatively all tumor free mice were rechallenged with $2.5x10^5$ D2F2/E2 cells on the contralateral side. An additional group of naïve mice also received D2F2/E2 inoculation as a control (n=8). Mice were monitored for an additional 18 days after the rechallenge for tumor growth.

As expected, all naïve mice developed palpable tumors 5-8 days after inoculation. Tumor excision (5/7), cryoablation (4/5), and cryoablation with CpG (6/7) treatments protected similar percentages of mice, which was significantly higher than naïve mice (Figure3.4C-D). Rechallenge tumors that did grow in treated groups had significantly delayed growth relative to naïve mice, and grew at comparable rates to one another with the exception of a rapid growing tumor in the excision group and a small stable tumor in the cryoablation + CpG group. These results indicate that D2F2/E2 induced immunity renders systemic protection once the primary tumor is cryoablated, but the effect is evident only after the necrotic tumor has completely resolved. Tumor excision produces comparable protection to cryoablation in this case as well. The discrepancy in tumor protection before and after resolution of the ablated tumor suggests cryoablation may cause transient immunosuppression (Figure3.3), which subsides once the tumor is cleared. Thus, to develop treatment strategies that compliment cryoablation in patients,

we examined the immune activation or suppressive mechanisms induced by cryoablation of D2F2/E2 tumors.

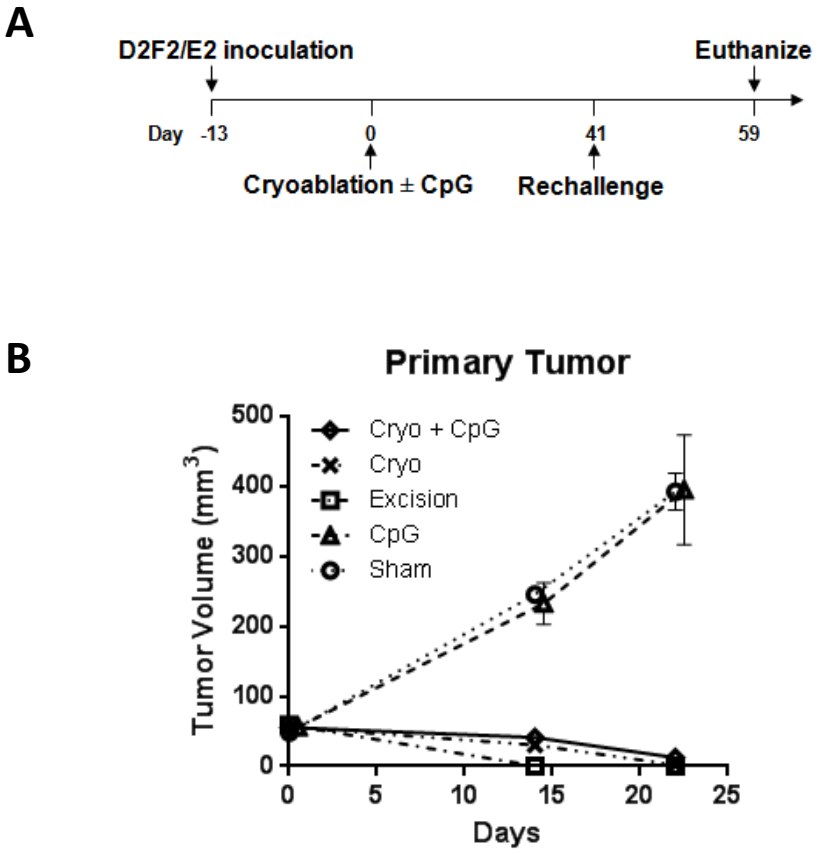

Figure 3.4. Cryoablation renders systemic protection after resolution of the treated tumor. (A) Experimental scheme outlining timing of tumor inoculation and treatments. Thirteen days after inoculation, D2F2/E2 mammary adenocarcinomas (~4x7mm) were treated with cryoablation with or without peritumoral CpG, tumor excision, peritumoral CpG injection, or sham surgery (n= 6-7). (B) Primary tumor growth of D2F2/E2 was monitored over time showing that mice treated with CpG or left untreated continued to have progressive tumor growth. Continued

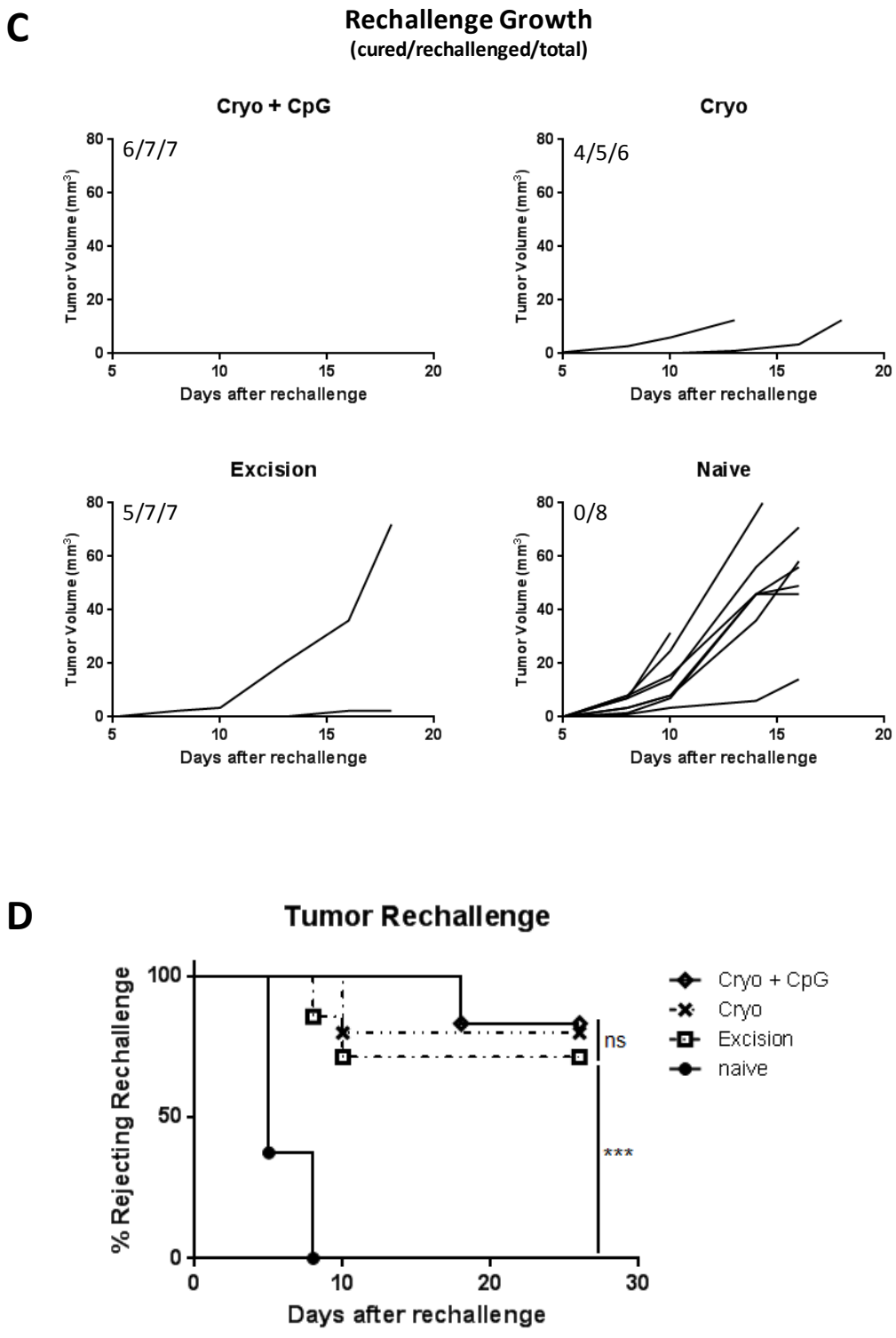

Figure 3.4. Tumor removal provides long term tumor protection. (C) Once cryoablated tumors had fully resolved (41 days), all tumor free mice were rechallenged with D2F2/E2 on the contralateral side. Mice were monitored for tumor growth over the course of 18 days, with any palpable tumor growing considered a failure in tumor protection. Number of mice protected shown. (D) Percent of mice rejecting tumor rechallenge. ****P*<0.001 Log-rank test.

Endogenous α-Her2 cell-mediated responses remain elevated after tumor removal. TDLNs from the rechallenged region were collected from mice in the previous experiment 59 days post-operatively. Single cell suspensions were prepared from TDLN and stimulated for 48 hours with 3T3/EKB. Supernatents were collected and analyzed with magnetic-bead protein multiplexing to detect GM-CSF, IFNγ, IL-1β, IL-2, IL-4, IL-5, IL-6, IL-10, IL-12 (p40/p70), and TNF-α, or TGFβ by ELISA. Mice treated with cryoablation ± CpG or tumor excision produced comparable results for all cytokines measured, however, these groups had significantly higher levels of IL-1β, IL-2, IL-4, IL-6, IL-10, IFNγ, TNFα, and GM-CSF relative to naïve mice, indicative of elevated endogenous α-Her2 immunity (Figure3.5). Together, these data indicate cryoablation or tumor excision promote systemic tumor immunity and protection, which is mediated by removal of the primary tumor.

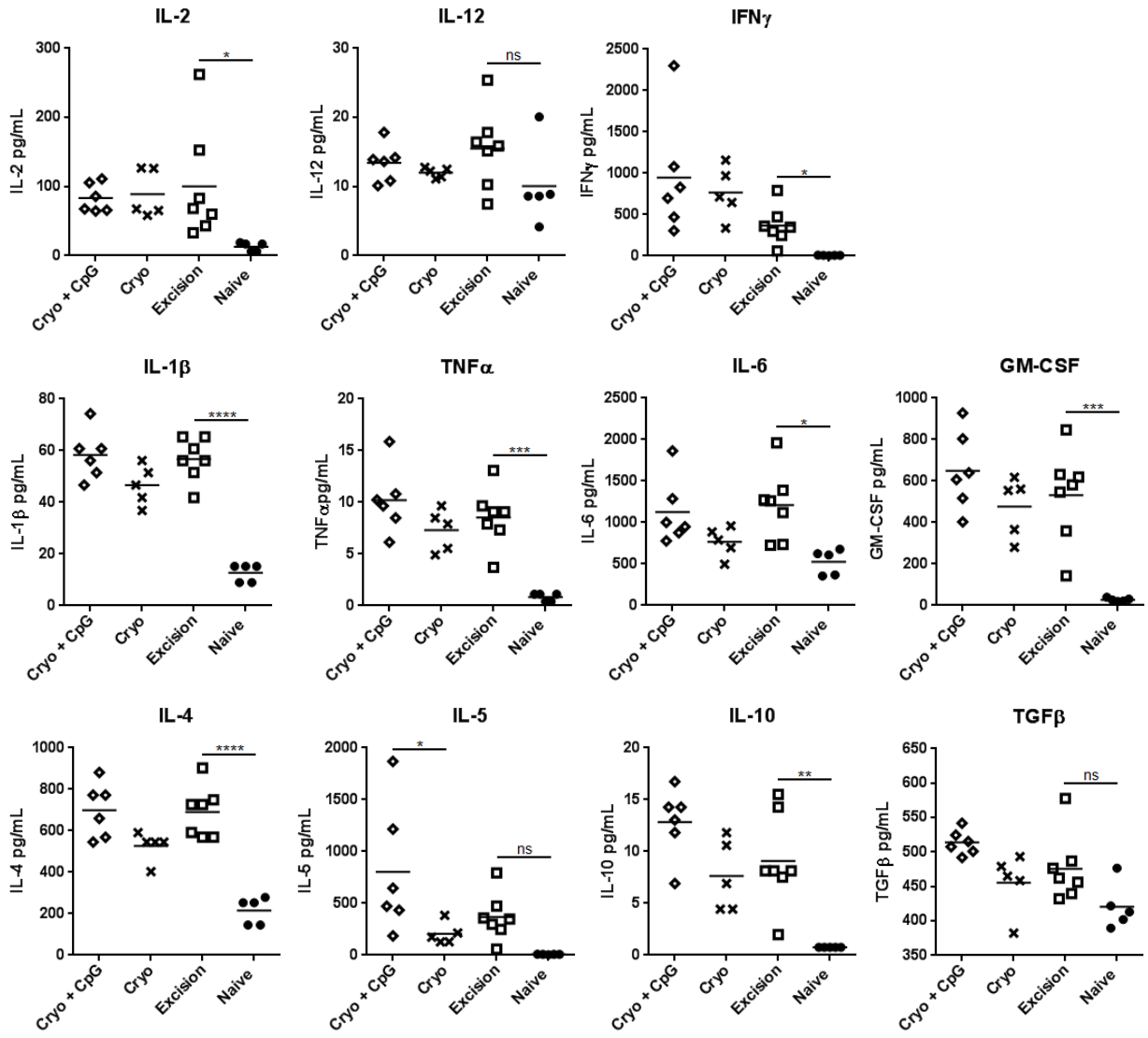

Figure 3.5. Endogenous α-Her2 immunity remains elevated after tumor removal. All mice rechallenged with tumor were euthanized 59 days post-operatively to collect TDLN from the tumor rechallenge region. TDLN from naïve mice were also collected as a negative control. $8x10^5$ LN cells were co-cultured with $8x10^4$ 3T3/EKB cells in a total volume of 0.5mL of 10% FBS RPMI at 10% CO_2 37˚C for 48 hours. Supernatents were collected and analyzed with Magpix based multiplexing. **P*<0.05 ***P*<0.01 ****P*<0.001 *****P*<0.0001 One-way ANOVA with Tukey's post-test.

Cryoablation does not diminish systemic α-Her2 immunity induced by D2F2/E2. To determine if cryoablation affects α-Her2 cell-mediated responses induced by the tumor, mice from Figure 3.3 were euthanized at day 30 to harvest spleens. Splenocytes were isolated and stimulated for 48 hours with either 3T3/EKB or 3T3/KB to assess IFNγ production by ELISPOT. All treatments produced a similar response, which was significantly higher than naïve mice (50-200 SFU) (Figure3.6A). All tumor-bearing mice had with a low level of α-Her2 Ab at the time of treatment when tumors were ~4x7 mm. In mice treated with excision, α-Her2 Ab levels plateaued (16±4 μg/mL) beginning 8 days post-operatively, whereas Ab continued to rise in mice treated with cryoablation (32±8 μg/mL) or cryoablation + CpG (45±7 μg/mL) until day 24 (Figure3.4B). Mice with untreated tumors had continuous induction of α-Her2 Ab (102±9 μg/mL) that correlated with tumor growth (Figure3.1B). Area under the curve (AUC) analysis found a significant difference between cryoablation + CpG and excision groups, with no difference between cryoablation and excision groups. IgG2a and IgG1 subclasses were also assessed using AUC analysis to assess Th1 or Th2 imbalance. Combination therapy of cryoablation and CpG significantly elevated IgG2a levels above cryoablation alone but did not impact IgG1 levels (Figure3.6C-D). Cryoablation did not significantly modulate α-Her2 cell-mediated responses relative to other groups, but α-Her2 IgG2a was significantly elevated when CpG was included in the regimen. These results indicate cryoablation did not compromise systemic tumor induced α-Her2 immunity, and with CpG, promotes a Th1 response.

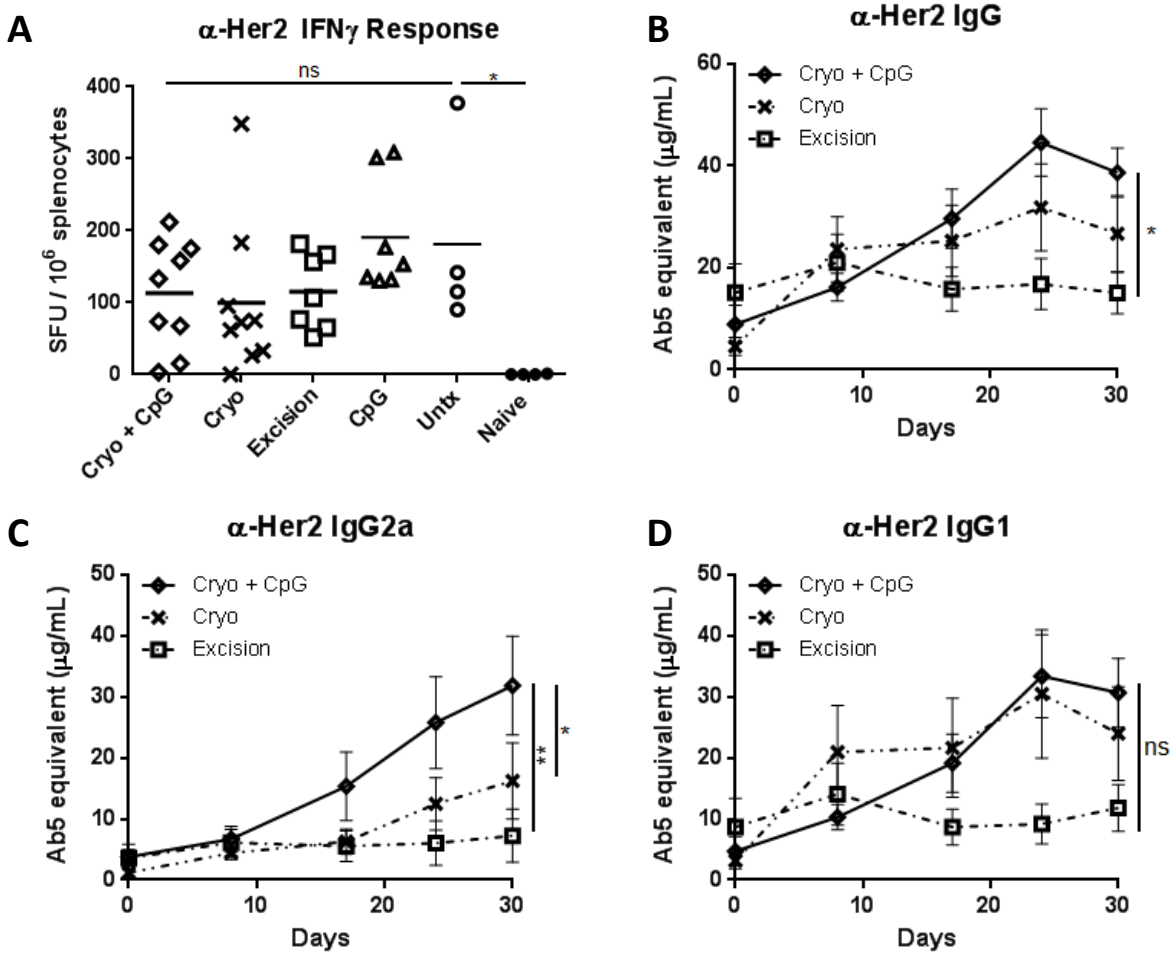

Figure 3.6. Cryoablatio does not diminish systemic α-Her2 immunity induced by D2F2/E2. (A) Spleens were harvested 30 days after cryoablation for IFNγ ELISPOT. Splenocytes were isolated and stimulated with either EKB or KB 3T3 lines for 48hr in an IFNγ ELISPOT. Results quantified in spot forming units (SFU) with KB subtracted from EKB. (B) Sera was collected throughout the experiment for α-Her2 IgG quantification. (C) IgG2a and (D) IgG1 levels at day 30. **P* <0.05 ***P* <0.01 One-way ANOVA with Tukey's post-test.

Cryoablation induces transcripts that favor a Th2 environment. To further characterize differences in systemic immunity induced by cryoablation with or without CpG we evaluated a panel of immune-related transcripts in tumor draining lymph nodes (TDLN) from mice in Figure 3.3 at day 30. Cryoablation alone upregulated TNFα, TGFβ, Foxp3, and IL-10 transcripts above all other treatments (Figure3.7). Interestingly, the addition of CpG to cryoablation reversed these changes, while increasing the chemokine CCL2 (monocyte chemotactic protein-1), which recruits monocytes, activated memory T-cells, and DCs (172, 173). Additionally, IFNγ levels were decreased in mice treated with cryoablation + CpG relative to untreated mice, which may be the result of transcriptional negative feedback due to high protein levels. Levels of Th2 promoting factors IL-4, IL-13, and Ptges (prostaglandin E synthase) were higher in mice without tumor debulking. These findings suggest that untreated tumors promote Th2 biased endogenous immunity, which can partially be abrogated by cryoablation and tumor exision. However, cryoablation alone increased levels of immunosuppressive cytokines (IL-10 and TGFβ) which were reversed with the addition of CpG, further supporting the role of CpG in promoting Th1 responses.

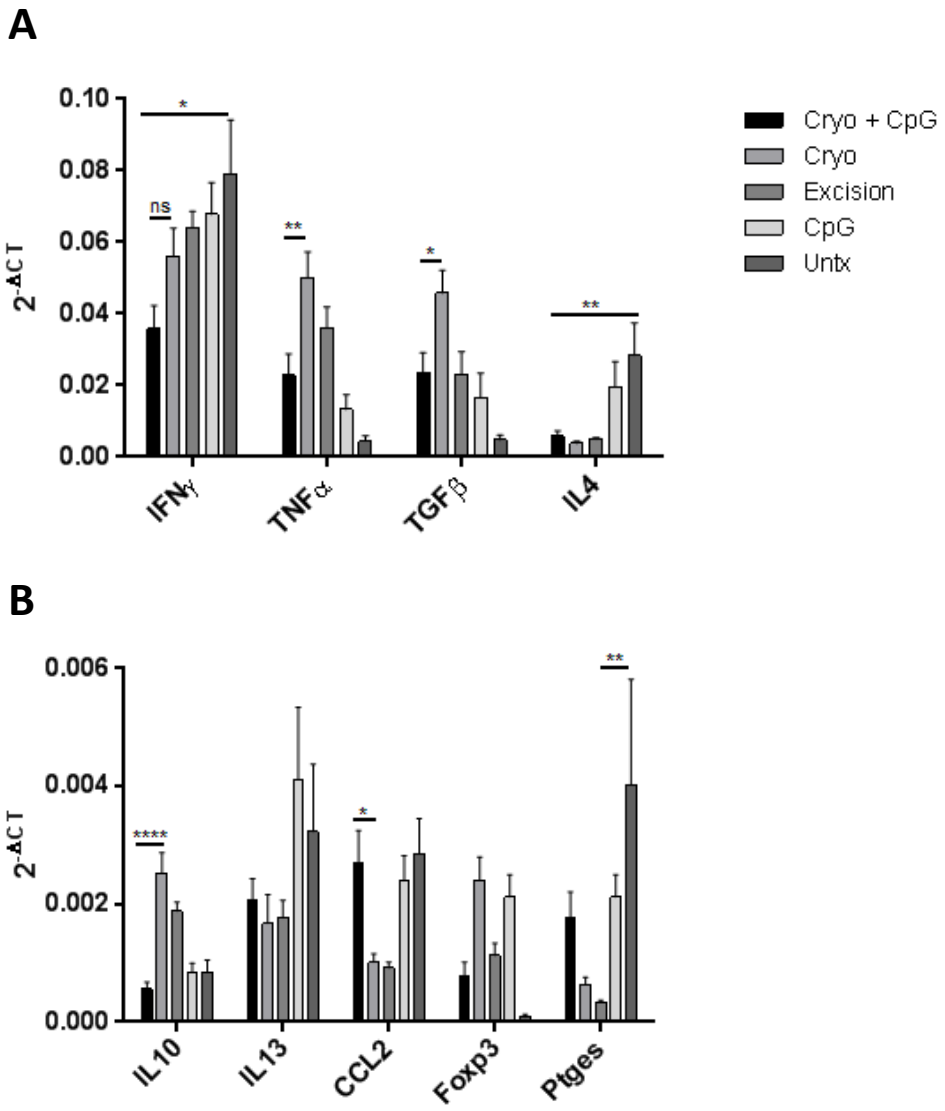

Figure 3.7. Addition of CpG to cryoablation reduces transcript levels of key suppressive factors. Tumor draining lymph nodes (TDLN) from the treated tumor were harvested 30 days post-operatively and lymphocytes stimulated for 3 hr using PMA / ionomycin. RNA was isolated for cDNA synthesis and subsequent qPCR analysis. Expression of each gene was normalized to B2M and is expressed as fold increase ($2^{-\Delta CT}$) (n=6-9). (A) $2^{-\Delta CT}$ axis range 0 - 0.10 (B) axis range 0 - 0.006. **P*<0.05 ***P*<0.01 *****P*<0.0001 One-way ANOVA with Tukey's post-test.

Cryoablation does not compromise cell-mediated α-Her2 immunity. To further analyze the impact of cryoablation on α-Her2 immunity we investigated whether cell-mediated responses in TDLN and spleen were affected 12 days post-operatively. BALB/c mice were inoculated with $2.5x10^5$ cells of D2F2/E2 cells which were allowed to grow until they measured ~4x7 mm in diameter. Tumors were treated with cryoablation ± peritumoral CpG, tumor excision, or sham surgery (n=6) (Figure3.8A). Splenocytes and LN cells were isolated and stimulated for 48 hours with 3T3/EKB. Supernatents were collected and analyzed with magnetic-bead protein multiplexing to detect GM-CSF, IFNγ, IL-1β, IL-2, IL-4, IL-5, IL-6, IL-10, IL-13, IL-12 (p40/p70), IL-17, CXCL10, MIP-1α, and TNF-α, or TGFβ by ELISA.

Splenocytes produced comparable responses between all groups, with the exception of small differences in IL-6 and GM-CSF between untreated and cryoablation + CpG treated mice (Figure3.8B). Conversely, within TDLNs, cryoablation in combination with CpG significantly elevated Her2 specific levels of IL-2, IL-12, IFNγ, CXCL10, MIP-1α, IL-4, and IL-13 (Figure3.8C). Elevation of IL-2, IL-12, and IFNγ are indicative of an active response biased toward Th1 immunity, with chemokines CXCL10 and MIP-1α (CCL3) likely upregulated in response to increased levels of IFNγ or IFNα/β (174-176). IL-4 and IL-13 were also moderately elevated, implicating activation of multiple pathways. Serum cytokine levels were at low or undetectable levels for the majority of targets except for IL-12 and TNFα, which were significantly increased with cryoablation and CpG treatment (Figure3.8D). Together, these data indicate cryoablation alone does not alter tumor induced α-Her2 cell-mediated immunity within regional or distant lymphoid tissues, but with the addition of CpG promotes a Th1 biased response in the regional TDLN.

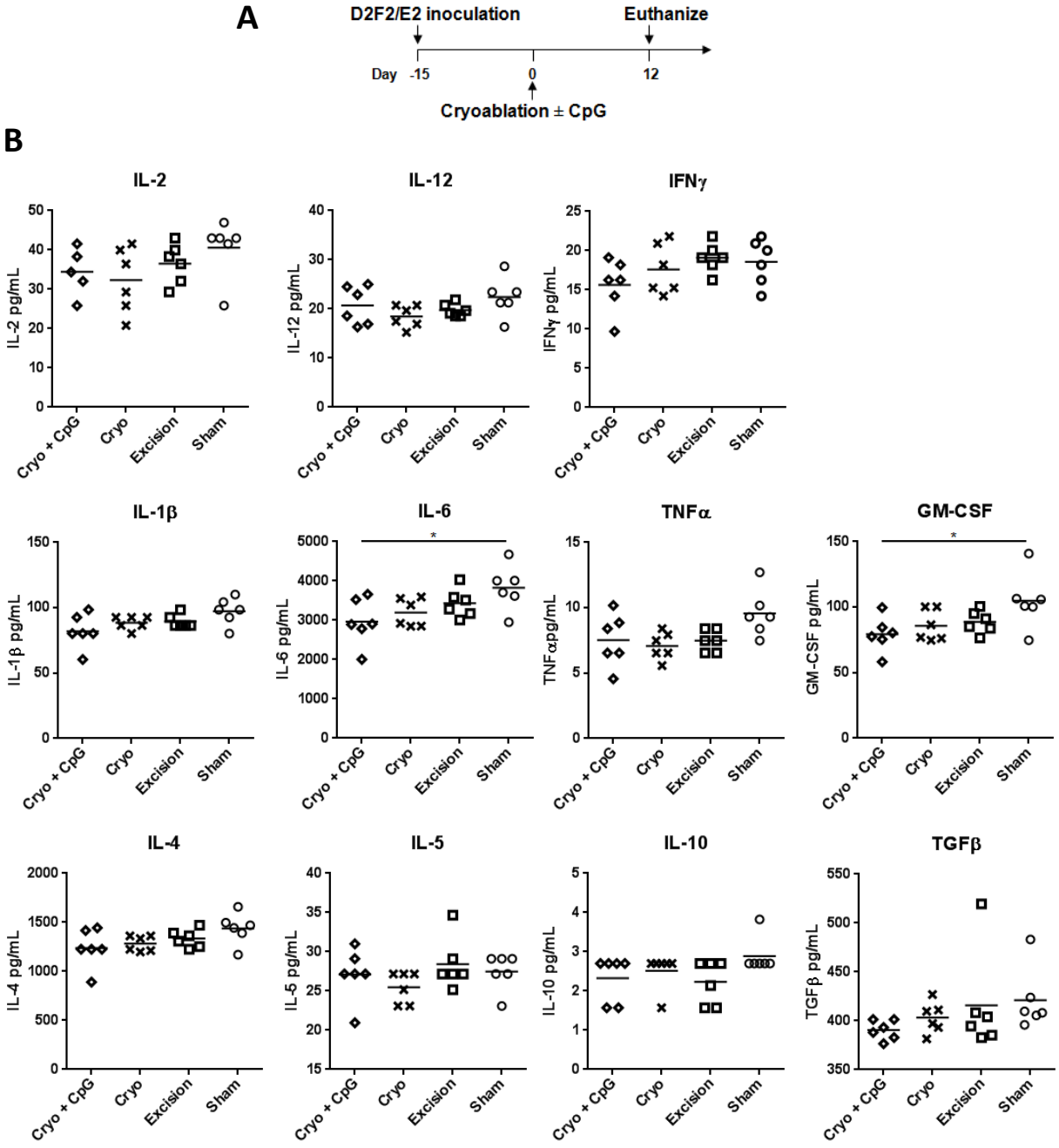

Figure 3.8. Cryoablation does not compromise cell-mediated α-Her2 immunity. (A) Experimental scheme outlining timing of tumor inoculation and treatments. Fifteen days after inoculation, D2F2/E2 mammary adenocarcinomas (~4x7mm) were treated with cryoablation ± peritumoral CpG, tumor excision, or sham surgery (n=6/group). Mice were euthanized 12 days post-operatively for spleen, TDLN, and sera collection. (B) $8x10^5$ splenocytes were co-cultured with $8x10^4$ 3T3/EKB cells in a total volume of 0.5mL of 10% FBS RPMI at 10% CO_2 37˚C for 48 hours. Supernatents were collected and analyzed with Magpix based multiplexing. (C) TDLN co-culture – same setup as described above. (D) Magpix of 12d sera. *P<0.05 **P<0.01 ***P<0.001 One-way ANOVA with Tukey's post-test. Continued

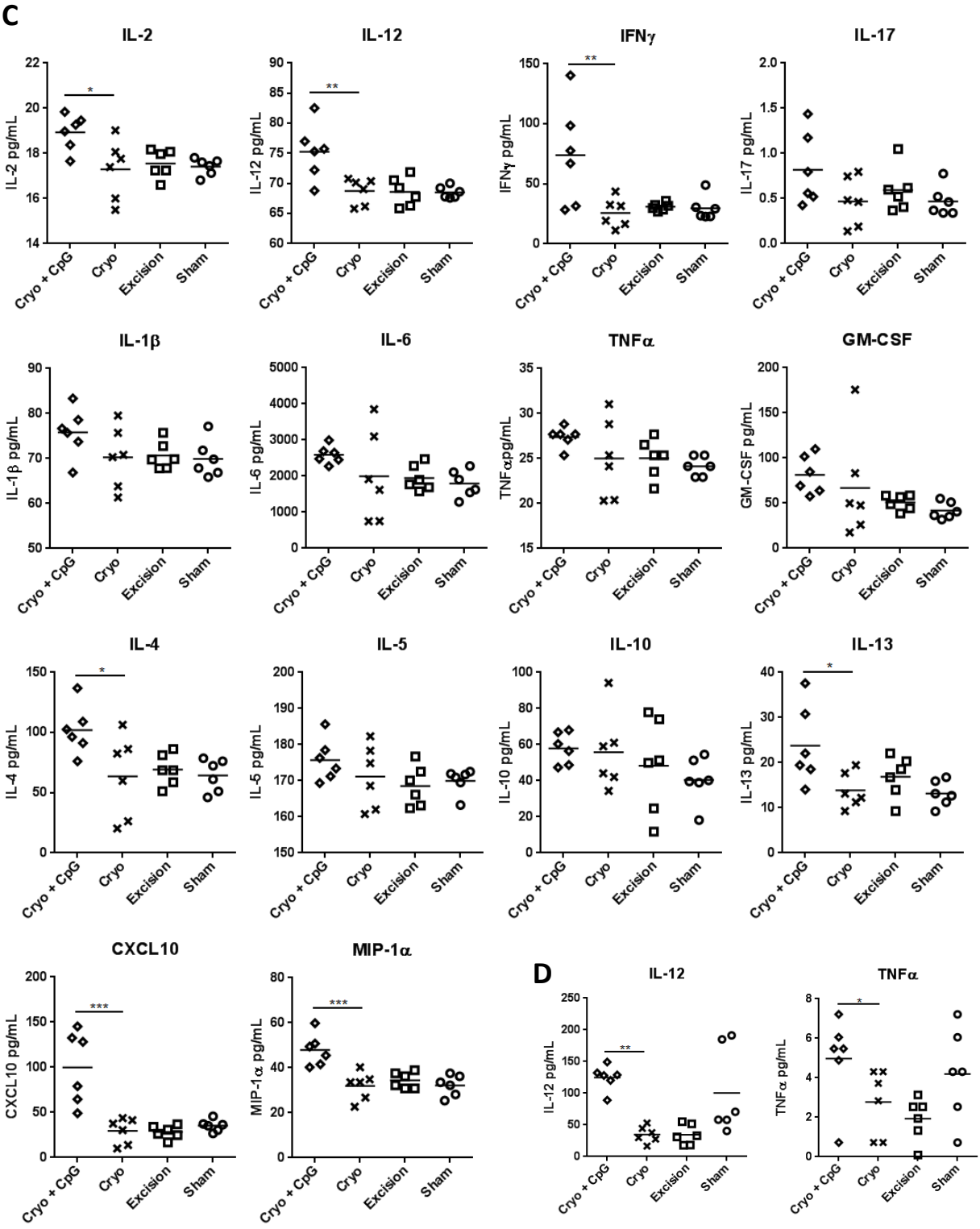
C
IL-2
IL-2 pg/mL
IL-12
IL-12 pg/mL
IFNγ
IFNγ pg/mL
IL-17
IL-17 pg/mL
IL-1β
IL-1β pg/mL
IL-6
IL-6 pg/mL
TNFα
TNFαpg/mL
GM-CSF
GM-CSF pg/mL
IL-4
IL-4 pg/mL
IL-5
IL-5 pg/mL
IL-10
IL-10 pg/mL
IL-13
IL-13 pg/mL
CXCL10
CXCL10 pg/mL
MIP-1α
MIP-1α pg/mL
Cryo + CpG
Cryo
Excision
Sham
D
IL-12
IL-12 pg/mL
TNFα
TNFα pg/mL

Cryoablation does not promote expansion of T-regulatory cells (Tregs) in circulation. Peripheral blood mononuclear cells (PBMCs) were collected from the previous experiment at day 12 to measure Treg populations by flow cytometry analysis, which were identified as $CD4^+$ $CD25^+$ $Foxp3^+$ cells. The percentage of Tregs present in total PBMCs (Figure3.9A) and total $CD4^+$ cells (Figure3.9B) were not different between treatment groups, indicating cryoablation, with or without CpG, did not affect circulating Treg populations 12 days post-operatively.

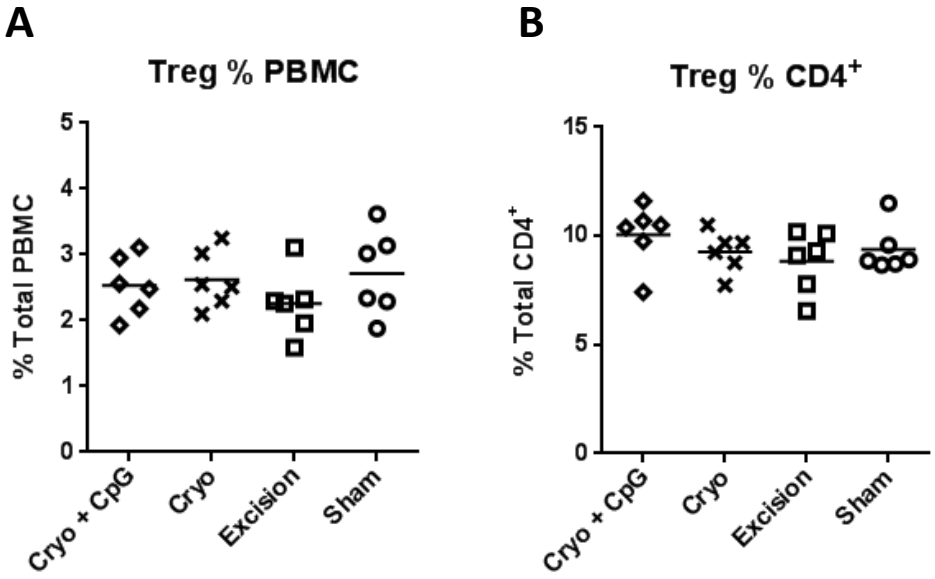

Figure 3.9. Cryoablation does not increase circulating Tregs. Fifteen days after inoculation, D2F2/E2 mammary adenocarcinomas (~4x7mm) were treated with cryoablation ± peritumoral CpG, tumor excision, or sham surgery (n=6/group). Mice were euthanized 12 days post-operatively for PBMC collection. Cells were stained for CD4, CD25, and Foxp3 for flow cytometry analysis. Tregs were identified as $CD4^+$ $CD25^+$ $Foxp3^+$ cells. (A) Percentage of Tregs in total PBMCs and (B) percentage among $CD4^+$ cells.

DISCUSSION

Similar to TUBO, D2F2/E2 expresses a tumor associated antigen the immune system can recognize. In contrast, D2F2/E2 is resistant to antigen specific Ab, and rejection, is in part dependent on cytotoxic T-cell activity (177). Additionally, D2F2/E2 does not rely on Her2/neu signaling for survival or growth, and only expresses Her2 due to stable transfection. Thus, D2F2/E2 may be representative of $Her2^{+}$ tumors which become resistant to Herceptin (Trastuzumab) and generate alternative survival pathways (i.e. phosphatidylinositol 3-kinase/Akt) (140).

We show that tumor growth of D2F2/E2 in BALB/c mice, without any manipulation, induces α-Her2 humoral and cell-mediated responses, indicating Her2 is actively presented and processed by the immune system from a growing D2F2/E2 tumor. However, resulting α-Her2 immunity was not sufficient to mediate regression of the primary tumor and also failed to protect mice from tumor challenge at a distant site 2 weeks post-treatment. Growth of tumors inoculated on the contralateral side were significantly delayed in tumor-bearing mice relative to naïve mice, indicating tumor induce α-Her2 immunity partially inhibits tumor growth (Figure3.3). This finding contends that tumor induced α-Her2 immunity is beneficial but may be too weak to mediate tumor regression due to concurrent tumor-specific immunosuppression. Furthermore, a portion of mice treated with cryoablation, with or without CpG, or excision were protected from tumor rechallenge, which suggests procedures that debulk the primary tumor may act to relieve tumor induced immunosuppression, thus supporting endogenous anti-tumor immunity and promoting greater tumor protection.

Although cryoablation resulted in effective tumor debulking, α-Her2 immunity was not amplified relative to surgical excision. Unlike TUBO, D2F2/E2 induces α-Her2 immunity without exogenous manipulation, which does not appear to benefit from additional antigen release by cryoablation. Furthermore, the resulting tissue inflammation may have contributed to increased

immune suppression, as evident by increased growth in rechallenge tumors relative to excision treated mice (Figure3.3C). This suppression is likely mediated by local factors *in vivo* (i.e. ablated tumor), because *ex vivo* stimulation of lymph node cells and splenocytes found no difference in α-Her2 responses. Circulating levels of Tregs were not different between groups 12 days post-treatment, although they could be increased within the tumor microenvironment as suggested by Waitz et al (36), which warrants additional investigation. The addition of CpG was able to partially abrogate cryoablated induced suppression as evident by the increased tumor protection observed (Figure3.3C). Our results suggest this effect was mediated by promoting Th1 responses, which reciprocally diminished transcripts favoring a Th2 biased environment (Figure3.7).

To further evaluate these findings, a similar experiment was performed with tumor rechallenge occurring after tumors treated with cryoablation had 41 days to resolve. Cryoablation, with or without CpG, or excision treated mice had much improved protection relative to mice rechallenged 2 weeks post-operatively, which suggests endogenous α-Her2 immunity is maintained, and potentially enhanced, after clearance of the primary tumor. α-Her2 cell mediated responses in TDLN, such as IL-1β, IL-2, IL-4, IL-6, IFNγ, TNFα, and GM-CSF, were elevated to comparable levels between treated groups, which were significantly higher than naïve mice. Additionally, IL-2, IFNγ, and GM-CSF levels were substantially higher in TDLN in mice 59 days post-operatively compared to 12 days, suggesting increased tumor protection resulted from elevation of α-Her2 cell-mediated responses (Figure3.5 and 3.8C). These findings provide additional evidence that D2F2/E2 tumor growth results in an immunosuppressive microenvironment which allows the tumor to escape immune effector responses. We also further validate that tumor debulking can reverse tumor induced immunosuppression to improve endogenous α-Her2 immunity resulting in increased tumor protection.

Similar to TUBO, CpG used in combination with cryoablation decreased cryoablation recurrences from 29% to 0%. In contrast to TUBO, all tumor bearing mice had comparable

levels of systemic α-Her2 immunity independent of treatment, which indicates the discrepancy in recurrence rates is not mediated by systemic immunity, but by local activity of CpG as initially suspected. Addition of CpG to cryoablation significantly increased levels of Th1 cytokines in TDLN 2 days post-operatively (chapter 1). Additionally, levels of IL-2, IL-12, IFNγ, CXCL10, and MIP-1α in TDLN remained elevated 12 days post-operatively (Figure3.8C). The combination of these factors creates an environment favoring immune mediated destruction of tumor (46-48) previously described in chapter 2. Thus, local Th1 responses activated by CpG are effective in eliminating recurrent tumor growth associated with tumor cryoablation.

GENERAL CONCLUSIONS

Although there are pre-clinical data supporting induction of protective tumor-specific immunity following cryoablation, similar responses have yet to be observed clinically. A lack of explanation and resolution for this discrepancy results from an incomplete understanding of how cryoablation directly and indirectly affects innate and adaptive immune responses. In an attempt to better understand these principles and identify areas for therapeutic intervention, we evaluated immune activation by cryoablation of two BALB/c mammary adenocarcinoma lines expressing Her2/neu antigen, TUBO and D2F2/E2. TUBO was originally induced by a constitutively activate rat neu and is sensitive to α-neu antibody, but growth of TUBO without intervention did not induce α-neu immunity. Thus, TUBO may resemble human cancers with viral etiology or gene mutations that result in expression of neo-antigens the immune system can recognize but does not without exogenous manipulation (47). D2F2/E2 expresses human Her2 by transfection and is resistant to α-Her2 antibody (Ab), but sensitive to T cells. Growth of D2F2/E2 induces both humoral and cellular immunity which are not sufficient to mediate regression of the primary tumor. Thus, D2F2/E2 may be representative of $Her2^{+}$ tumors which become resistant to Herceptin (Trastuzumab) and generate alternative survival pathways (140).

We found that cryoablation of TUBO resulted in protective immunity in a ~65% mice, but observed, in contrast to popular opinion (13), resulting immunity was not Th1 biased, but favored a Th2 response as evident by a dominant IgG1 Ab response. Cryoablation of D2F2/E2 protected ~80% of mice if secondary inoculation was performed after the ablated tumor had been cleared (41 d). However, secondary inoculation 2 weeks after cryoablation resulted in accelerated growth relative to surgical incision, suggesting cryoablation may induce transient immune suppression until the tumor debris is fully resolved. In support of this, increased transcript levels of factors involved in wound healing, such as prostaglandin E2, thymic stromal lymphopoietin, OX40 ligand, TGFβ and IL-10, were observed in tumor draining lymph nodes

(TDLN). Importantly, these factors also favor Th2 biased responses. Furthermore, recurrences of the primary tumor occurred in 26 – 29% of treated mice, which suggests cryoablation did not induce sufficient immunity to eliminate residual tumor foci.

In attempt to reverse Th2 biased immunity and subsequent immunosuppression, the Th1 promoting TLR9 agonist CpG was used in combination with cryoablation. When TUBO was treated with combination therapy we saw a dramatic increase in tumor-specific immunity Ab production following Th1 skewed immunity relative to cryoablation alone, as evident by increased IgG2a Ab. A similar enhancement in Ab was observed with D2F2/E2 as well. This response protected nearly 100% of TUBO-bearing mice from tumor rechallenge and also improved protection in D2F2/E2-bearing mice. These findings are further corroborated by Nierkens and den Brok, who reported similar Th1 induction with CpG treatment (30-34). Importantly, tumor recurrences of both TUBO and D2F2/E2 significantly dropped to 0% in BALB/c mice, and to 12% in NeuT mice. The clearing of residual tumor foci may be mediated by local activation of innate immunity due to increased Th1 responses. Furthermore, upregulation of Th1 cytokines detected in TDLNs created a reciprocal decrease in transcripts favoring a Th2 biased environment, thereby reducing cryoablation induced suppression.

A portion of D2F2/E2 bearing mice treated with cryoablation, with or without CpG, or excision were protected from secondary inoculation 13 days after treatment, which suggests procedures that debulk the primary tumor may act to relieve tumor induced immunosuppression, thus supporting endogenous anti-tumor immunity and promoting greater tumor protection. Although cryoablation resulted in effective tumor debulking, α-Her2 immunity was not amplified relative to surgical excision. Unlike TUBO, D2F2/E2 induces α-Her2 immunity without exogenous manipulation, which does not appear to benefit from additional antigen release by cryoablation. Furthermore, the resulting tissue inflammation may have contributed to increased immune suppression, as evident by increased growth in rechallenge tumors relative to excision treated mice (Figure3.3C). This suppression is likely mediated by local factors *in vivo* (i.e.

ablated tumor), because *ex vivo* stimulation of lymphocytes and splenocytes found no difference in α-Her2 responses.

These results, along with current CpG clinical trial data, highly support concurrent CpG treatment with cryoablation to improve local tumor control with the potential to induce or amplify systemic tumor-specific immunity. Although not tested in this study, the use of therapeutics directly targeting immunosuppressive cells, such as Tregs or myeloid derived suppressor cells, may provide further benefit to cryoablation and CpG treatment. Reducing tissue inflammation following cryoablation and the consequent immune suppression with a short course of anti-inflammatory agents, such as steroids or COX2 inhibitors, may also improve outcomes with cryoablation. As new immunotherapeutic options emerge, it becomes increasingly important that we understand the mechanisms by which cryoablation affects the immune system so appropriate therapeutic intervention can be used to achieve the best outcome.

APPENDIX

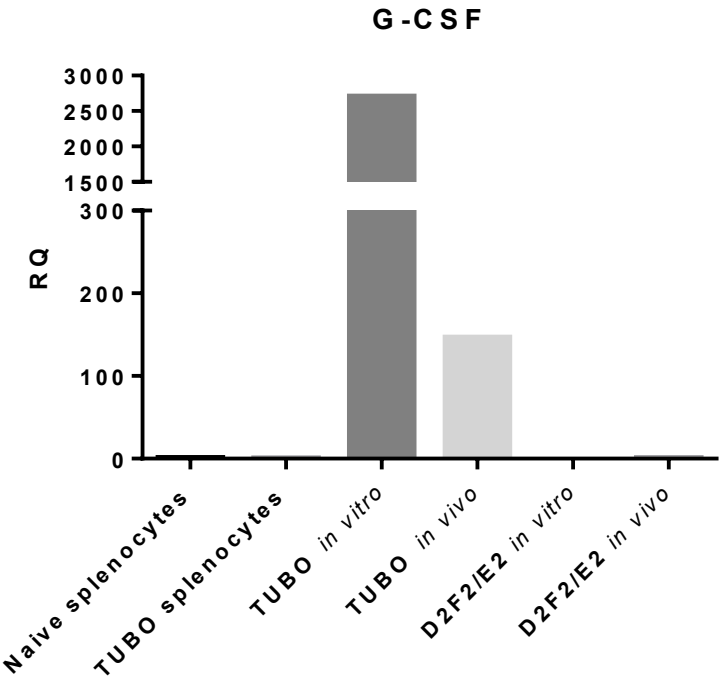

Supplemental Figure 1. TUBO has high transcript levels of G-CSF. RNA was isolated from TUBO and D2F2/E2 growing *in vitro* and *in vivo*. RNA from splenocytes in a TUBO bearing mouse and naïve mouse were also collected. cDNA synthesis and subsequent qPCR analysis was performed. G-CSF transcript levels measured are relative to naïve splenocytes (RQ).

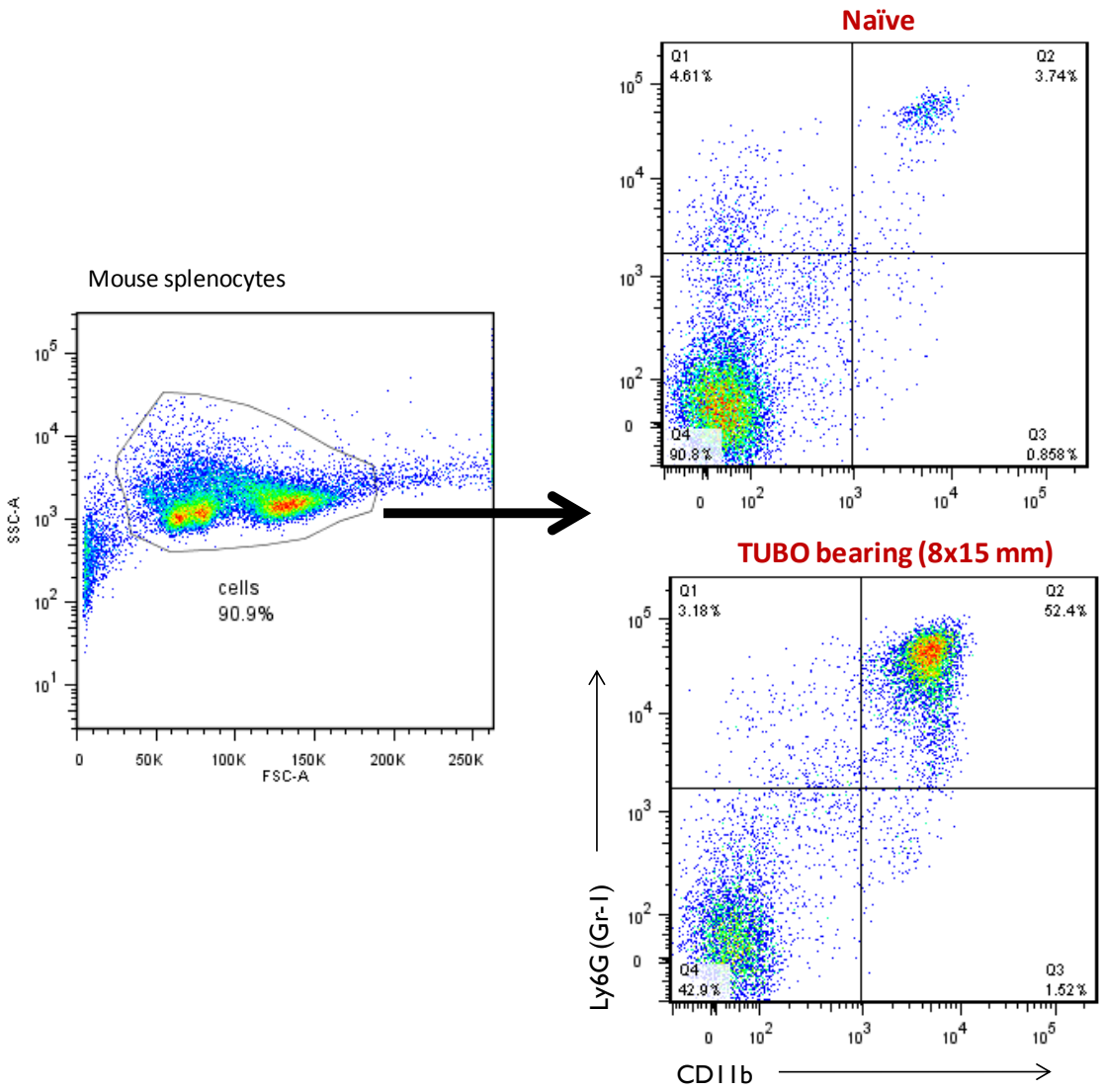

Supplemental Figure 2. TUBO growth induces expansion of myeloid derived suppressor cells (MDSC). A TUBO bearing mouse with tumor measuring ~8x15 mm was euthanized along with a naïve mouse. Splenocytes were isolated and stained for CD11b and Ly6G (GR-1). MDSC were identified by $CD11b^{+}$ $Ly6G^{+}$ cells.

REFERENCES

1. Hoffmann NE, Bischof JC. The cryobiology of cryosurgical injury. Urology. 2002;60:40-9.
2. Karlsson JO, Cravalho EG, Borel R, I, Tompkins RG, Yarmush ML, Toner M. Nucleation and growth of ice crystals inside cultured hepatocytes during freezing in the presence of dimethyl sulfoxide. BiophysJ. 1993;65:2524-36.
3. Fraser J, Gill W. Observations on ultra-frozen tissue. BrJ Surg. 1967;54:770-6.
4. Whittaker DK. Mechanisms of tissue destruction following cryosurgery. AnnRCollSurgEngl. 1984;66:313-8.
5. Korpan NN. A history of cryosurgery: its development and future. J AmCollSurg. 2007;204:314-24.
6. Li C, Wu L, Song J, Liu M, Lv Y, Sequeiros RB. MR imaging-guided cryoablation of metastatic brain tumours: initial experience in six patients. European radiology. 2010;20:404-9.
7. Bang HJ, Littrup PJ, Currier BP, Goodrich DJ, Aoun HD, Klein LC, et al. Percutaneous cryoablation of metastatic lesions from non-small-cell lung carcinoma: initial survival, local control, and cost observations. Journal of vascular and interventional radiology : JVIR. 2012;23:761-9.
8. Littrup PJ, Jallad B, Chandiwala-Mody P, D'Agostini M, Adam BA, Bouwman D. Cryotherapy for breast cancer: a feasibility study without excision. J VascIntervRadiol. 2009;20:1329-41.
9. Solomon LA, Munkarah AR, Vorugu VR, Deppe G, Adam B, Malone JM, Jr., et al. Image-guided percutaneous cryotherapy for the management of gynecologic cancer metastases. GynecolOncol. 2008;111:202-7.

10. Wang H, Littrup PJ, Duan Y, Zhang Y, Feng H, Nie Z. Thoracic masses treated with percutaneous cryotherapy: initial experience with more than 200 procedures. Radiology. 2005;235:289-98.

11. Kaufman CS, Littrup PJ, Freeman-Gibb LA, Smith JS, Francescatti D, Simmons R, et al. Office-based cryoablation of breast fibroadenomas with long-term follow-up. Breast J. 2005;11:344-50.

12. Kerkar S, Carlin AM, Sohn RL, Steffes C, Tyburski J, Littrup P, et al. Long-term follow up and prognostic factors for cryotherapy of malignant liver tumors. Surgery. 2004;136:770-9.

13. Sabel MS. Cryo-immunology: a review of the literature and proposed mechanisms for stimulatory versus suppressive immune responses. Cryobiology. 2009;58:1-11.

14. Soanes WA, Gonder MJ, Ablin RJ. A possible immuno-cryothermic response in prostatic cancer. ClinRadiol. 1970;21:253-5.

15. Ablin RJ, Soanes WA, Gonder MJ. Elution of in vivo bound antiprostatic epithelial antibodies following multiple cryotherapy of carcinoma of prostate. Urology. 1973;2:276-9.

16. Blackwood J, Moore FT, Pace WG. Cryotherapy for malignant tumors. Cryobiology. 1967;4:33-8.

17. Si T, Guo Z, Hao X. Immunologic response to primary cryoablation of high-risk prostate cancer. Cryobiology. 2008;57:66-71.

18. Callstrom MR, Dupuy DE, Solomon SB, Beres RA, Littrup PJ, Davis KW, et al. Percutaneous image-guided cryoablation of painful metastases involving bone: multicenter trial. Cancer. 2013;119:1033-41.

19. Bang HJ, Littrup PJ, Goodrich DJ, Currier BP, Aoun HD, Heilbrun LK, et al. Percutaneous cryoablation of metastatic renal cell carcinoma for local tumor control:

feasibility, outcomes, and estimated cost-effectiveness for palliation. Journal of vascular and interventional radiology : JVIR. 2012;23:770-7.

20. El Dib R, Touma NJ, Kapoor A. Cryoablation vs radiofrequency ablation for the treatment of renal cell carcinoma: a meta-analysis of case series studies. BJU international. 2012;110:510-6.

21. Chin JL, Al-Zahrani AA, Autran-Gomez AM, Williams AK, Bauman G. Extended followup oncologic outcome of randomized trial between cryoablation and external beam therapy for locally advanced prostate cancer (T2c-T3b). J Urol. 2012;188:1170-5.

22. Breen DJ, Bryant TJ, Abbas A, Shepherd B, McGill N, Anderson JA, et al. Percutaneous cryoablation of renal tumours: outcomes from 171 tumours in 147 patients. BJU international. 2013.

23. Elkjaer MC, Borre M. Oncological outcome after primary prostate cryoablation compared with radical prostatectomy: A single-centre experience. Scandinavian journal of urology. 2013.

24. Klatte T, Mauermann J, Heinz-Peer G, Waldert M, Weibl P, Klingler HC, et al. Perioperative, oncologic, and functional outcomes of laparoscopic renal cryoablation and open partial nephrectomy: a matched pair analysis. Journal of endourology / Endourological Society. 2011;25:991-7.

25. Davol PE, Fulmer BR, Rukstalis DB. Long-term results of cryoablation for renal cancer and complex renal masses. Urology. 2006;68:2-6.

26. Aron M, Kamoi K, Remer E, Berger A, Desai M, Gill I. Laparoscopic renal cryoablation: 8-year, single surgeon outcomes. J Urol. 2010;183:889-95.

27. Thakur A, Littrup P, Paul EN, Adam B, Heilbrun LK, Lum LG. Induction of specific cellular and humoral responses against renal cell carcinoma after combination therapy with cryoablation and granulocyte-macrophage colony stimulating factor: a pilot study. J Immunother. 2011;34:457-67.

28. Urano M, Tanaka C, Sugiyama Y, Miya K, Saji S. Antitumor effects of residual tumor after cryoablation: the combined effect of residual tumor and a protein-bound polysaccharide on multiple liver metastases in a murine model. Cryobiology. 2003;46:238-45.

29. Osada S, Imai H, Tomita H, Tokuyama Y, Okumura N, Matsuhashi N, et al. Serum cytokine levels in response to hepatic cryoablation. J SurgOncol. 2007;95:491-8.

30. den Brok MH, Nierkens S, Wagenaars JA, Ruers TJ, Schrier CC, Rijke EO, et al. Saponin-based adjuvants create a highly effective anti-tumor vaccine when combined with in situ tumor destruction. Vaccine. 2012;30:737-44.

31. den Brok MH, Sutmuller RP, Nierkens S, Bennink EJ, Frielink C, Toonen LW, et al. Efficient loading of dendritic cells following cryo and radiofrequency ablation in combination with immune modulation induces anti-tumour immunity. BrJCancer. 2006;95:896-905.

32. den Brok MH, Sutmuller RP, Nierkens S, Bennink EJ, Toonen LW, Figdor CG, et al. Synergy between in situ cryoablation and TLR9 stimulation results in a highly effective in vivo dendritic cell vaccine. Cancer Res. 2006;66:7285-92.

33. Nierkens S, den Brok MH, Roelofsen T, Wagenaars JA, Figdor CG, Ruers TJ, et al. Route of administration of the TLR9 agonist CpG critically determines the efficacy of cancer immunotherapy in mice. PloS one. 2009;4:e8368.

34. Nierkens S, den Brok MH, Sutmuller RP, Grauer OM, Bennink E, Morgan ME, et al. In vivo colocalization of antigen and CpG [corrected] within dendritic cells is associated with the efficacy of cancer immunotherapy. Cancer Res. 2008;68:5390-6.

35. Levy MY, Sidana A, Chowdhury WH, Solomon SB, Drake CG, Rodriguez R, et al. Cyclophosphamide Unmasks an Antimetastatic Effect of Local Tumor Cryoablation. The Journal of Pharmacology and Experimental Therapeutics2009. p. 596-601.

36. Waitz R, Solomon SB, Petre EN, Trumble AE, Fasso M, Norton L, et al. Potent induction of tumor immunity by combining tumor cryoablation with anti-CTLA-4 therapy. Cancer Res. 2012;72:430-9.

37. Autorino R, Kaouk JH. Cryoablation for small renal tumors: current status and future perspectives. Urologic oncology. 2012;30:S20-7.

38. Pisters LL, Leibovici D, Blute M, Zincke H, Sebo TJ, Slezak JM, et al. Locally recurrent prostate cancer after initial radiation therapy: a comparison of salvage radical prostatectomy versus cryotherapy. J Urol. 2009;182:517-25; discussion 25-7.

39. Panumatrassamee K, Kaouk JH, Autorino R, Lenis AT, Laydner H, Isac W, et al. Cryoablation versus minimally invasive partial nephrectomy for small renal masses in the solitary kidney: impact of approach on functional outcomes. J Urol. 2013;189:818-22.

40. Mu F, Niu L, Li H, Liao M, Li L, Liu C, et al. Percutaneous comprehensive cryoablation for metastatic hepatocellular cancer. Cryobiology. 2013;66:76-80.

41. Littrup PJ, Ahmed A, Aoun HD, Noujaim DL, Harb T, Nakat S, et al. CT-guided percutaneous cryotherapy of renal masses. J VascIntervRadiol. 2007;18:383-92.

42. Ahrar K, Ahrar JU, Javadi S, Pan L, Milton DR, Wood CG, et al. Real-time magnetic resonance imaging-guided cryoablation of small renal tumors at 1.5 T. Investigative radiology. 2013;48:437-44.

43. Bilchik AJ, Wood TF, Allegra DP. Radiofrequency ablation of unresectable hepatic malignancies: lessons learned. The oncologist. 2001;6:24-33.

44. Littman DR, Rudensky AY. Th17 and regulatory T cells in mediating and restraining inflammation. Cell. 2010;140:845-58.

45. Mosmann TR, Cherwinski H, Bond MW, Giedlin MA, Coffman RL. Two types of murine helper T cell clone. I. Definition according to profiles of lymphokine activities and secreted proteins. J Immunol. 1986;136:2348-57.

46. Kalinski P, Moser M. Consensual immunity: success-driven development of T-helper-1 and T-helper-2 responses. Nature reviews Immunology. 2005;5:251-60.

47. Restifo NP, Dudley ME, Rosenberg SA. Adoptive immunotherapy for cancer: harnessing the T cell response. Nature reviews Immunology. 2012;12:269-81.

48. Haabeth OA, Lorvik KB, Hammarstrom C, Donaldson IM, Haraldsen G, Bogen B, et al. Inflammation driven by tumour-specific Th1 cells protects against B-cell cancer. Nature communications. 2011;2:240.

49. Zhu J, Yamane H, Paul WE. Differentiation of effector CD4 T cell populations (*). Annu Rev Immunol. 2010;28:445-89.

50. Mosmann TR, Coffman RL. TH1 and TH2 cells: different patterns of lymphokine secretion lead to different functional properties. Annu Rev Immunol. 1989;7:145-73.

51. Kalinski P. Regulation of immune responses by prostaglandin E2. J Immunol. 2012;188:21-8.

52. Nishimura T, Nakui M, Sato M, Iwakabe K, Kitamura H, Sekimoto M, et al. The critical role of Th1-dominant immunity in tumor immunology. Cancer Chemother Pharmacol. 2000;46 Suppl:S52-61.

53. Nishimura T, Iwakabe K, Sekimoto M, Ohmi Y, Yahata T, Nakui M, et al. Distinct Role of Antigen-specific T Helper Type 1 (Th1) and Th2 Cells in Tumor Eradication In Vivo. JExpMed. 1999;190:617-27.

54. Ikeda H, Chamoto K, Tsuji T, Suzuki Y, Wakita D, Takeshima T, et al. The critical role of type-1 innate and acquired immunity in tumor immunotherapy. Cancer science. 2004;95:697-703.

55. Kalinski P, Hilkens CMU, Wierenga EA, Kapsenberg ML. T-cell priming by type-I and type-2 polarized dendritic cells: the concept of a third signal. Immunology Today. 1999;20:561-7.

56. Pulendran B, Kumar P, Cutler CW, Mohamadzadeh M, Van Dyke T, Banchereau J. Lipopolysaccharides from distinct pathogens induce different classes of immune responses in vivo. J Immunol. 2001;167:5067-76.

57. de Jong EC, Vieira PL, Kalinski P, Schuitemaker JH, Tanaka Y, Wierenga EA, et al. Microbial compounds selectively induce Th1 cell-promoting or Th2 cell-promoting dendritic cells in vitro with diverse th cell-polarizing signals. J Immunol. 2002;168:1704-9.

58. Paul WE, Zhu J. How are T(H)2-type immune responses initiated and amplified? Nature reviews Immunology. 2010;10:225-35.

59. Pulendran B, Tang H, Manicassamy S. Programming dendritic cells to induce T(H)2 and tolerogenic responses. Nat Immunol. 2010;11:647-55.

60. Green DR, Ferguson T, Zitvogel L, Kroemer G. Immunogenic and tolerogenic cell death. Nature reviews Immunology. 2009;9:353-63.

61. Ohtani T, Mizuashi M, Nakagawa S, Sasaki Y, Fujimura T, Okuyama R, et al. TGF-beta1 dampens the susceptibility of dendritic cells to environmental stimulation, leading to the requirement for danger signals for activation. Immunology. 2009;126:485-99.

62. Chen GY, Nunez G. Sterile inflammation: sensing and reacting to damage. Nature reviews Immunology. 2010;10:826-37.

63. Zhang X, Mosser DM. Macrophage activation by endogenous danger signals. J Pathol. 2008;214:161-78.

64. Caminschi I, Shortman K. Boosting antibody responses by targeting antigens to dendritic cells. Trends Immunol. 2012;33:71-7.

65. Zhang JG, Czabotar PE, Policheni AN, Caminschi I, Wan SS, Kitsoulis S, et al. The dendritic cell receptor Clec9A binds damaged cells via exposed actin filaments. Immunity. 2012;36:646-57.

66. Viorritto IC, Nikolov NP, Siegel RM. Autoimmunity versus tolerance: can dying cells tip the balance? ClinImmunol. 2007;122:125-34.

67. Peng Y, Martin DA, Kenkel J, Zhang K, Ogden CA, Elkon KB. Innate and adaptive immune response to apoptotic cells. J Autoimmun. 2007;29:303-9.

68. Buckwalter MR, Srivastava PK. Mechanism of dichotomy between CD8+ responses elicited by apoptotic and necrotic cells. Cancer Immun. 2013;13:2.

69. Rand RW, Rand RP, Eggerding FA, Field M, DenBesten L, King W, et al. Cryolumpectomy for breast cancer: an experimental study. Cryobiology. 1985;22:307-18.

70. Joosten JJ, Muijen GN, Wobbes T, Ruers TJ. In vivo destruction of tumor tissue by cryoablation can induce inhibition of secondary tumor growth: an experimental study. Cryobiology. 2001;42:49-58.

71. Ohkuma T, Otagiri K, Ikekawa T, Tanaka S. Augmentation of antitumor activity by combined cryo-destruction of sarcoma 180 and protein-bound polysaccharide, EA6, isolated from Flammulina velutipes (Curt. ex Fr.) Sing. in ICR mice. J Pharmacobiodyn. 1982;5:439-44.

72. Sabel MS, Nehs MA, Su G, Lowler KP, Ferrara JL, Chang AE. Immunologic response to cryoablation of breast cancer. Breast Cancer Res Treat. 2005;90:97-104.

73. Sabel MS, Arora A, Su G, Chang AE. Adoptive immunotherapy of breast cancer with lymph node cells primed by cryoablation of the primary tumor. Cryobiology. 2006;53:360-6.

74. Hoffmann NE, Coad JE, Huot CS, Swanlund DJ, Bischof JC. Investigation of the mechanism and the effect of cryoimmunology in the Copenhagen rat. Cryobiology. 2001;42:59-68.

75. Matsumura K, Sakata K, Saji S, Misao A, Kunieda T. Antitumor immunologic reactivity in the relatively early period after cryosurgery: experimental studies in the rat. Cryobiology. 1982;19:263-72.

76. Muller LC, Micksche M, Yamagata S, Kerschbaumer F. Therapeutic effect of cryosurgery of murine osteosarcoma--influence on disease outcome and immune function. Cryobiology. 1985;22:77-85.

77. Yamashita T, Hayakawa K, Hosokawa M, Kodama T, Inoue N, Tomita K, et al. Enhanced tumor metastases in rats following cryosurgery of primary tumor. Gann. 1982;73:222-8.

78. Hayakawa K, Yamashita T, Suzuki K, Tomita K, Hosokawa M, Kodama T, et al. Comparative immunological studies in rats following cryosurgery and surgical excision of 3-methylcholanthrene-induced primary autochthonous tumors. Gann. 1982;73:462-9.

79. Miya K, Saji S, Morita T, Niwa H, Takao H, Kida H, et al. Immunological response of regional lymph nodes after tumor cryosurgery: experimental study in rats. Cryobiology. 1986;23:290-5.

80. Miya K, Saji S, Morita T, Niwa H, Sakata K. Experimental study on mechanism of absorption of cryonecrotized tumor antigens. Cryobiology. 1987;24:135-9.

81. Wing MG, Rogers K, Jacob G, Rees RC. Characterisation of suppressor cells generated following cryosurgery of an HSV-2-induced fibrosarcoma. Cancer Immunol Immunother. 1988;26:169-75.

82. Blackwood CE, Cooper IS. Response of experimental tumor systems to cryosurgery. Cryobiology. 1972;9:508-15.

83. Shibata T, Suzuki K, Yamashita T, Takeichi N, Mark M, Hosokawa M, et al. Immunological analysis of enhanced spontaneous metastasis in WKA rats following cryosurgery. Anticancer Res. 1998;18:2483-6.

84. Shibata T, Yamashita T, Suzuki K, Takeichi N, Micallef M, Hosokawa M, et al. Enhancement of experimental pulmonary metastasis and inhibition of subcutaneously transplanted tumor growth following cryosurgery. Anticancer Res. 1998;18:4443-8.

85. Friedman EJ, Orth CR, Brewton KA, Ponniah S, Alexander RB. Cryosurgical ablation of the normal ventral prostate plus adjuvant does not protect Copenhagen rats from Dunning prostatic adenocarcinoma challenge. JUrol. 1997;158:1585-8.

86. Udagawa M, Kudo-Saito C, Hasegawa G, Yano K, Yamamoto A, Yaguchi M, et al. Enhancement of immunologic tumor regression by intratumoral administration of dendritic cells in combination with cryoablative tumor pretreatment and Bacillus Calmette-Guerin cell wall skeleton stimulation. Clin Cancer Res. 2006;12:7465-75.

87. Yokokawa J, Cereda V, Remondo C, Gulley JL, Arlen PM, Schlom J, et al. Enhanced functionality of CD4+CD25(high)FoxP3+ regulatory T cells in the peripheral blood of patients with prostate cancer. ClinCancer Res. 2008;14:1032-40.

88. Zhou L, Fu JL, Lu YY, Fu BY, Wang CP, An LJ, et al. Regulatory T cells are associated with post-cryoablation prognosis in patients with hepatitis B virus-related hepatocellular carcinoma. Journal of gastroenterology. 2010;45:968-78.

89. Lucchini F, Sacco MG, Hu N, Villa A, Brown J, Cesano L, et al. Early and multifocal tumors in breast, salivary, harderian and epididymal tissues developed in MMTY-Neu transgenic mice. Cancer Lett. 1992;64:203-9.

90. Boggio K, Nicoletti G, Di CE, Cavallo F, Landuzzi L, Melani C, et al. Interleukin 12-mediated prevention of spontaneous mammary adenocarcinomas in two lines of Her-2/neu transgenic mice. J ExpMed. 1998;188:589-96.

91. Nanni P, Pupa SM, Nicoletti G, De GC, Landuzzi L, Rossi I, et al. p185(neu) protein is required for tumor and anchorage-independent growth, not for cell proliferation of transgenic mammary carcinoma. Int J Cancer. 2000;87:186-94.

92. Rovero S, Amici A, Carlo ED, Bei R, Nanni P, Quaglino E, et al. DNA vaccination against rat her-2/Neu p185 more effectively inhibits carcinogenesis than transplantable carcinomas in transgenic BALB/c mice. J Immunol. 2000;165:5133-42.

93. Mahoney KH, Miller BE, Heppner GH. FACS quantitation of leucine aminopeptidase and acid phosphatase on tumor-associated macrophages from metastatic and nonmetastatic mouse mammary tumors. J LeukocBiol. 1985;38:573-85.

94. Wei WZ, Shi WP, Galy A, Lichlyter D, Hernandez S, Groner B, et al. Protection against mammary tumor growth by vaccination with full-length, modified human ErbB-2 DNA. Int J Cancer. 1999;81:748-54.

95. Wei WZ, Jacob JB, Zielinski JF, Flynn JC, Shim KD, Alsharabi G, et al. Concurrent induction of antitumor immunity and autoimmune thyroiditis in CD4+ CD25+ regulatory T cell-depleted mice. Cancer Research. 2005;65:8471-8.

96. Vollmer J, Weeratna R, Payette P, Jurk M, Schetter C, Laucht M, et al. Characterization of three CpG oligodeoxynucleotide classes with distinct immunostimulatory activities. Eur J Immunol. 2004;34:251-62.

97. Livak KJ, Schmittgen TD. Analysis of relative gene expression data using real-time quantitative PCR and the 2(-Delta Delta C(T)) Method. Methods. 2001;25:402-8.

98. Machin D, Cheung YB, Parmar MKB, Parmar MKB. Survival analysis : a practical approach. 2nd ed. Chichester, England ; Hoboken, NJ: Wiley; 2006.

99. Rubinsky B. Cryosurgery. Annual review of biomedical engineering. 2000;2:157-87.

100. Maccini M, Sehrt D, Pompeo A, Chicoli FA, Molina WR, Kim FJ. Biophysiologic considerations in cryoablation: a practical mechanistic molecular review. International braz j urol : official journal of the Brazilian Society of Urology. 2011;37:693-6.

101. Baust JG, Gage AA. The molecular basis of cryosurgery. BJUInt. 2005;95:1187-91.

102. Erinjeri JP, Clark TW. Cryoablation: mechanism of action and devices. Journal of vascular and interventional radiology : JVIR. 2010;21:S187-91.

103. Weber SM, Lee FT, Jr., Chinn DO, Warner T, Chosy SG, Mahvi DM. Perivascular and intralesional tissue necrosis after hepatic cryoablation: results in a porcine model. Surgery. 1997;122:742-7.

104. Matin SF, Sharma P, Gill IS, Tannenbaum C, Hobart MG, Novick AC, et al. Immunological response to renal cryoablation in an in vivo orthotopic renal cell carcinoma murine model. J Urol. 2010;183:333-8.

105. O'Neill LA. The interleukin-1 receptor/Toll-like receptor superfamily: 10 years of progress. Immunol Rev. 2008;226:10-8.

106. Matsushima H, Ogawa Y, Miyazaki T, Tanaka H, Nishibu A, Takashima A. Intravital imaging of IL-1beta production in skin. The Journal of investigative dermatology. 2010;130:1571-80.

107. Vasselon T, Detmers PA. Toll receptors: a central element in innate immune responses. Infect Immun. 2002;70:1033-41.

108. Klinman DM. Immunotherapeutic uses of CpG oligodeoxynucleotides. Nature reviews Immunology. 2004;4:249-58.

109. Bauer S, Kirschning CJ, Hacker H, Redecke V, Hausmann S, Akira S, et al. Human TLR9 confers responsiveness to bacterial DNA via species-specific CpG motif recognition. Proc Natl Acad Sci U S A. 2001;98:9237-42.

110. Rankin R, Pontarollo R, Ioannou X, Krieg AM, Hecker R, Babiuk LA, et al. CpG motif identification for veterinary and laboratory species demonstrates that sequence recognition is highly conserved. Antisense & nucleic acid drug development. 2001;11:333-40.

111. Klinman DM, Yi AK, Beaucage SL, Conover J, Krieg AM. CpG motifs present in bacteria DNA rapidly induce lymphocytes to secrete interleukin 6, interleukin 12, and interferon gamma. Proc Natl Acad Sci U S A. 1996;93:2879-83.

112. Sun S, Zhang X, Tough DF, Sprent J. Type 1 interferon-mediated stimulation of T cells by CpG DNA. JExpMed. 1998;188:2335-42.

113. Stacey KJ, Sweet MJ, Hume DA. Macrophages ingest and are activated by bacterial DNA. J Immunol. 1996;157:2116-22.

114. Ballas ZK, Rasmussen WL, Krieg AM. Induction of NK activity in murine and human cells by CpG motifs in oligodeoxynucleotides and bacterial DNA. J Immunol. 1996;157:1840-5.

115. Halpern MD, Kurlander RJ, Pisetsky DS. Bacterial DNA induces murine interferon-gamma production by stimulation of interleukin-12 and tumor necrosis factor-alpha. Cell Immunol. 1996;167:72-8.

116. Yamamoto S, Yamamoto T, Kataoka T, Kuramoto E, Yano O, Tokunaga T. unique palindromic sequences in synthetic oligonucleotides are required to induce INF and augment INF-mediated natural killer activity. The Journal of Immunology. 1992;148:4072-6.

117. Krieg AM, Yi AK, Matson S, Waldschmidt TJ, Bishop GA, Teasdale R, et al. CpG motifs in bacterial DNA trigger direct B-cell activation. Nature. 1995;374:546-9.

118. Jones TR, Obaldia NI, Gramzinski RA, Charoenvit Y, Kolodny NK, Kitov S, et al. Synthetic oligodeoxynucleotides containing CpG motifs enhance immunogenicity of a peptide malaria vaccine in *Aotus* monkeys. Vaccine. 1999;17:3065-71.

119. Dalpke AH, Zimmermann S, Albrecht I, Heeg K. Phosphodiester CpG oligonucleotides as adjuvants: polyguanosine runs enhance cellular uptake and improve immunostimulative activity of phosphodiester CpG oligonucleotides in vitro and in vivo. Immunology. 2002;106:102-12.

120. Marshall JD, Fearon K, Abbate C, Subramanian S, Yee P, Gregorio J, et al. Identification of a novel CpG DNA class and motif that optimally stimulate B cell and plasmacytoid dendritic cell functions. J Leukoc Biol. 2003;73:781-92.

121. Krug A, Rothenfusser S, Hornung V, Jahrsdorfer B, Blackwell S, Ballas ZK, et al. Identification of CpG oligonucleotide sequences with high induction of IFN-alpha/beta in plasmacytoid dendritic cells. Eur J Immunol. 2001;31:2154-63.

122. Verthelyi D, Ishii KJ, Gursel M, Takeshita F, Klinman DM. Human peripheral blood cells differentially recognize and respond to two distinct CPG motifs. J Immunol. 2001;166:2372-7.

123. Brody JD, Ai WZ, Czerwinski DK, Torchia JA, Levy M, Advani RH, et al. In situ vaccination with a TLR9 agonist induces systemic lymphoma regression: a phase I/II study. J Clin Oncol. 2010;28:4324-32.

124. Gurtner GC, Werner S, Barrandon Y, Longaker MT. Wound repair and regeneration. Nature. 2008;453:314-21.

125. Maslin B, Alexandrescu DT, Ichim TE, Dasanu CA. Newer developments in the immunotherapy of malignant melanoma. Journal of oncology pharmacy practice : official publication of the International Society of Oncology Pharmacy Practitioners. 2013.

126. Lin Y, Roberts TJ, Sriram V, Cho S, Brutkiewicz RR. Myeloid marker expression on antiviral CD8+ T cells following an acute virus infection. Eur J Immunol. 2003;33:2736-43.

127. Huleatt JW, Lefrancois L. Antigen-driven induction of CD11c on intestinal intraepithelial lymphocytes and CD8+ T cells in vivo. J Immunol. 1995;154:5684-93.

128. Kim SK, Schluns KS, Lefrancois L. Induction and visualization of mucosal memory CD8 T cells following systemic virus infection. J Immunol. 1999;163:4125-32.

129. McFarland HI, Nahill SR, Maciaszek JW, Welsh RM. CD11b (Mac-1): a marker for CD8+ cytotoxic T cell activation and memory in virus infection. J Immunol. 1992;149:1326-33.

130. Christensen JE, Andreasen SO, Christensen JP, Thomsen AR. CD11b expression as a marker to distinguish between recently activated effector CD8(+) T cells and memory cells. Int Immunol. 2001;13:593-600.

131. Kim YH, Seo SK, Choi BK, Kang WJ, Kim CH, Lee SK, et al. 4-1BB costimulation enhances HSV-1-specific CD8+ T cell responses by the induction of CD11c+CD8+ T cells. Cell Immunol. 2005;238:76-86.

132. Nathan C. Points of control in inflammation. Nature. 2002;420:846-52.

133. Wynn TA, Ramalingam TR. Mechanisms of fibrosis: therapeutic translation for fibrotic disease. Nat Med. 2012;18:1028-40.

134. Faler BJ, Macsata RA, Plummer D, Mishra L, Sidawy AN. Transforming growth factor-beta and wound healing. Perspectives in vascular surgery and endovascular therapy. 2006;18:55-62.

135. Li MO, Flavell RA. Contextual regulation of inflammation: a duet by transforming growth factor-beta and interleukin-10. Immunity. 2008;28:468-76.

136. Taylor A, Verhagen J, Blaser K, Akdis M, Akdis CA. Mechanisms of immune suppression by interleukin-10 and transforming growth factor-beta: the role of T regulatory cells. Immunology. 2006;117:433-42.

137. Blackwell TS, Debelak JP, Venkatakrishnan A, Schot DJ, Harley DH, Pinson CW, et al. Acute lung injury after hepatic cryoablation: correlation with NF-kappa B activation and cytokine production. Surgery. 1999;126:518-26.

138. Menard S, Pupa SM, Campiglio M, Tagliabue E. Biologic and therapeutic role of HER2 in cancer. Oncogene. 2003;22:6570-8.

139. Slamon DJ, Godolphin W, Jones LA, Holt JA, Wong SG, Keith DE, et al. Studies of the HER-2/neu proto-oncogene in human breast and ovarian cancer. Science. 1989;244:707-12.

140. Nahta R, Yu D, Hung MC, Hortobagyi GN, Esteva FJ. Mechanisms of disease: understanding resistance to HER2-targeted therapy in human breast cancer. Nature clinical practice Oncology. 2006;3:269-80.

141. Gullick WJ, Bottomley AC, Lofts FJ, Doak DG, Mulvey D, Newman R, et al. Three dimensional structure of the transmembrane region of the proto-oncogenic and oncogenic forms of the neu protein. EMBO J. 1992;11:43-8.

142. Zindl CL, Chaplin DD. Immunology. Tumor immune evasion. Science. 2010;328:697-8.

143. Drake CG, Jaffee E, Pardoll DM. Mechanisms of immune evasion by tumors. Adv Immunol. 2006;90:51-81.

144. Heimberger AB, Archer GE, Crotty LE, McLendon RE, Friedman AH, Friedman HS, et al. Dendritic cells pulsed with a tumor-specific peptide induce long-lasting immunity and are effective against murine intracerebral melanoma. Neurosurgery. 2002;50:158-64; discussion 64-6.

145. Jacob JB, Quaglino E, Radkevich-Brown O, Jones RF, Piechocki MP, Reyes JD, et al. Human Her-2 DNA vaccines containing heterologous rat neu sequence overcome immune tolerance to induce elevated anti-tumor immunity. Cancer Res2009.

146. Soares MM, Mehta V, Finn OJ. Three different vaccines based on the 140-amino acid MUC1 peptide with seven tandemly repeated tumor-specific epitopes elict distinct immune effector mechanisms in wild-type versus MUC1-transgenic mice with different potential for tumor rejection. The Journal of Immunology. 2001;166:6555-63.

147. Xiang R, Silletti S, Lode HN, Dolman CS, Ruehlmann JM, Niethammer AG, et al. Protective immunity against human carcinoembryonic antigen (CEA) induced by an oral DNA vaccine in CEA-transgenic mice. Clinical Cancer Research. 2001;7:856s-64s.

148. Aurisicchio L, Mennuni C, Giannetti P, Calvaruso F, Nuzzo M, Cipriani B, et al. Immunogenicity and safety of a DNA prime/adenovirus boost vaccine against rhesus CEA in nonhuman primates. IntJ Cancer. 2007;120:2290-300.

149. Straetemans T, Coccoris M, Berrevoets C, Treffers-Westerlaken E, Scholten CE, Schipper D, et al. T-cell receptor gene therapy in human melanoma-bearing immune-

deficient mice: human but not mouse T cells recapitulate outcome of clinical studies. Hum Gene Ther. 2012;23:187-201.

150. Pupa SM, Iezzi M, Di CE, Invernizzi A, Cavallo F, Meazza R, et al. Inhibition of mammary carcinoma development in HER-2/neu transgenic mice through induction of autoimmunity by xenogeneic DNA vaccination. Cancer Res. 2005;65:1071-8.

151. Quaglino E, Iezzi M, Mastini C, Amici A, Pericle F, Di CE, et al. Electroporated DNA vaccine clears away multifocal mammary carcinomas in her-2/neu transgenic mice. Cancer Res. 2004;64:2858-64.

152. Farkas AM, Marvel DM, Finn OJ. Antigen choice determines vaccine-induced generation of immunogenic versus tolerogenic dendritic cells that are marked by differential expression of pancreatic enzymes. J Immunol. 2013;190:3319-27.

153. Jacob J, Radkevich O, Forni G, Zielinski J, Shim D, Jones RF, et al. Activity of DNA vaccines encoding self or heterologous Her-2/neu in Her-2 or neu transgenic mice. Cellular Immunology. 2006;240:96-106.

154. Jacob JB, Kong YC, Nalbantoglu I, Snower DP, Wei WZ. Tumor regression following DNA vaccination and regulatory T cell depletion in neu transgenic mice leads to an increased risk for autoimmunity. J Immunol. 2009;182:5873-81.

155. Jacob JB, Quaglino E, Radkevich-Brown O, Jones RF, Piechocki MP, Reyes JD, et al. Combining human and rat sequences in her-2 DNA vaccines blunts immune tolerance and drives antitumor immunity. Cancer Res. 2010;70:119-28.

156. Whittington PJ, Radkevich-Brown O, Jacob JB, Jones RF, Weise AM, Wei WZ. Her-2 DNA versus cell vaccine: immunogenicity and anti-tumor activity. Cancer ImmunolImmunother. 2008.

157. Whittington PJ, Piechocki MP, Heng HH, Jacob JB, Jones RF, Back JB, et al. DNA vaccination controls Her-2+ tumors that are refractory to targeted therapies. Cancer Res. 2008;68:7502-11.

158. Rolla S, Marchini C, Malinarich S, Quaglino E, Lanzardo S, Montani M, et al. Protective immunity against neu-positive carcinomas elicited by electroporation of plasmids encoding decreasing fragments of rat neu extracellular domain. HumGene Ther. 2008;19:229-40.

159. Curcio C, E DC, Clynes R, MJ S, Boggio K, E Q, et al. Nonredundant roles of antibody, cytokines and perforin for the immune eradication of established Her-2/neu carcinomas. Journal of Clinical Investigation. 2003;111:1161-70.

160. Lipford GB, Sparwasser T, Zimmermann S, Heeg K, Wagner H. CpG-DNA-mediated transient lymphadenopathy is associated with a state of Th1 predisposition to antigen-driven responses. The Journal of Immunology. 2000;165:1228-35.

161. Luther SA, Cyster JG. Chemokines as regulators of T cell differentiation. Nat Immunol. 2001;2:102-7.

162. Thomas DA, Massague J. TGF-beta directly targets cytotoxic T cell functions during tumor evasion of immune surveillance. Cancer Cell. 2005;8:369-80.

163. Roda JM, Parihar R, Carson WE, 3rd. CpG-containing oligodeoxynucleotides act through TLR9 to enhance the NK cell cytokine response to antibody-coated tumor cells. J Immunol. 2005;175:1619-27.

164. Kawai T, Akira S. The role of pattern-recognition receptors in innate immunity: update on Toll-like receptors. Nat Immunol. 2010;11:373-84.

165. Wegmann M, Hauber HP. Experimental approaches towards allergic asthma therapy-murine asthma models. Recent patents on inflammation & allergy drug discovery. 2010;4:37-53.

166. Boehm U, Klamp T, Groot M, Howard JC. Cellular responses to interferon-gamma. Annu Rev Immunol. 1997;15:749-95.

167. Yu H, Pardoll D, Jove R. STATs in cancer inflammation and immunity: a leading role for STAT3. Nature reviews Cancer. 2009;9:798-809.

168. Yu H, Kortylewski M, Pardoll D. Crosstalk between cancer and immune cells: role of STAT3 in the tumour microenvironment. Nature reviews Immunology. 2007;7:41-51.

169. Panopoulos AD, Watowich SS. Granulocyte colony-stimulating factor: molecular mechanisms of action during steady state and 'emergency' hematopoiesis. Cytokine. 2008;42:277-88.

170. Barbieri I, Quaglino E, Maritano D, Pannellini T, Riera L, Cavallo F, et al. Stat3 is required for anchorage-independent growth and metastasis but not for mammary tumor development downstream of the ErbB-2 oncogene. Mol Carcinog. 2010;49:114-20.

171. Kawarada Y, Ganss R, Garbi N, Sacher T, Arnold B, Hammerling GJ. NK- and CD8(+) T cell-mediated eradication of established tumors by peritumoral injection of CpG-containing oligodeoxynucleotides. J Immunol. 2001;167:5247-53.

172. Xu LL, Warren MK, Rose WL, Gong W, Wang JM. Human recombinant monocyte chemotactic protein and other C-C chemokines bind and induce directional migration of dendritic cells in vitro. J Leukoc Biol. 1996;60:365-71.

173. Carr MW, Roth SJ, Luther E, Rose SS, Springer TA. Monocyte chemoattractant protein 1 acts as a T-lymphocyte chemoattractant. Proc Natl Acad Sci U S A. 1994;91:3652-6.

174. Maurer M, von Stebut E. Macrophage inflammatory protein-1. The international journal of biochemistry & cell biology. 2004;36:1882-6.

175. Salazar-Mather TP, Lewis CA, Biron CA. Type I interferons regulate inflammatory cell trafficking and macrophage inflammatory protein 1alpha delivery to the liver. J Clin Invest. 2002;110:321-30.

176. Kelly-Scumpia KM, Scumpia PO, Delano MJ, Weinstein JS, Cuenca AG, Wynn JL, et al. Type I interferon signaling in hematopoietic cells is required for survival in mouse polymicrobial sepsis by regulating CXCL10. J Exp Med. 2010;207:319-26.

177. Pilon SA, Piechocki MP, Wei WZ. Vaccination with cytoplasmic ErbB-2 DNA protects mice from mammary tumor growth without anti-ErbB-2 antibody. J Immunol. 2001;167:3201-6.

ABSTRACT

IMPACT OF CRYOABLATION ON TUMOR IMMUNITY

by

JESSE J. VEENSTRA

May 2015

Advisor: Dr. Wei-zen Wei

Major: Cancer Biology

Degree: Doctor of Philosophy

Background and Objectives: Percutaneous cryoablation is a minimally invasive procedure for tumor debulking, which has the potential to initiate or amplify tumor immunity through the release of tumor-associated antigens and endogenous danger signals. However, enhanced immunity is rarely observed in treated patients, suggesting the need for mechanistic analysis. The goal is to determine how cryoablation affects tumor specific immunity and if the response can be improved through exogenous TLR9 stimulation.

Methodology: We evaluated α-Her2/Neu immunity following cryoablation in wt BALB/c and tolerant NeuT mice inoculated with Neu or Her2 expressing mammary tumors TUBO and D2F2/E2 respectively. Mice were treated with cryoablation, tumor excision, sham surgery, and/or 100 μg peritumoral (p.t.) CpG ODN. NeuT mice received vaccination with plasmid DNA encoding Neu/Her2 and GM-CSF to induce an initial response. Specific IgG antibody (Ab) subclasses and T-cell responses were assessed using flow cytometry and IFNγ ELISPOT assays respectively. Inflammatory transcript and protein levels from stimulated tumor draining lymph nodes (TDLN) were quantified using qPCR and magnetic bead multiplexing respectively. Phenotyping of peripheral blood leukocytes and TDLN was performed using flow cytometry.

Results: Cryoablation of Ab-sensitive TUBO induced α-neu Ab that protected ~65% of wt mice from tumor re-challenge which increased to ~95% when p.t. CpG was used in combination

therapy. Cryoablation of D2F2/E2 protected ~80% of mice if rechallenge was performed after the ablated tumor had been cleared (41 d). However, rechallenge 2 weeks after cryoablation resulted in accelerated growth relative to surgical incision. In vaccinated tolerant NeuT mice, protection was not amplified after cryoablation, even with the addition of CpG. However, tumor excision provided significantly greater tumor protection. Cryoablation primarily induced α-Neu IgG1 relative to IgG2a, which was inversed with the addition of CpG. Cryoablation elevated many inflammatory transcripts, with the most significantly elevated transcripts indicative of a Th2 phenotype (*Il10* and *Il4*) and suppression (*Foxp3* and *Tgfb*). Recurrences of tumors treated with cryoablation occurred in 26-29% of wt mice which was significantly decreased to 0% with the addition of CpG.

Conclusions: These findings suggest cryoablation induces a Th2 dominant response, which may be detrimental if residual disease is present. To promote the shift to a Th1 phenotype, which is associated with greater anti-tumor activity, CpG was used in combination with cryoablation. This led to significantly elevated IgG2a/IgG1 relative to cryoablation alone and greater tumor protection in wt mice, suggesting Th1 activation. Furthermore, the addition of CpG elevated IFNγ responses above that of cryoablation alone, which appeared to primarily be localized to the treated region. Cryoablation can be an effective tool for both tumor debulking and immune priming if Th1-promoting adjuvants are used in combination therapy.

AUTOBIOGRAPHICAL STATEMENT

Jesse J. Veenstra

Education

INSTITUTION	DEGREE	YEAR(s)	FIELD OF STUDY
Grand Valley State University Allendale, MI	BS	2003-2007	Biomedical Science
Wayne State University School of Medicine Detroit, MI	MD/PhD	2007-2015	Medicine / Cancer Biology

Positions

ACTIVITY/OCCUPATION	BEGINNING DATE (mm/yy)	ENDING DATE (mm/yy)	FIELD	INSTITUTION
Research Assistant	06/05	4/07	Molecular Biology and Genetics	Grand Valley State University
Tutor	09/05	4/07	Biomedical Science	Grand Valley State University

Academic and Professional Honors

Grand Valley State University

- 2006 - S^3 Research Grant Recipient
- 2007 - Magna Cum Laude

Wayne State University School of Medicine

- 2007: Wayne State University School of Medicine Board of Governors Scholarship
- 2007 – 2009: Honors in year 1 and 2 at Wayne State University School of Medicine
- 2007 – 2009: MD/PhD Preclinical Academic Excellence Award
- 2009: Alpha Omega Alpha Medical Honor Society Inductee
- 2010: 2nd place at Wayne State University Graduate Exhibition
- 2010 – 2011: Selection to the NCI funded T32
- 2011: F30 fellowship from National Institute on Aging
- 2011: 2nd place at Wayne State University Cancer Biology Symposium
- 2011 – 2012: MD/PhD Student Representative
- 2012: 1st place poster award Karmanos Cancer Institute retreat